BMR JOURNAL of Australian Geology & Geophysics

VOLUME 6 NUMBER 2 JUNE 1981

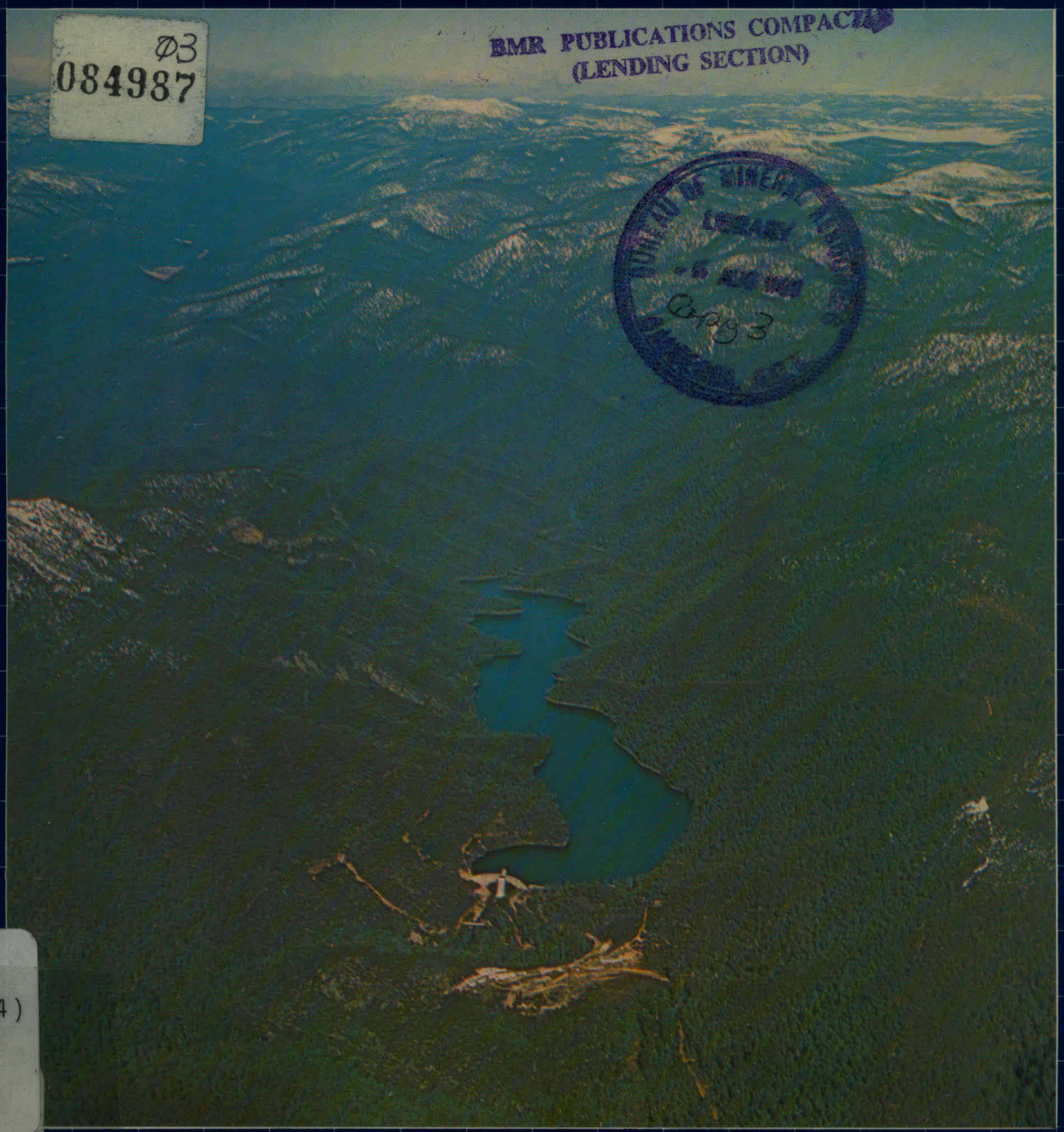

BMR JOURNAL of Australian Geology & Geophysics

Volume 6, No. 2
June 1981

AUSTRALIAN GOVERNMENT PUBLISHING SERVICE
CANBERRA 1981

Department of National Development and Energy, Australia

Minister: Senator the Hon. J. L. Carrick

Secretary: A. J. Woods

Bureau of Mineral Resources, Geology and Geophysics

Director: R. W. R. Rutland

Editor, BMR Journal: I. M. Hodgson

The BMR Journal of Australian Geology and Geophysics is a quarterly journal of research and related activities. Contributions are from officers of the BMR, from BMR officers working in collaboration with others, or requested work sponsored by the BMR. In addition to articles the Journal may include shorter notes and discussion of papers published in it. Discussion of papers is invited from anyone.

Annual subscription to the Journal is at the rate of $14 (Australian). Individual numbers, if available, cost $4. Subscriptions, etc., made payable to the Receiver of Public Moneys in Australian dollars should be sent to the Director, Bureau of Mineral Resources, Geology and Geophysics, P.O. Box 378, Canberra, A.C.T. 2601, Australia.

Other matters concerning the Journal should be sent to the Director, marked for the attention of the Editor, BMR Journal.

Front cover:

Two of Canberra's water supply dams: aerial view (1966), looking south towards Bendora Dam, and Corin Dam under construction (upper left). The importance of geology in the siting and design of such dams is described in a paper in this issue. Photo by courtesy of Australian Information Service.

Cover design: Stuart Fereday.

The text figures in this issue were drawn by a cartographic team of R. Bates, I. Hartig, R. Anderson, and C. Fitzgerald.

ISSN 0312-9608

Printed by Graphic Services Pty Ltd, 516-518 Grand Junction Road, Northfield, S.A. 5085

BMR Journal of Australian Geology & Geophysics, 6, 1981, 117-122

A model for sulfide band formation under epigenetic conditions — a study based on simulated sedimentary systems

B. Bubela[1]

The formation of sulfide bands in sediments has been investigated in the past, but in all the cases described they have formed by the diffusion of solutes from stationary fluids in the pores of the sediments. Experimental work with liquids flowing through sediments has shown that such bands may be formed even in a dynamic environment. A model based on experimental work with simulated sedimentary systems explaining the mechanism responsible for the formation of such bands under epigenetic conditions is presented in this paper.

Introduction

The investigation of problems associated with various branches of geology, sedimentology and geobiology is usually based on two approaches:

(a) fieldwork; and
(b) laboratory investigation.

The fieldwork approach has, of course, a distinct advantage of direct observation of systems or their results in nature, and usually adequate amounts of material available for studies.

However, field investigations are frequently hindered by the complexity of the systems being studied and the investigator is handicapped by lack of experimental control. Furthermore, although very slow processes may have been operating long enough for the results to be measurable, their original operating environment may have been very different to that at the time of observation.

As the field approach can be disadvantaged by the complexity of systems, laboratory investigation of individual parameters, their evaluation, and significant application to the field may be limited by over-simplification of systems. Individual processes, as studied, do not operate independently in the field, but are highly interactive in their effects. However, one of the primary advantages of laboratory experiments is that the starting conditions of processes being studied are known, which is frequently essential for subsequent evaluation of the systems. In many cases the size of an experiment may be a limiting factor: frequent sampling over a long time may be necessary, for example, or the walls of a small container may affect processes associated with surface tension, microbiological activity, and permeability. On the other hand, such experiments are usually readily monitored and the answers to many basic questions are relatively easy to obtain.

Finally one of the most important advantages of laboratory investigations is the operator's experimental freedom, lacking in most cases of field investigations.

After consideration of all the advantages and disadvantages of the above approaches, an attempt was made to utilise their advantages and eliminate as many of their short-comings as possible, by devising another approach. A concept of a simulating system was formulated.

The simulating system represents an attempt, in the laboratory, to move closer to the field environment, while eliminating some of the non-essential complexity, and facilitating experimental control. There is, of course, no sharp division between laboratory experiments and simulation. Ideally, there should be continuity from the simple laboratory system, through the experimentally manageable simulating system, to the naturally complex field environment.

In the designing of a simulating system, the questions to be answered should be carefully defined. To reduce the complexity of the system as much as possible, the number of parameters to be monitored simultaneously should be limited. Therefore the selection of these parameters is of the greatest importance. The problems of continuous sampling and side-wall effects can be reduced, if not eliminated, with proper planning, although requirements for specific minerals and fluids in quantities of kilograms or even tonnes can create logistic problems, especially where uniformity of chemical composition or mineralogy is important. In the cases where fully automatic monitoring and automatic control are desirable the instrumentation may become very complex. The same would apply to a field study, of course.

History of investigations

Probably the earliest attempt to simulate a geobiological environment was made by Winogradsky (1945) when he investigated the effect of organic material on carbonate mineralogy. Later, Weiss & Amstutz (1966) devised a system to study the extraction of lead and other metals from clay in the presence of sodium sulfide solution.

The genesis of Mansfield copper shale was simulated by Suckow & Schwartz (1968), and the ionic movement of iron through sediments in the presence of organic matter and the diffusion processes involved were simulated by Berner (1969), who also previously worked on the effect of organic matter in carbonates (Berner, 1968). Experimental work simulating multi-ionic diffusion through sediments and the consequent separation of metals into monomineralic strata has been described by Bubela & McDonald (1969), Lambert & Bubela (1970), and by Bubela (1981).

Thorstenson & Mackenzie (1971) and Deelman (1975) investigated, by simulating systems, the effects of microbiological sulfate reduction and carbonate precipitation, and Hargrave (1972) was simulating some aspects of eutropic lakes for his investigation of Eh and O_2 concentration in such a lake.

A more complex system was developed by Graetz & others (1973) to study Eh and nitrogen transformation in lake sediment—water environments, and photosynthetic sulfide oxidation and its response to heat and light were simulated by Blackburn & others (1975).

A more sophisticated system was developed by Bubela & Ferguson (1973) where the relative large

[1] **Baas Becking Geobiological Laboratory, P.O. Box 378, Canberra City, ACT 2601.**

size of the simulating system (over 1000 litres) permitted continuous sampling and monitoring over a long time without undue disturbance to the system. The system simulated diagenetic processes in unconsolidated sediments in the presence of carbonates, heavy metals, microbiological sulfate reduction and algal growth (Bubela, 1970; Bubela & Powell, 1973; Bubela & others, 1975; Ferguson & others, 1975; Davies & others, 1978).

All of the systems mentioned so far were static, where the systems, except for molecular diffusion, evaporation, and biological activity, were at a steady state.

However, natural systems are usually dynamic, and thus simulation studies have evolved to include dynamic factors such as water movement and varying energy states.

Several systems have been developed where the liquid phase was forcibly circulated. Jorgensen & others (1975) circulated seawater through an experimental column and measured the rate of sulfate reduction and the oxygen uptake by the water of the sediments. A similar system simulating oxygen uptake by sediment waters was constructed by Fenchel (1960).

A high energy environment favourable to the formation of carbonate ooids was simulated and the effect of high molecular weight organic substances on the processes involved was described by Ferguson & others (1978) and Davies & others (1978).

To study the effects of metal chelation on transport and deposition, Hallberg & others (1980) developed a system where continuous sedimentation of mineral particles took place for several months. A mathematical evaluation of such a simulating system was done by Mooney & others (1978).

Movement of interstitial waters through sediments is important during diagenesis of carbonates and organic matter (Bubela, 1980), and a complex system was developed by Bubela & others (1978), to provide horizontal and vertical water movement, climatic simulation and continuous monitoring of a variety of parameters (Johns & Bubela, 1979).

Hydrological studies with simulating systems

The two main areas concerned with the hydrology of sediments as studied with simulating systems are: (a) movement of fluids through sediments and the effect on associated processes; and (b) hydrochemistry.

The movement of water through sediments is influenced by a number of factors. Possibly, the most pertinent is the permeability of the sediments, which is directly linked to the useful porosity of the sediments. The porosity and permeability may be affected in a number of ways, both biological and abiological (Bubela, 1980). Biological factors may be the production of organic matter in pores, development of low-permeability algal mats sealing the water-sediment interface, formation of low permeability strata of high organic content, should such mats become buried in sediments, and diagenesis and cementation processes involving carbonates, owing to the release or consumption of CO_2 by the biological component of the sediments. Abiological processes may consist of compaction of sediments, a decrease of pore space, owing to pressure, diagenetic responses of carbonates to temperature and pressure, and pH changes. Only rarely would any of these factors be involved singularly.

The heteropermeability of sediments is important, as direction of flow of interstitial fluids and the length of the pathway the fluids travel may be altered considerably and result in changes in the chemical and physical properties of the fluids, thus affecting the conditions governing deposition or solution of minerals (Bubela, 1980). Direct evidence of such an influence was obtained by Bubela (1980). While the growth of an algal mat limited free movement of interstitial fluids, it permitted the passage of at least some ions. At pH 7.7 and 20°C and concentration gradient of 500 μmoles over 1 mm of mat thickness, 75 μmoles of copper passed per 1 cm^2 per day. However, no metal passage was detected if the metal was bound as an organo-complex.

To some extent, the composition of interstitial and supernatant waters reflects the biological activity of a system. When the algal mat mentioned above (Bubela, 1980) was active at the water-sediment interface, the Ca/Mg ratio in the interstitial water increased—owing to the relative solubilities of the calcium and magnesium carbonate respectively, the CO_2 concentration decreased—because of its consumption by the algae, and the pH of the system rose to 8.4. During the bacterial decay of the algae mat, the total concentration of CO_2 in the waters increased, the Ca/Mg ratio decreased and the pH value was lowered to 6.5. A similar fluctuation of the above parameters was noticeable during diurnal changes in microbiological activities.

Mineralogical studies with simulating systems

Weiss & Amstutz (1966) reported that a mixture of metals adsorbed to clay separates into a form of metal sulfide when H_2S is diffused through the clays. Similar results were obtained by Bubela & McDonald (1969) and Lambert & Bubela (1970) when they separated a mixture of lead, zinc, and copper into individual mineral zones by counter-diffusion of metals and hydrogen sulfide through stationary interstitial fluids. The metals did not separate into the zone sequences according to their solubiiities, as was expected. Copper with the lowest solubility ($K_S = 8.5 \times 10^{-45}$) spread through the whole zone of observation, while lead ($K_S = 3.5 \times 10^{-28}$) accumulated in the middle of the zone, and zinc ($K_S = 1.2 \times 10^{-23}$) travelled furthest before it precipitated as the corresponding sulfide.

This observation indicates that other factors besides solubility may determine the zone of precipitation. The separation of metal sulfides into individual bands from two converging streams, carrying metal and sulfide ions respectively, was demonstrated by Bubela (1981). The sulfide bands were formed parallel to the resulting flow.

It is evident from the experimental work by Hallberg & others (1980) that organic matter has a considerable influence on metal precipitation, in certain cases even preventing it. It is possible that under some conditions the supersaturation threshold is considerably increased by the presence of organic matter and metal precipitation is delayed until a higher degree of supersaturation is reached.

Diagenetic changes in carbonates have been studied in simulating systems in some detail. The earliest experimental work was concerned with participation of organic matter and the involvement of sulfate reducing organisms in the diagenesis of carbonates (Berner, 1968; Thorstenson & Mackenzie, 1971; Deelman, 1975). Lambert & Bubela (1970) described the participation of carbonates in the formation of framboidal hydrocerussite, which was converted to galena by passing biologically produced H_2S through the sediments.

When deposits of nesquehonite were exposed to biological activity associated with endogenous organic

material in a simulating system (Davies & others, 1973) chemical changes were noted leading to the formation of dypingite, protohydromagnesite, high-magnesium calcite, huntite, and protodolomite. Formation of a crust was observed at the water-sediment interface, composed of monohydrocalcite spherules embodied in nesquehonite matrix (Davies & others, 1973). During this experiment the aqueous phase always covered the surface of the sediments. Under different experimental conditions (Bubela, 1980), when the surface of the sediments was allowed to dry out and the surface temperature was maintained at 30°C, a surface crustation formed of residues of algal mat, halite, gypsum, anhydrite, and high-magnesium calcite. At a later stage the high-magnesium calcite disappeared and dolomite was detected.

The formation of carbonate spherules in the static simulating system of Bubela & others (1975) is important, as general opinion was that such structures are only inorganic precipitates formed during motion in suspension after heterogenous nucleation, and the organic matter found within the ooids (spherules) is an accidental accessory unrelated to their growth (Berner, 1974). Experimental work employing simulating systems (Davies & others, 1978) has shown that ooid formation may take place in both high and low-energy regions, but each will produce a different geometry in the crystals composing the ooids. Ooids formed in a high-energy environment (waves) exhibit a tangential orientation of baton-like crystals and the endogenous organic matter is accidental. Quiet-water ooids have radial arrangement of their crystals, and they are formed from supersaturated seawater containing organic matter. The factors most important in the quiet-water formation are the molecular weight of the organic matter, the presence of carboxyl groups, and an ability of the matter to participate in hydrophobic-hydrophilic interactions. The organic matter has to be able to form organic membranes, which form the bases of concentric shells for the growth of the crystals and induce the periodicity in the carbonate precipitation. The membranes have been shown (Ferguson & others, 1978) to form by association of individual organic molecules through metal bridging and hydrophobic/hydrophilic interactions, which are known to contribute to the stability of biological membranes.

Simulating studies of diagenesis of organic matter

The diagenesis of organic material has been simulated in several systems. The organic content of the sediments undergoes a number of changes, both qualitatively and quantitatively. It is at least partially biodegraded, which results generally in the evolution of gases, mostly a mixture of methane and carbon dioxide. A system operating under highly saline conditions and being anaerobic (approx.—150 mV) produced a mixture of gases containing hydrogen (80%), carbon dioxide (5%), methane (2%), and cyclobutane, n-butane, isobutane, n-pentane, and isopentane (13%) (Bubela & others, 1975). Such short paraffines have been detected frequently in natural gases, but their presence has been attributed to the catagenetic processes acting at high temperatures on type-2 kerogen (Tissot & Welte, 1978). The system described by Bubela was operating at temperatures around 20°C and at a pressure not exceeding 100kPa above atmospheric pressure. The biodegradation of organic matter under extremely halophilic and anaerobic conditions is not well known. Significant changes in biological activity due to environmental stresses have been described (Bubela, 1970). It is therefore feasible that such hydrocarbons may be produced directly at low temperatures and pressures from biopolymers without them first being changed into geopolymers (Tissot & Welte, 1978).

An increase in organic matter in sediments has been described by Bubela & others, 1975; Bubela, 1980. Such an increase is primarily due to fixation of carbon dioxide by photosynthetic organisms in the water column above the sediments or the biological population at the water-sediment interface. The biomass produced by such a process is not confined to the region of its genesis, but is transported by diffusion or water movements down into the sediments, where it serves as a substrate for development of the endogenous biological population. Therefore, the organic matter in the sediments consists at any time of the residual syngenetic component, material introduced by diffusion or water movement, the biomass that developed in the sediments after their deposition, and finally, the metabolic by-products of the biological activity taking place.

The composition of the organic matter changes quite rapidly. Bubela & Philips (in prep.) have observed that the buried organic matter, which originally exhibited an abundance of hydrocarbons of about C_{17}, thus demonstrating its algal origin, altered significantly after 18 months. The algal characteristics of the organic matter decreased, and hydrocarbons in the C_{20-30} range became predominant, thus indicating its predominantly bacterial origin. The significance of this observation lies in the fact, that it was the bacterial and not algal material, which, at least to some degree, underwent further diagenetic changes, leading eventually to the formation of geopolymers. As the original sediments become more and more covered by new sediments, the introduction of fresh organic matter suitable as the substrate for the endogenous population diminishes and the chemical, abiological changes become more and more predominant, resulting eventually in the formation of kerogen type-1 (Tissot & Welte, 1978).

Some conclusions from simulating studies

From data obtained from the above simulation studies it is possible to derive some conclusions regarding the behaviour of natural marine evaporative sedimentary systems.

(a) The movement of interstitial waters through sediments may be greatly influenced by biological activity, the major effect of which is to change permeability. Such changes affect not only the quantitative aspect of flow, but the directional component as well, and may result in the alteration of conditions governing the mechanisms of deposition and/or solution of components of the sediments. An example would be chemical and physico-chemical changes in the fluid composition, a decrease in the evaporation drive through the surface of the sediments and selective passage of metals through algal mats (Bubela, 1980).

(b) The mineralogy and morphology of sediments becomes affected by the presence and composition of organic material, and may, in certain cases, such as in the presence of dolomite or ooids, be used as indicators of the environmental conditions during their formation (Davies & others, 1978; Ferguson & others, 1978).

(c) The production of cyclic and iso-paraffines of 4-carbons by biological processes makes their value as

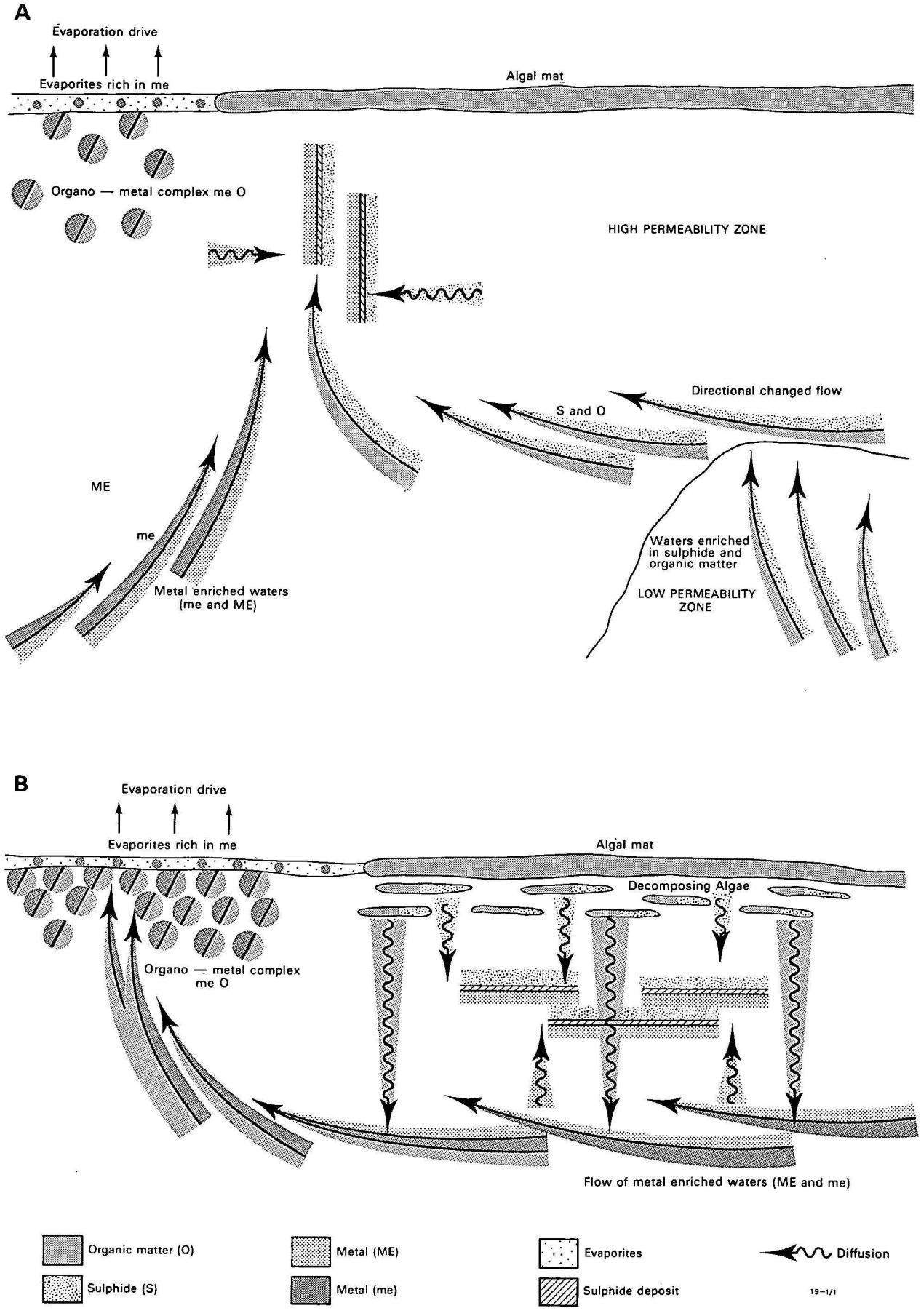
A
Evaporation drive
Evaporites rich in me
Algal mat
Organo — metal complex me O
HIGH PERMEABILITY ZONE
Directional changed flow
S and O
ME
me
Metal enriched waters
(me and ME)
Waters enriched
in sulphide and
organic matter
LOW PERMEABILITY
ZONE
B
Evaporation drive
Evaporites rich in me
Algal mat
Decomposing Algae
Organo — metal complex
me O
Flow of metal enriched waters (ME and me)
Organic matter (O)
Metal (ME)
Evaporites
Diffusion
Sulphide (S)
Metal (me)
Sulphide deposit
19-1/1

indicators of high temperatures and pressures in the sediments during their formation rather questionable (Bubela & others, 1975).

(d) Biological processes resulting in the production and/or consumption of CO_2 affect the Ca/Mg ratio in interstitial waters, and therefore directly influence the solution and deposition of carbonates and their mineralogy. These processes, frequently observed during diurnal changes in nature, are even more active during the establishment of algal mats and their subsequent biological decomposition (up to several months), when their effect can be very pronounced. The effects of diurnal changes tend to be mutually cancelling (Bubela, 1980).

(e) The formation of predominantly monomineralic sulfide deposits is not necessarily a manifestation of subsequent changes in the depositional environment (sequential introduction of metals, changes in pH and Eh, etc), but may be the result of diffusion in stationary interstitial fluids or converging and/or parallel flow patterns (Bubela & McDonald, 1969; Lambert & Bubela, 1970; Bubela, 1980, Bubela, 1981).

(f) The distribution of metals through sediments will be affected by their capacity to form organic complexes and the relative stability of such complexes compared with that of their corresponding sulfides (Hallberg & others, 1980).

Model for sulfide band formation under epigenetic conditions

A number of models have been suggested for environments where, owing to an evaporation drive, underground supply of metals and biologically or abiologically produced S^{2-}, metal sulfides are deposited. One such model has been described by Renfro (1974). This model describes the formation of mixed sulfide deposits, but cannot explain the formation of predominantly monomineralic strata in the sediments. Considering some of the observations described above and demonstrated in and by the simulating systems, it is possible to construct a model that does explain simply the separation of individual metals into distinct zones, not necessarily conforming to the direction of the sedimentary beds.

Basically, the model starts from the same concept as Renfro's, visualising an environment where metals and sulfide ions are supplied from their individual sources. The first modification of Renfro's model is to take into consideration the heteropermeability of the sediments. It has been shown that, owing to differences in permeability, significant directional variation of fluid movement will result. The second modification is due to the fact that algal mats may considerably reduce the evaporation drive and therefore alter the directional components of flow of the interstitial fluids. The next difference in the concept is due to the observation that organic complexing of metals may influence their availability to be precipitated as sulfides. Finally, the formation of banded sulfides from converging or parallel-moving fluids is taken into account.

The model is presented in Figure 1A. The surface of the sediments is partially covered by low-permeability algal mat. Interstitial waters emerging from a low-permeability zone of buried organic matter, where biological activity results in the production of S^{2-}, are enriched in organic complexing matter and S^{2-}. Owing to the change in permeability, the S^{2-}-rich waters deviate from their original direction. This trend is further enhanced by the evaporation drive operating at the mat-free surface. The metal-enriched waters, from their separate source, converge on the sulfide/organic matter stream. Because of the negligible compressibility of liquids, these streams eventually run parallel to each other with limited mixing, if the flow rate is sufficiently slow, to result in laminar flow. The same mechanism (Liesegang phenomenon) responsible for the formation of monomineralic sulfide bands during counter-current diffusion (Bubela & McDonald, 1969) will be operative and sulfide bands parallel to the flow will be formed. The orientation of the bands may be at a variety of angles to that of the sedimentary layers.

A variation to the above model is presented in Figure 1B. In this case, the metal-bearing waters move parallel to the sedimentary layers. The decomposing buried algae produce sulfide, which, owing to its concentration gradient, diffuses in a direction perpendicular to the flow of the metal enriched waters. Similarly to the situation described in Figure 1A, metal-sulfide bands will form parallel to the flow and the bedding.

The system on which this model is based varies significantly from that described by Bubela & McDonald (1969) and Lambert & Bubela (1970), where, in all the cases investigated, only the molecular movement of the solutes (metals and sulphide) was considered, and the solvent (water) was stationary. Therefore, in principle, the process leading to banding as described previously (Bubela & McDonald, 1969; Lambert & Bubela, 1970) may be classified as a diagenetic process, while the present model describes the formation of bands under epigenetic conditions. In both cases, these terms are used as defined by Williams (1979). In many instances it may be difficult to decide by which of these two processes the sulphide bands were formed. The epigenetic model indicates the feasibility of the processes envisaged by Williams (1979) for the McArthur River deposits: if some of the metals form organocomplexes of sufficient stability, they may be moved for a considerable distance from the precipitation zone and may eventually follow the evaporation drive, finishing as an enrichment in the surface evaporites.

In summary, the model presented here is capable of explaining certain problems associated with sulfide deposits in sediments and is believed to complement Renfro's model by providing plausible mechanisms for the formation of banded metal deposits at various angles to the sediments.

Acknowledgements

The Baas Becking Laboratory is supported by the Australian Mining Industry Research Association, Bureau of Mineral Resources, Geology and Geophysics, and the Commonwealth Scientific and Industrial Research Organisation.

Figure 1. Models of sulphide band formation under epigenetic conditions.
A: Waters enriched in S= and organic matter (O) converge on metal-bearing waters (ME and me); ME does not form an organo-complex and is precipitated as a ME sulfide band. Metal me forms a stable organo-complex and is not readily precipitated as a sulfide, but is removed from the zone of precipitation and accumulates in the evaporites.
B: Sulfide ions produced by decaying algal mat diffuse down into the sediments' metal-bearing waters, and produce sulfide bands parallel to the bedding.

References

BERNER, R. A., 1968—Calcium carbonate concretions formed by the decomposition of organic matter. *Science*, 159, 195-7.

BERNER, R. A., 1969—Migration of iron and sulfur within anaerobic sediments during early diagenesis. *American Journal of Science*, 267, 19-42.

BERNER, R. A., 1974—Principles of chemical sedimentology. *McGraw-Hill, New York.*

BLACKBURN, T. H., KLEIBER, P., & FENCHEL, T., 1975—Photosynthetic sulfide oxidation in marine sediments. *Oikos*, 26, 103-8.

BUBELA, B., 1970—Chemical and microbiological changes in *Bacillus stearothermophilus* induced by copper. *Chemical and Biological Interactions*, 2, 107-16.

BUBELA, B., 1973—Effect of copper on the growth characteristics of *Bacillus stearothermophilus. Zentralblatt fur Bakteriologie*, 128, 457-66.

BUBELA, B., 1980—Some aspects of interstitial water movements in simulated sedimentary systems. *BMR Journal of Australian Geology & Geophysics*, 5, 257-63.

BUBELA, B., 1981—Banded sulphide ores. The experimental formation of sulphide bands in sediments from flowing liquids. *Economic Geology*, 76, 171-2.

BUBELA, B., & FERGUSON, James, 1973—Apparatus for studies of artificial sediments. *Journal of Sedimentary Petrology*, 43, 1167-70.

BUBELA, B., & MCDONALD, J. A., 1969—Formation of banded sulphides: metal ion separation and precipitation by inorganic and microbial sulphide sources. *Nature*, 221, 465-6.

BUBELA, B., & PHILLIPS, P., in preparation—Diagenetic changes in organic matter: simulation study.

BUBELA, B., & POWELL, T. C., 1973—Effect of copper on the composition of bacterial cell wall peptides. *Zentralblatt fur Bakteriologie*, 128, 451-66.

BUBELA, B., FERGUSON, James, & DAVIES, P. J., 1975—Biological and abiological processes in simulated sedimentary systems. *Journal of the Geological Society of Australia*, 22(2), 135-42.

BUBELA, B., JOHNS, I. A., & FERGUSON, James, 1978—A system for simulation of evaporative sedimentary environments. *BMR Journal of Australian Geology & Geophysics*, 3, 166-71.

DAVIES, P. J., BUBELA, B., & FERGUSON, James, 1973—Simulation of carbonate diagenetic processes: Formation of dolomite, huntite and monohydrocalcite by the reaction between nesquehonite and brine. *Chemical Geology*, 19, 187-214.

DAVIES, P. J., BUBELA, B., & FERGUSON, James, 1978—The formation of ooids. *Journal of Sedimentology*, 25, 703-30.

DEELMAN, J. C., 1975—Bacterial sulfate reduction affecting carbonate sediments. *Soil Science*, 119, 73-80.

FENCHEL, T., 1960—The ecology of marine microbenthos IV. Structure and function of the benthic ecosystem, its chemical and physical factors and the microfauna communities with special reference to the ciliated protozoa. *Ophelic*, 6, 1-182.

FERGUSON, James, BUBELA, B., & DAVIES, P. J., 1975—Simulation of sedimentary ore-forming processes. Concentration of Pb and Zn from brines into organic and Fe-bearing carbonate sediments. *Geologische Rundschau*, 64, 767-82.

FERGUSON, James, BUBELA, B., & DAVIES, P. J., 1978—Synthesis and possible mechanisms of formation of radial carbonate ooids. *Chemical Geology*, 22, 285-308.

GRAETZ, D. A., KEENEY, D. R., & ASPIRAS, R. B., 1973—Eh status of lake sediment-water systems in relation to nitrogen transformations. *Limnology and Oceanography*, 18, 908-17.

HALLBERG, R. O., BUBELA, B., & FERGUSON, James, 1980—Simulation of metal chelating in two reducing systems, *Journal of Geomicrobiology*, 2, 99-113.

HARGRAVE, B. T., 1972—Oxidation-reduction potentials, oxygen uptake of profundal sediments in a eutropic lake. *Oikos*, 23, 167-77.

JOHNS, I. A., & BUBELA, B., 1979—Multichannel pH-Eh-specific ion monitoring systems. *BMR Journal of Australian Geology & Geophysics*, 4, 398-402.

JORGENSEN, S. E., KAMP-NIELSEN, L., & JACOBSON, O. S., 1975—A submodel for anaerobic mud water exchange of phosphate. *Ecological Modelling*, 1, 133-46.

LAMBERT, I. B., & BUBELA, B., 1970—Banded sulphide ores. The experimental production of monomineralic sulphide bands in sediments. *Mineralium Deposita*, 5, 97-102.

MOONEY, J., BUBELA, B., FERGUSON, James, & HALLBERG, R. O., 1978—Mathematical modelling of experimental systems simulating metal chelating in reducing sedimentary environments. *BMR Journal of Australian Geology & Geophysics*, 3, 93-100.

RENFRO, A. R., 1974—Genesis of evaporite-associated stratiform metalliferous deposits—a sabkha process. *Economic Geology*, 69, 33-45.

SUCKOW, R., & SCHWARTZ, W., 1968—Geomicrobiological studies. The problem of the genesis of Mansfield copper shale. *Zeitschrift fur Allgemeime Mikrobiologie*, 8, 47-64.

THORSTENSON, D. C., & MACKENZIE, F. T., 1971—Experimental decomposition of algae in seawater and early diagenesis. *Nature*, 234, 593-45.

TISSOT, B. P., & WELTE, D. H., 1978—Petroleum formation and occurrence. *Springer Verlag, Berlin.*

WEISS, D., & AMSTUTZ, G. C., 1966—Ion-exchange reactions on clay minerals and cation selective membrane properties as possible mechanisms of economic metal concentration. *Mineralium Deposita*, 1, 60-6.

WILLIAMS, N., 1979—Studies of the base metal sulphide deposits at McArthur River, Northern Territory, Australia: II The sulphide-S and organic-C relationship of the concordant deposits and their significance. *Economic Geology*, 74, 1695-7.

WINOGRADSKY, S., 1945—Microbiology du Sol. *Masson, Paris.*

BMR Journal of Australian Geology & Geophysics, 6, 1981, 123-135

Crustal structure of the Precambrian terrains of northwest Australia from seismic refraction data

B. J. Drummond

The crust of the Pilbara Craton is 28-33 km thick, and its boundary with the upper mantle dips south at slightly less than one degree. The southern edge of the craton is marked by a sharp increase in crustal thickness about 40 km south of the Sylvania Dome in the east and along the northern boundary of the Ashburton Trough in the west. Seismically, the crust has two layers, an upper one with P-wave velocity 6.0-6.1 km s^{-1}, and a lower of 6.4-6.6 km s^{-1}. The boundary between them is depressed beneath the deepest part of the Hamersley Basin, and rises along the southern part of the basin and craton, beneath a topographic ridge of higher grade metamorphic rocks. The velocities in the lower crustal layer are highest along the southern part of the Hamersley Basin, an area known to have been depressed during the formation and filling of the basin, and then uplifted. The crust of the northern Yilgarn Craton is at least 50 km thick and, seismically, has three layers. The uppermost layer has P-wave velocities of 6.1-6.2 km s^{-1}, the middle layer, at 10-16 km depth, 6.4 km s^{-1}, and the lowest, at 32 km depth, 6.7-7.0 km s^{-1}. A zone of crust, about 50 km wide, along the northern margin of the craton was extensively reworked during Proterozoic orogenesis, and is now characterised by thinner crust than the rest of the Yilgarn Craton, extensive granitoid emplacement, intense deformation and folding of the upper crustal rocks, and low gravity values. The Capricorn Orogen between the cratons is marked by high velocities in the lower crust, probably caused by dense mafic intrusions or a higher metamorphic grade. The seismic layering within the crust is most likely caused by increasing metamorphic grade with depth. The crust is probably of average acid to intermediate chemical composition, and has a low metamorphic grade at the surface. The velocities are attributed to metamorphic grade increasing to felsic granulite at 9-16 km depth, and garnet granulite at 32 km depth in the Yilgarn Craton.

Introduction

During 1979, seismic refraction measurements were made along five profiles in the Pilbara region of Western Australia (Drummond, 1979a). Seven open-cut iron-ore mines in the northern Pilbara Block and the Hamersley Basin regularly fired large quarrying blasts, and these were used as seismic sources.

The seismic survey was planned so that the refraction profiles would traverse all the Precambrian geological provinces in the region. The survey design is superimposed on the geological map in Figure 1. BMR recorded along lines ABC, FDB and ADHE (Drummond, 1979a), and the Research School of Earth Sciences at the ANU recorded along lines GF and DC. Drummond (1979b) and Drummond & others (1981) used the intercept method (Mota, 1954) to interpret the data from lines ABC and FDB, and extended their interpretation by using computer ray tracing through their models to test for lateral structural changes.

In this paper the results of the earlier interpretations are summarised, the data from the three remaining traverses (ADHE, DC and FG) are interpreted, and the results from all five profiles are used to derive a picture of the crustal structure of the region.

Geology

The regional geology is shown in Figure 1. The tectonic nomenclature follows that of Gee (1979a, c); accordingly, a 'block' is the exposed part of an old, stabilised region called a 'craton'. In the survey area, two Archean cratons, the Pilbara and Yilgarn Cratons, are overlapped and separated by younger sediments and volcanics of several sedimentary basins.

The greenstone belts of the Pilbara Block have provided Australia's oldest isotopic ages of 3400 to 3500 m.y. (Richards, 1977; Pidgeon, 1978a; Hamilton & others, 1980), and sinuously enclose large, ovoid domes of younger, intrusive granitoid, with isotopic ages grouped around 3000 m.y. (Oversby, 1975; Pidgeon, 1978b; de Laeter & Blockley, 1972; de Laeter & others 1980, 1981) and 2600-2800 m.y. (Oversby, 1975; de Laeter & Blockley, 1972; de Laeter & others, 1980). The younger granitoids are a minor proportion of the granitoids of the Pilbara Block, and may have resulted from partial remelting of the older crust (de Laeter & Blockley, 1972).

The Yilgarn Block, which extends about 1000 km south of the area shown in Figure 1, also has a granitoid/greenstone stratigraphy. In the north, the majority of the granitoids have isotopic ages of about 2600 m.y. (Compston & Arriens, 1968; Oversby, 1975; de Laeter & others, 1980).

Volcanic and sedimentary rocks and banded iron formations of the Hamersley Basin overlap the southern edge of the Pilbara Block. Trends in the regional gravity pattern (Fraser, 1973; Wellman, 1978), and inliers of Archaean basement (e.g. the Sylvania Dome) indicate that the Pilbara Craton forms the basement of the Hamersley Basin. The rocks of this basin have marked lateral continuity, and are thought to have originally covered most of the Pilbara Craton. They are now restricted to the southern part of the craton, where the basin was deepest (Trendall, 1975; Horwitz & Smith, 1978). Where the basal unconformity of the basin is exposed, the basal volcanics are restricted to the centre of greenstone belts, implying that the granitoid plutons were still rising when the basin formed (Trendall, 1975). The intensity of folding in the basin increases southwards (Trendall, 1975).

Abutting the southern edge of the Hamersley Basin is the Ashburton Trough (the Wyloo Trough of Horwitz & Smith, 1978), which contains thick clastic sediments, turbidites, and olistostromes. The Ashburton Trough is younger than the Hamersley Basin, and

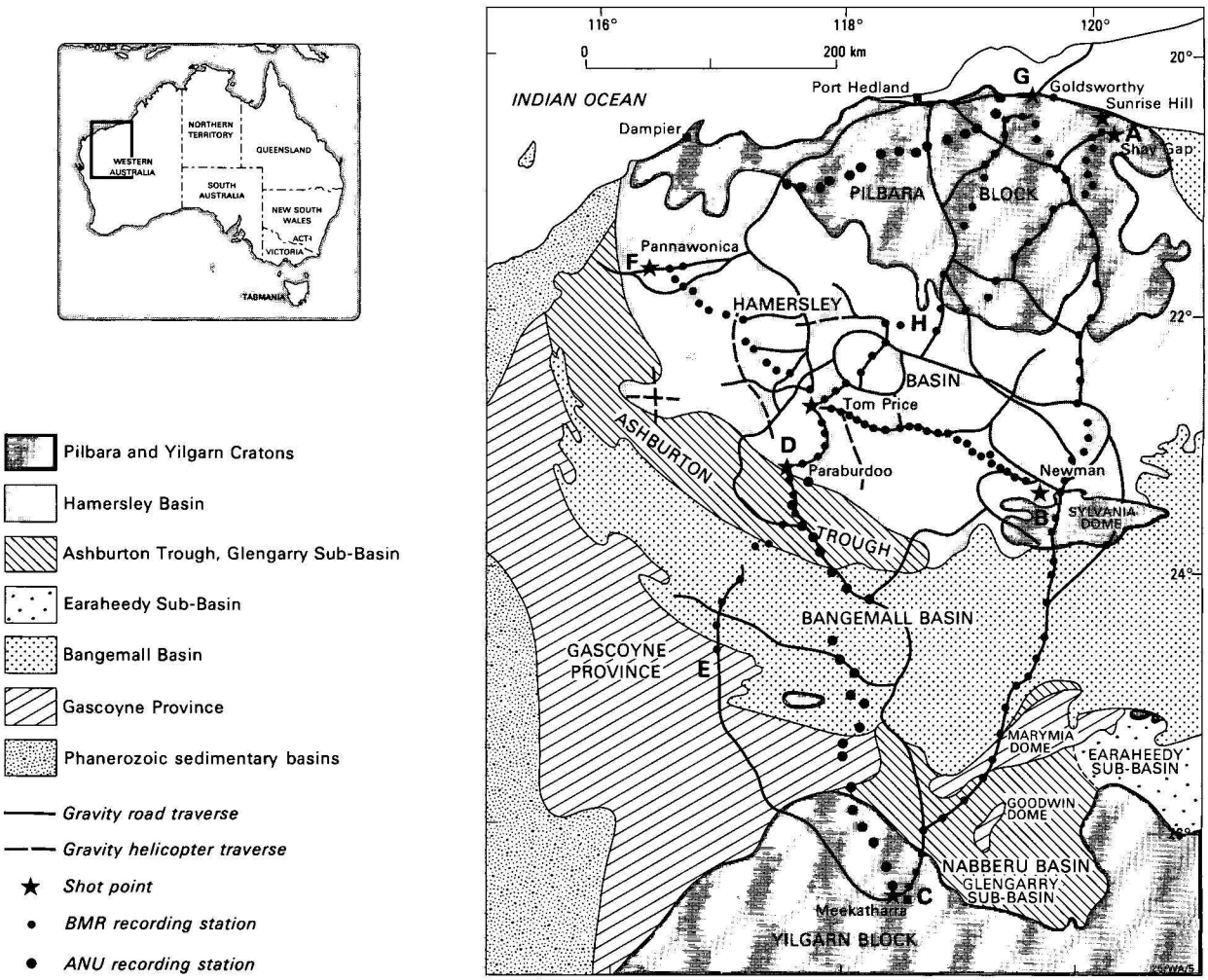

Figure 1. Geology and survey design.

is possibly contemporaneous with the Glengarry Sub-basin of the Nabberu Basin, which bounds the northern edge of the Yilgarn Craton (Gee, 1979a).

The Glengarry Sub-basin contains clastic sediments, volcanic rocks, and turbidites, which dip gently off the Yilgarn Craton. The dip and deformation of the sediments increase northwestwards across the basin (Hall & Goode, 1978; Gee, 1979b) and, although the structural relations between the Nabberu Basin and the Hamersley Basin are masked by the younger cover of the Bangemall Basin, Horwitz (1975) was able to show a mirror image symmetry of the structures in the two basins.

Clastic sediments, dolomites and cherts are the principal rock types of the Bangemall Basin; volcanic rocks are not common. Changes of facies and structural style reflect the stability of the basement on which the basin formed. Stable basement parallelled the southern boundary of the Pilbara Craton in the north, and the northern edge of the Yilgarn Craton in the south. The western and central portions of the basin had an active basement (Brakel & Muhling, 1976).

The Gascoyne Province in the west of the survey area contains reworked Archaean basement rocks, and reworked sediments from the Bangemall and Nabberu Basins and Ashburton Trough (Daniels, 1975; Williams & others, 1979). Granitoids which crop out in the province were derived from reworked Archaean basement, possibly mixed with younger magmatic or supracrustally reworked material (de Laeter, 1976; Williams & others, 1978).

The Gasycoyne Province, Bangemall Basin, and Ashburton Trough occupy the Proterozoic Capricorn Orogenic Belt (Gee, 1979c). Palaeozoic sedimentary basins bound the region on the west, north, and east.

Seismic wavegroup nomenclature

The nomenclature used in this paper is similar to that used by Drummond & others (1981), which is derived from Giese (1976).

Pg — Direct waves, which travel through the near-surface crystalline basement with velocities of 6.0-6.2 km s^{-1}.

P* — Waves critically refracted at an intracrustal boundary, and with velocities of 6.4-6.55 km s^{-1}.

P^I — Waves reflected from the intracrustal boundary and travelling with velocities intermediate between those of the Pg and P* wavegroups.

Pn — Waves critically refracted at the crust/mantle boundary, and having apparent velocities in the range 7.6-8.6 km s^{-1}.

P^M Waves reflected from the crust/mantle boundary, and with apparent velocities in-

termediate between those of the P* and Pn wavegroups.

P_1,P_2 — Near-surface wavegroups observed where the Hamersley Basin strata are underlain by lower velocity rocks. P_1 waves have velocities of about 5.9 km s^{-1}, and P_2 waves have velocities of 6.3-6.7 km s^{-1}.

PL — Near-critical point reflections from a deep crustal layer in the northern Yilgarn Craton. They have apparent velocities of about 7.0 km s^{-1}.

Results

Line ABC, including blasts at G (Shay Gap, Sunrise Hill, Goldsworthy-Newman-Meekatharra)

The data from line ABC (and line GBC) were interpreted by Drummond (1979b), and a slightly revised model, shown here as Figure 2, was given by Drummond & others (1981).

In the north, along segment Shay Gap-Newman, the crust is 28 km thick at Shay Gap, 32 km thick at Newman, and is two-layered. The upper crust has a seismic velocity of 6.0 km s^{-1}, and at about 13 km depth the velocity increases to 6.4 km s^{-1}. The upper mantle velocity is 8.34 km s^{-1}. The Hamersley Basin north of Newman is represented by a thin layer with a low (5.86 km s^{-1}) velocity.

Along the segment from Newman to Meekatharra, the Pn arrivals are delayed beyond 250 km, and as no such delay is apparent in the Pn data in the reverse direction, crustal thickening to the south is inferred. Crustal thickening is consistent with intercept times from recordings of Newman and Meekatharra shots, and with delays of teleseismic arrivals from earthquakes in the Fijian region (Drummond, 1979c), and the Indonesian Arc to the north (Drummond & others, in prep.). Ray tracing has shown that, in the most likely models, the crust thickens from about 33 km south of Newman to more than 50 km at Meekatharra. The principal differences in the models occur in the lower crust along the segment between Newman and Meekatharra.

The seismic velocity in the upper crust between Newman and Meekatharra is 6.1-6.2 km s^{-1}. At 10 km depth in the north and at 16 km depth in the south, the velocity increases to 6.4 km s^{-1}. In the south of segment BC, a lower crustal layer, with a velocity of about 7 km s^{-1}, is implied by a band of large-amplitude reflections at about 7 s and 140-200 km. The crust in the south is therefore three-layered. The upper mantle velocity may decrease from 8.34 to 8.1 km s^{-1} southwards along segment BC.

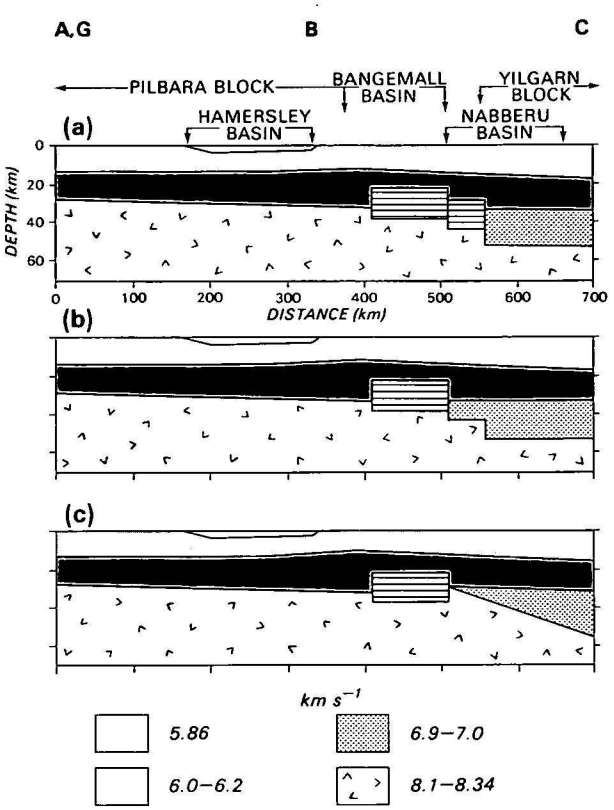

Figure 2. Three alternative seismic models for line GBC (and line ABC).
The models are those of Drummond & others (1981).

Line FDB (Pannawonica-Tom Price-Newman)

Drumond & others (1981) reported the results from line FDB, and Figure 3 shows their model. It is preliminary, because several features of their record sections could not be explained by ray-tracing methods alone.

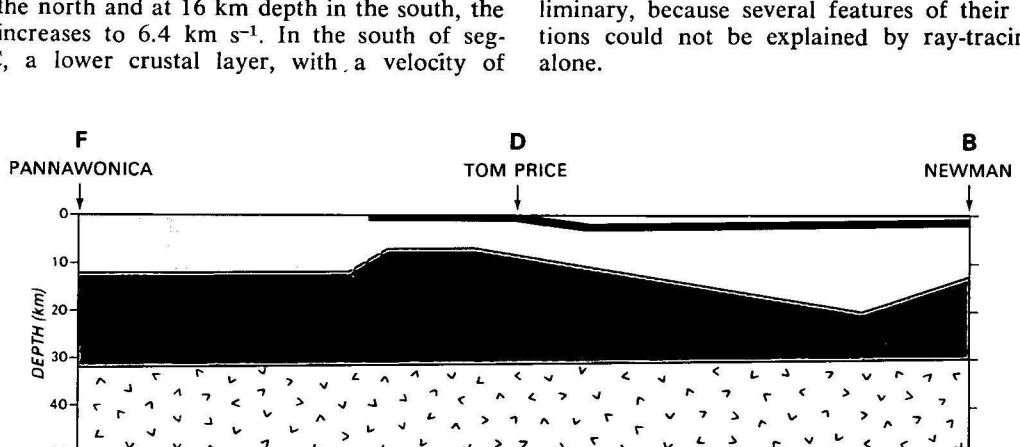

Figure 3. The crustal model derived by Drummond & others (1981) for line FDB.

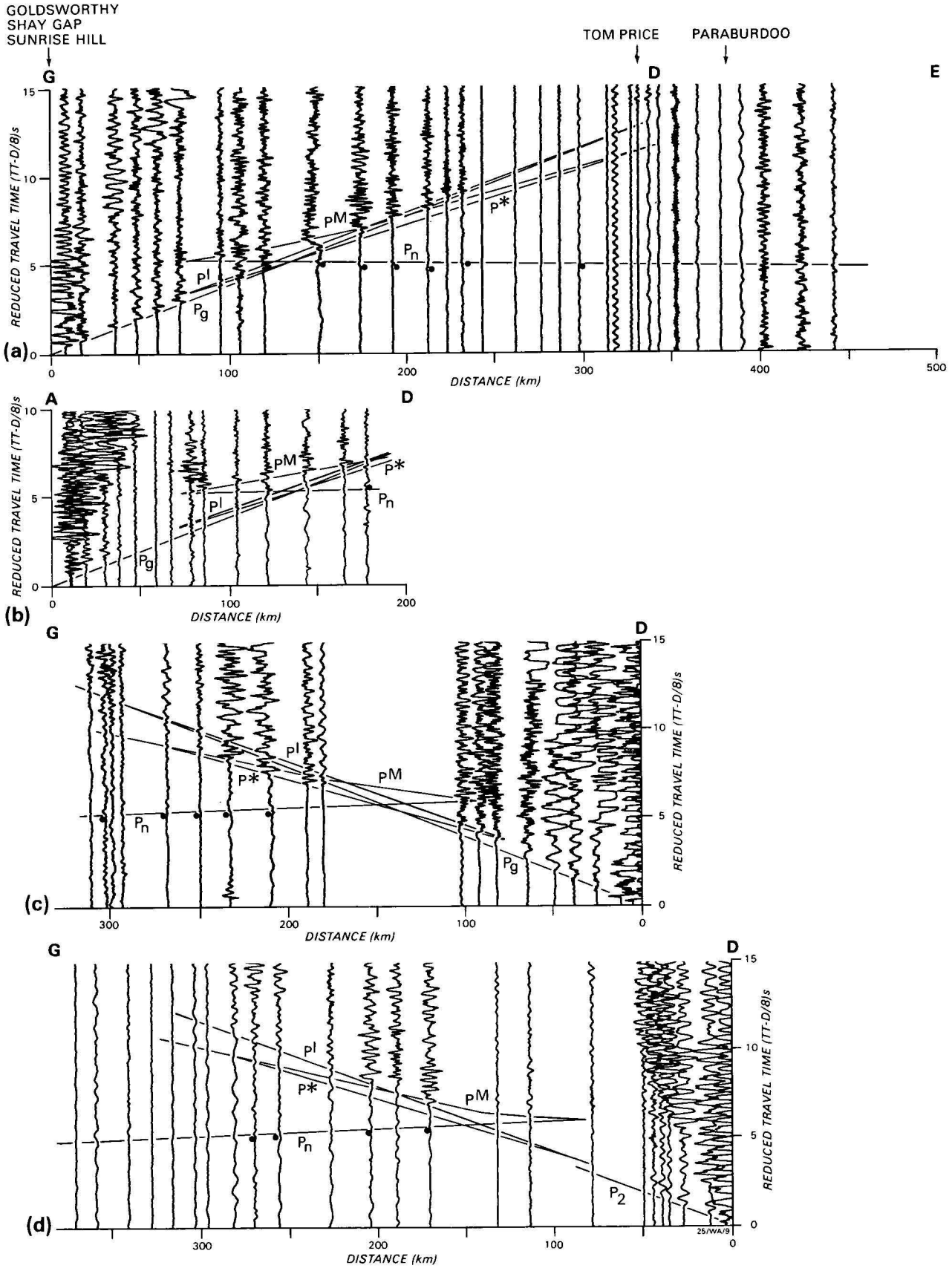

Figure 4. Record sections for line GD.
Sections a, b, c and d are for shotpoints G southwards, A southwards, Tom Price northwards and Paraburdoo northwards respectively. The superimposed travel-time curves are for the model in Figure 8a. The trace amplitudes are as recorded, and all traces were digitally filtered in the bandpass 0.5 to 8 Hz. The dots indicate the times of P_n arrivals picked from these and large amplitude records.

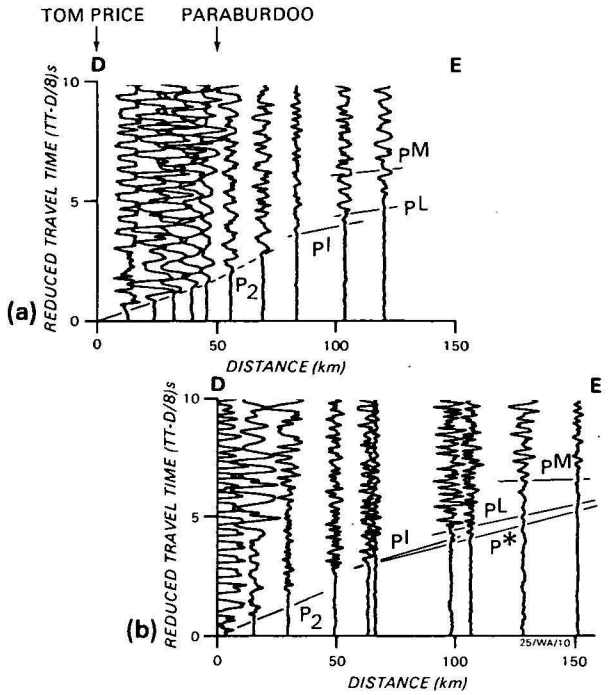

Figure 5. Record sections for line DE.
Section a is for Tom Price southwards, and section b is for Paraburdoo southwards. The superimposed travel-time curves are for the model in Figure 8b. The trace amplitudes are as recorded, and all traces were digitally filtered in the bandpass 0.5 to 8 Hz.

Between Tom Price and Newman, thin, near-surface layers with velocities of 5.9 and 6.3-6.7 km s^{-1} are interpreted as Hamersley Basin banded iron formations and volcanic and sedimentary rocks. They overlie a deeper crust in which the seismic velocities are less; the velocity of 6.07 km s^{-1} used throughout the profile was the unreversed velocity measured in the western part of the basin from a blast at Pannawonica. A lower crustal layer under the basin has a slightly higher velocity (6.54-6.56 km s^{-1}) than the corresponding layer under Newman measured along the north-south profile (Figure 2).

The boundary between the upper (6.07 km s^{-1}) and lower crustal layers has considerable topography. It is 12 km deep under Pannawonica, and shallows to 7 km depth to the west of Tom Price. Further east it deepens, perhaps reaching 20 km before shallowing to about 13 km under Newman.

Sub-Moho refracted arrivals are poorly observed along this profile, the reversed upper mantle seismic velocity was estimated at 7.8 km s^{-1}, which is considerably lower than along profile ABC. The crust/mantle boundary was modelled with very little topography; it is 31 km deep under Pannawonica, and 30 km deep under Newman. It may deepen slightly in the centre of the profile.

Lines GDC (including blasts at A) and DE (Goldsworthy-Tom Price-Meekatharra; and Tom Price towards SW)

The data from lines GD, DE, and DC are depicted as record sections in Figures 4, 5 and 6 respectively and the velocities and intercepts for the refracted phases and the P^L phase identified in, and scaled from, these record sections are listed in Table 1. In all cases, and in the following discussion, the travel times are reduced by the factor, distance/8.0. In Figures 4 and 5, the traces were digitally filtered in the bandpass 0.5 to 8.0 Hz, and the trace amplitudes are not normalised; normalised amplitudes were used in some cases in the identification and correlation of phases, but these are not shown here. In Figure 6, all record sections have had the trace amplitudes normalised so that the maximum amplitude for each trace is the same; the traces in Figure 6 were filtered in the bandpass 1.0 to 8.0 Hz. The models derived from the record sections are shown in Figure 7. The travel-time curves superimposed on the record sections in Figures 4, 5, and 6 were derived by computer ray tracing through the models in Figure 7; the following discussion serves to illustrate the wave groups used to derive the models.

Representative record sections from the line between Goldsworthy and Tom Price (GD) are shown in Figure 4. Two mines are located near D. The northern one is at Tom Price, and the southern one at Paraburdoo (Figure 1). They were treated as separate shotpoints and record sections from both are depicted.

The record section of blasts from the Goldsworthy shotpoint (G) is presented in Figure 4a. Coherent seismic energy was not observed beyond 240 km. The near-surface Pg phase is clearly seen as a first arrival to the crossover point with Pn at about 130 km. The Pn phases are very weak; dots indicate the arrivals that can be identified on larger scale records. A P^*/P^I cusp can be identified about 0.5 s after Pg, at about 70 km, and the P^M phase is clearly seen as large amplitude later arrivals in the 80-240 km distance range.

The smaller blasts at shoptpoint A (Shay Gap and Sunrise Hill), generate less seismic energy and, therefore, smaller amplitude arrivals than those at Goldsworthy. The P^M phase is, therefore, more clearly seen because the earlier arrivals do not obscure it (Figure 4b).

The Tom Price record section for line GD is shown in Figure 4c. The modelled P^M travel-times are about 0.5 s later than the recorded times. This was interpreted by Drummond (1979b) for data from shotpoint G along line GB as evidence for positive velocity gradients in the lower crust. The P^I wavegroup is clearly identified as a high-frequency phase following the low-frequency Pg arrivals.

In the record section of the Paraburdoo blasts recorded northwards (Figure 4d), the first arrivals from the shotpoint to about 50 km show a very rapid fall off in amplitude. This is indicative of a low-velocity zone in the upper crust north of the shotpoint. As will be shown in Figures 5 and 6, the near-source first arrivals probably belong to the P_2 phase which travels through the high-density, high-velocity, near-surface Hamersley Basin rocks. The P^*/P^I cusp is not clearly seen in this record section. The P^M phase is clearly seen, but the Pn phase is very weak.

The record section of Tom Price shots recorded southwards on line DE is shown in Figure 5a. The P_2 phase is recorded with strong amplitudes to about 60 km, whereafter it is delayed and its amplitudes weaken. The delay and weakening of amplitudes is also observed southwards from Paraburdoo (Figure 5b), but at only a few stations within 20 km of the blast. The delay and fall off in amplitudes corresponds, for both shotpoints, with the southern boundary of the Hamersley Basin about 10-15 km south of Paraburdoo (Gee, 1979a). The near-source upper crustal phase has, therefore, been interpreted as the P_2 phase, and not the

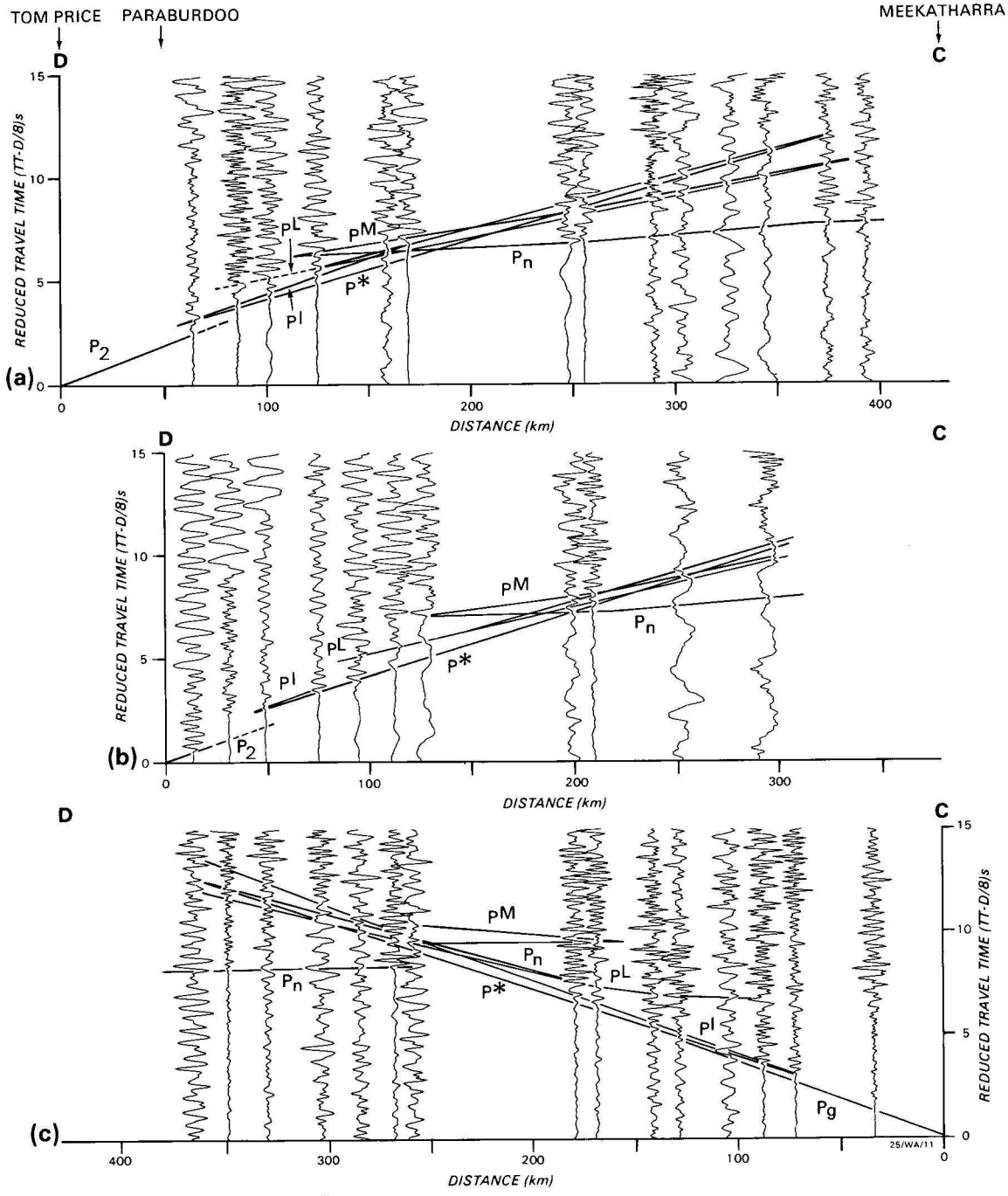

Figure 6. Record sections from line DC.
The sections a, b and c are for Tom Price southwards, Paraburdoo southwards, and shotpoint c northwards, respectively. The superimposed travel-time curves are for the model in Figure 8a. The trace amplitudes have been normalised so that the maximum amplitude is the same for all traces, and the traces in section c were digitally filtered in the bandpass 1.0 to 8.0 Hz. For some recorders, one of the horizontal components had clearer arrivals than the vertical component and has been plotted in its place. Note that the P^L cusp (the dashed curve) is closer to the shotpoint than predicted by the model.

Pg phase. This is the main reason for interpreting the near-source first arrivals in Figure 4d as P_2. Some of the lower crustal phases can also be identified in Figure 5b, in particular, the P^I and P^L phases.

Figure 6 contains the data from the ANU line between Paraburdoo and Meekatharra (DC). In Figure 6a, the P_2 phase is identified by only one early arrival, but it is identified with confidence because, at that point, the ANU line is coincident with the BMR line DE, on which the data in Figure 5a were recorded. The Pn phase is observed as strong arrivals on two traces at 240 to 260 km, but beyond that it is not clear. The traces at 375 and 395 km have large amplitude arrivals at about 8.5 s, which are delayed in time relative to Pn between 120 and 260 km, but may still be Pn arrivals. Figure 6a is similar to the record section from the line between Newman and Meekatharra (BC), where large-amplitude Pn phases are clearly evident, and can be correlated from trace to trace, and Pn is delayed beyond 250 km (Drummond, 1979b).

The P^L phase is very clearly seen in Figure 6a; the cusp on the travel-time curve for the model (Figure

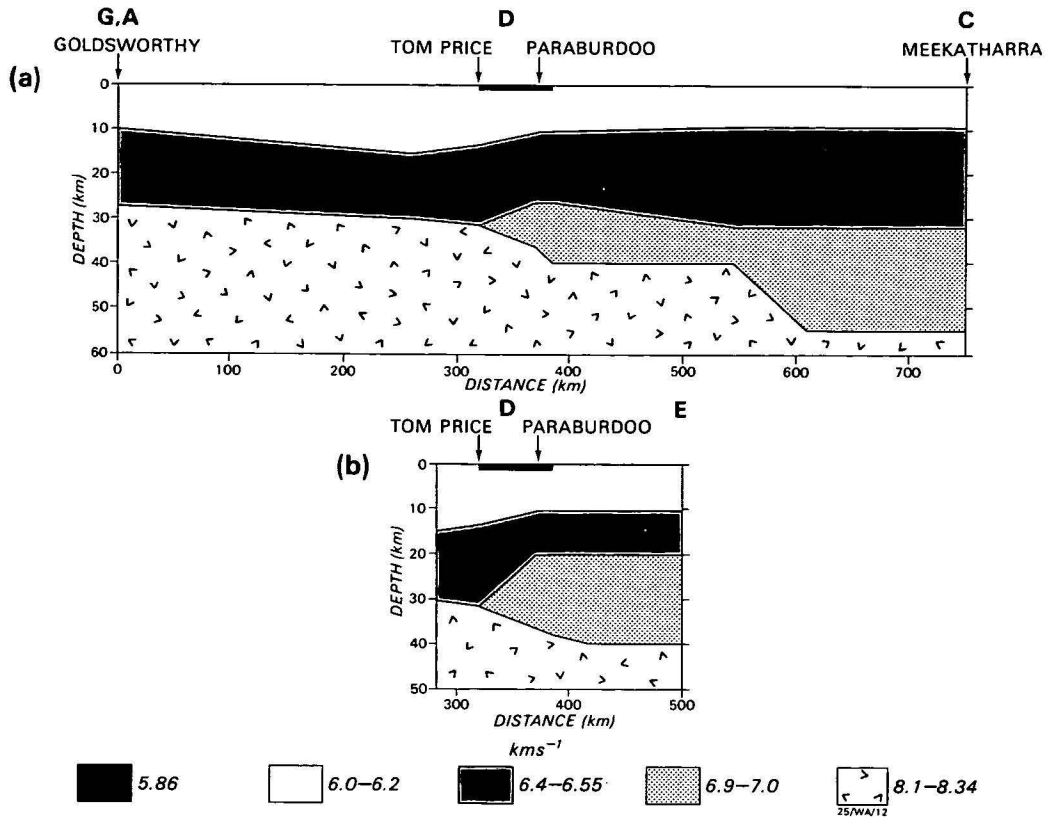

Figure 7. Seismic model for lines GDC and DE.
Figure 7a is the model for line GDC, and Figure 7b is the model for line DE.

LINE GD (Goldsworthy, Shay Gap and Sunrise Hill to Tom Price and Paraburdoo)

	Goldsworthy southwards		*Shay Gap & Sunrise Hill southwards*		*Tom Price northwards*		*Paraburdoo northwards*	
	V	*ti*	*V*	*ti*	*V*	*ti*	*V*	*ti*
P_2							6.19	0.0
Pg	6.11	0.0	6.15	0.0	6.10			
P*	6.36	1.0			6.55	1.6	6.54	1.2
Pn	8.13	5.5			8.23	6.2	8.23	6.2

LINE DE (Tom Price and Paraburdoo southwards)

	Tom Price southwards		*Paraburdoo southwards*	
	V	*ti*	*V*	*ti*
P_2	6.25	0.0		
Pg				
P*			6.25	1.2
Pn				

LINE DC (Tom Price and Paraburdoo to Meekatharra)

	Tom Price southwards		*Paraburdoo southwards*		*Meekatharra northwards*	
	V	*ti*	*V*	*ti*	*V*	*ti*
P_2						
Pg					6.13	0.0
P*	6.54	1.30	6.54	1.30	6.37	0.85
PL	6.99	3.40	6.99	3.40	7.04	4.46
Pn	7.89	6.23	7.89	6.80	8.17	10.15[1]
					8.12	8.70[2]

[1] Later arrivals between 120-180 km.
[2] First arrivals beyond 180 km.

Table 1. Velocities (km s^{-1}) and intercepts (seconds) scaled from record sections (Figures 4, 5 & 6).

7) is at 130 km, but the clearest P^L phases are observed between 80 and 100 km. The P^L cusp is also closer to the blast than the model would predict in Figure 6b, the southwards record section of Paraburdoo blasts. This may imply that the lower crustal, 7.0 km s^{-1}, layer should be shallower in the model. Pn is not clear in Figure 6b.

The record section for shotpoint C at Meekatharra is shown in Figure 6c. The Pg phase is weak, but it is neverthless clear on large scale plots. The P^L cusp is clearer on the lower gain records, and the P^M phase is not as clear as it is for the same shotpoint along line CB towards Newman (Drummond, 1979b). Pn is observed clearly on only two traces—those at 265 and 350 km.

The data from Figure 4 were interpreted by taking reciprocal pairs of refracted phases between Goldsworthy and Tom Price (GD), and inverting them, using the intercept method, for refractor depths. velocities, and dips. The data from line DE are unreversed, and were interpreted by assuming that the layers were horizontal and that the apparent velocities were refractor velocities. The Pn delays at distances beyond 250 km in Figure 6a imply structures on the crust/mantle boundary; the boundaries between the layers and the crust/mantle boundary at either end of line from Tom Price to Meekatharra (DC) were assumed to be horizontal and the velocities to be the refractor velocities. The models from these various lines were then combined. The calculated depths were assumed to apply only beyond the offset distances to the refractors, and the composite models were then adjusted using ray tracing so that the final models (Figure 7) satisfied the travel-time data.

Figure 7a depicts the preferred model for line GDC (Goldsworthy-Tom Price-Meekatharra) and Figure 7b the preferred model for line DE (Tom Price towards the SW).

The upper crustal velocity along the profile is 6.0-6.1 km s^{-1}. In the centre of the profile, near Tom Price (D), a thin, high-velocity, near-surface layer corresponds to the Hamersley Basin rocks. It has been modelled as 1 km thick, but it may be thicker. Assessment of the thickness of such layers is difficult with ray tracing alone, and further modelling with synthetic seismograms is required. A lower crustal layer, with velocities of 6.37-6.55 km s^{-1} is present along the profile. It is 10 km deep under shotpoint G at Goldsworthy, deepens to 15 km about 260 km south of G, but then shallows again to 10 km between Tom Price and Meekatharra (DC). An even deeper crustal layer, with a velocity of 6.7-7.0 km s^{-1} is present along DC. It is 10 km thick south of Tom Price (D), and thickens rapidly in the centre of the line, to be 20-25 km thick under Meekatharra (C). The interpreted upper mantle velocity along the Goldsworthy-Tom Price-Meekatharra line varies between 8.0 and 8.2 km s^{-1}. The crust/mantle boundary is 28 km deep under Goldsworthy, deepens steadily to 31.5 km under Tom Price, and then rapidly to 40 km, and then to 55 km southwards towards Meekatharra.

The model for line DE (Figure 7b) is similar to the equivalent part of line DC to the east, except that the lowermost, 6.98 km s^{-1}, crustal layer is thicker. This may not be significant, because the seismic line is unreversed.

Line FG (Pannawonica-Goldsworthy)

Only 15 stations were installed along line FG. The data are shown in Figure 8. The recorders were set up along the northeastern half of the line, but not all operated successfully, and consequently, it is not possible to interpret the data with any degree of confidence. The model adopted for the line is shown in Figure 9 and was derived by taking the refractor depths under Pannawonica (F) from line FDG (Figure 3), and those under Goldsworthy (G) from line GDC (Figure 7), and assuming that the refractors were plane layered between F and G. The velocities used were averages of those from the northern part of line GDC (Figure 7) and the western part of line FDB (Figure 3). The travel-time curves for the model were then derived by computer ray tracing, and are superimposed on the record sections. They are generally consistent with the observed data, so the model in Figure 9 is taken to be the best available for the line between Pannawonica and Goldsworthy.

Accuracy of the models

The refracted travel-time branches for the models in Figure 7 fit the observed data to within 0.1 to 0.2 s, thereby implying an accuracy of one or, perhaps, two kilometres in the calculated refractor depths. However, greater errors may be caused by assuming that the refractor velocities are constant through the layers.

Berry (1971) showed that errors of up to 20% can arise in the refractor depths, owing to use of oversimple velocity/depth functions, such as those used here, where the velocity is assumed constant through each refractor and the boundaries between the layers are sharp. Drummond (1979b) suggested, on the basis of a study of reflected travel-time branches, that the crust/mantle boundary of the Pilbara Craton was transitional, and this may be so for the other boundaries as well. Consequently, the refractor depths from this study are probably minimum values. This should be considered when the refractor depths are quoted in the ensuing discussion. It should be noted, however, that the under-estimate of refractor depth probably applies to all profiles, so that the relative thicknesses are maintained from one area to another.

Discussion

The models from all the seismic lines are combined as a fence diagram in Figure 10. The refractor depths generally agree at the junction of the profiles within the accuracy of the modelling. Figure 11 depicts the interpretation of the seismic models in terms of the geology .

Pilbara Craton

The Pilbara Craton is 28 km thick in the north and 30-33 km thick in the south, where its boundary with the Capricorn Orogen is interpreted as the zone where the crust thickens sharply to the south. This is about 40 km to the south of the Sylvania Dome in the east, and corresponds to the northern boundary of the Ashburton Trough in the west. The crust/mantle boundary under the craton, therefore, has a dip of slightly less than one degree to the south. The dip is observed on all profiles except FDP, which lies approximately east/west and on which there is no significant dip from the west on the crust/mantle boundary.

An intracrustal boundary is indicated by the increase of seismic velocities from between 6.0-6.2 km to 6.4-6.55 km s^{-1} within the Pilbara Craton. The depth to the boundary varies throughout the region. Drummond (1979b) modelled it as 13 km deep under the eastern Pilbara Craton, but suggested that it could dip from 9 km in the north to 14 km in the south. The latter values are more in agreement with the depths from the central Pilbara Craton (Figure 7a), where the boundary dips from 10 km in the north to 15 km to the north of Tom Price. It shallows to the south of Newman in the east (Figure 2) and between Tom Price and Paraburdoo (Figure 7a). Along the southern edge of the craton, it is deepest betwen Newman and Tom Price, shallows to 7 km to the west of Tom Price, and then deepens again to 11 km in the west (Figure 3).

Southwards across the Pilbara Craton, the top of the intracrustal boundary defines a basin-like structure with a general southeast/northwest axis. The basin cuts the seismic profiles west of Newman and north of Tom Price. The basin-like structure corresponds to the

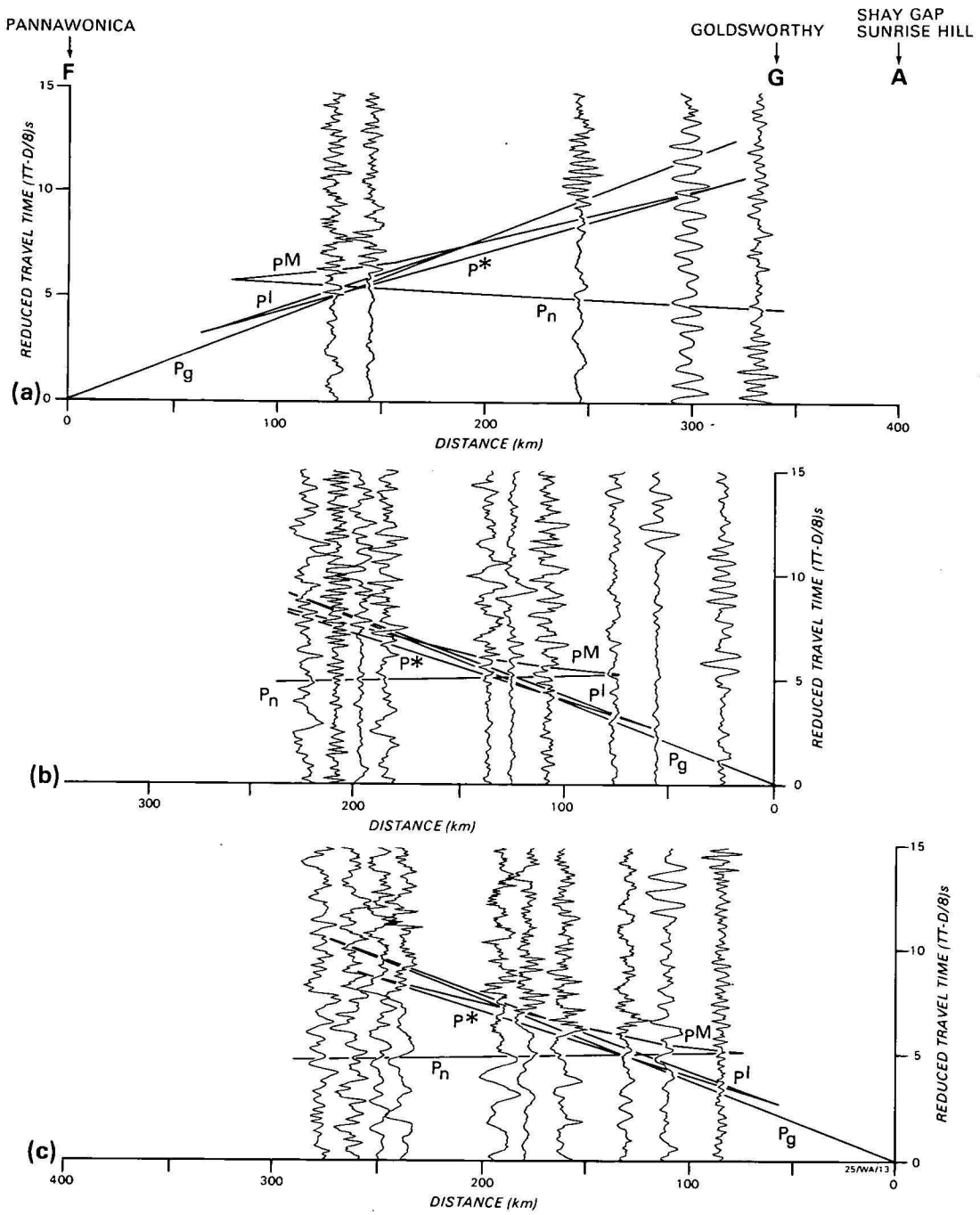

Figure 8. Record sections from line FG.
Sections a, b and c are for shotpoint F northeast, G southwest, and A southwest respectively. The superimposed travel-time curves are for the model in Figure 9. The trace amplitudes have been normalised as in Figure 6. For some recorders, one of the horizontal components had clearer arrivals than the vertical component and has been plotted in its place.

deepest part of the Hamersley Basin inferred from Trendall's (1975) isopach maps and structural diagrams. Horwitz & Smith (1978) defined an Archaean ridge along the southern edge of the Pilbara Craton which corresponds to the shallowing of the intracrustal boundary south of Newman and south and west of Tom Price.

The highest velocities (6.55 km s^{-1}) observed below the intracrustal boundary occur along the southern basement ridge and the axis of the Hamersley Basin. These velocities are due to higher metamorphic grades in the lowermost crust, caused by the depression of the crust into higher pressure and temperature regimes during the formation of the Hamersley Basin (Drummond & others, 1981). Uplift occurred after the filling of the Hamersley Basin, and can be divided into two types, regional isostatic rebound and localised diapirism of basement rocks.

Regional isostatic rebound followed the filling of the basin. This can be inferred from the exposure at the surface of some of the stratigraphically lowest members of the Hamersley Basin sequence. As well, R. E. Smith & others (personal communication) used the metamorphic grades mapped at surface exposures to estimate uplifts of 10-12 km, west of Tom Price, and 5-7 km, near Newman. The second type of uplift was localised

diapirism of basement rocks to form Archean inliers within the Hamersley Basin. The largest of these is the Sylvania Dome, but several smaller ones are observed or inferred to the west and east of Tom Price. Those near Tom Price correspond to the region where the intracrustal boundary shallows to 7 km depth along profile FDB (Figures 3 and 10).

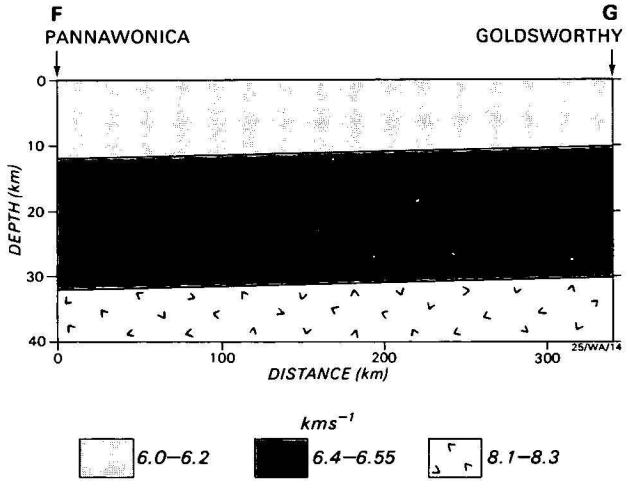

Figure 9. Seismic model for line FD.
The model was not derived from the data in Figure 8, but is an average of the models for the northern end of line GD and the western end of line FD (see the text).

The diapirism may have been caused by density inversions near the surface. Where rocks of the Hamersley Basin are seismically distinct from the underlying basement rocks, they have velocities which are higher than those of the basement. They are highest in the southeast of the basin. Further west and north, the velocities of the P_1 and P_2 wavegroups decrease as the metamorphic grade decreases (Drummond & others, 1981), and the basin rocks have not achieved sufficiently high velocities to be seen to be independent of the underlying Archaean basement. Gravity data also infer that the Hamersley Basin rocks are denser than the Archaean basement (Drummond & Shelley, 1981).

Yilgarn Craton

The crust of the Yilgarn Craton is much thicker (> 50 km) than the crust of the Pilbara Craton, and extends further north than the area mapped by Gee (1979a) as the Yilgarn Block. Intracrustal seismic boundaries occur at 10-16 km and at 32 km depth.

In the Proterozoic, the northern limit of the stable Yilgarn Craton was probably just south of the present day northern edge of the Nabberu Basin. A zone along the northern edge of the Yilgarn Craton, where the crustal thickness is intermediate between that of the Yilgarn Craton and the thinner crust of the Capricorn Orogen, probably represents part of the northern Yilgarn Craton which was reworked by tectonism in the Proterozoic. It corresponds to a large, negative gravity anomaly to the north of the Yilgarn Block. Fraser (1973) suggested that the anomaly was too intense to

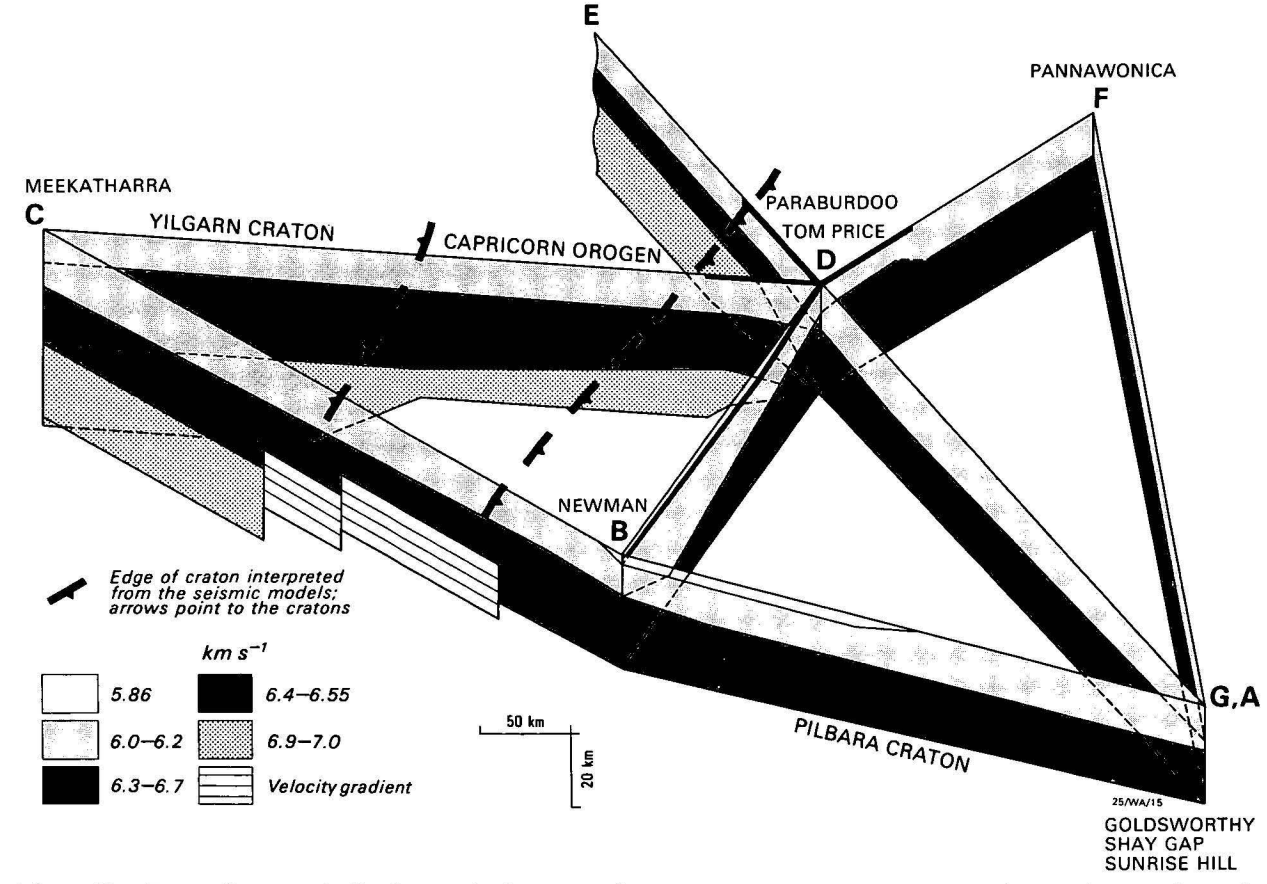

Figure 10. Fence diagram of all of the seismic models from the Intercept Method interpretation of the data from the 1977 Pilbara Crustal Survey.
The interpreted margins of the cratons are based on crustal thicknesses. The edge of the Pilbara Craton corresponds to the southern margin of thin crust, and the northern edge of the Yilgarn Craton corresponds to the northern margin of thick crust. The Capricorn Orogen between the cratons has crust of intermediate thickness.

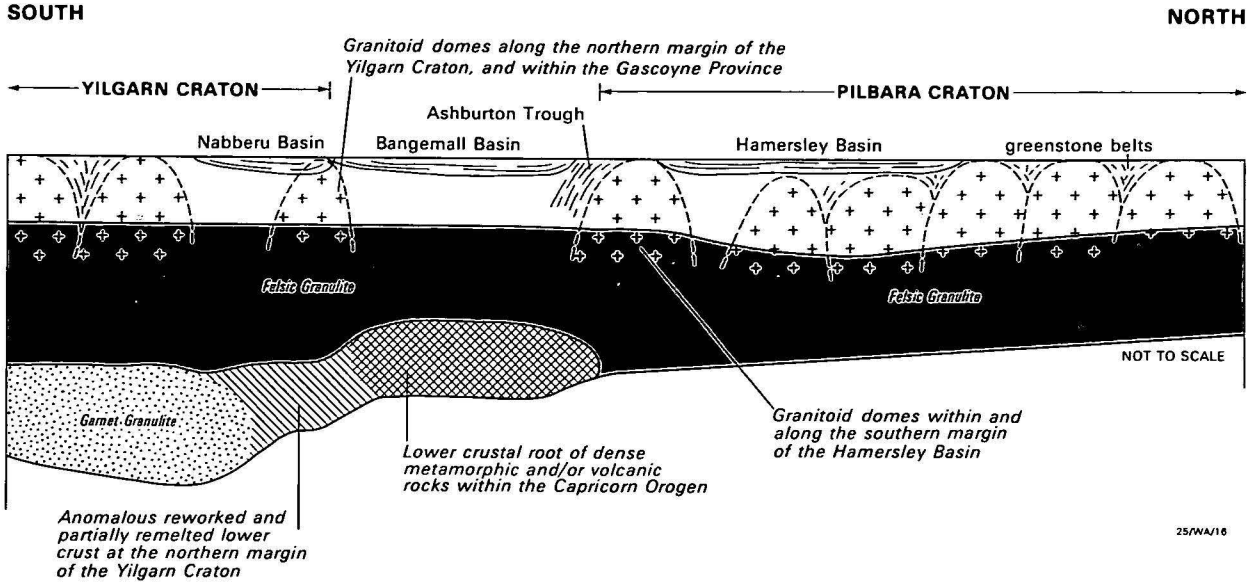

Figure 11. Cartoon sketch of a north/south section of crust through the survey area, in which the seismic models are interpreted in terms of the geology.

be purely a gravity edge effect of the Yilgarn Craton, and Horwitz & Smith (1978) correlated it with 'certain granitic and metamorphic rocks of the Gascoyne Province'.

The area contains, in the Gascoyne Province, granitoid intrusions, which have been interpreted as remelted basement and younger sediments (de Laeter, 1976; Williams & others, 1978), and, further east, the Marymia Dome at the northern edge of the Nabberu Basin. It also includes the northwestern part of the Nabberu Basin, where the sedimentary rocks and underlying basement were intensely deformed (Hall & Goode, 1978). The southern belt of stable basement in the western Bangemall Basin falls within and marks the northern limit of this zone.

Capricorn Orogen

No shotpoints were located in the Bangemall Basin or Ashburton Trough, and because the basin and trough rocks do not cause any noticebale deviation of the travel-times from those expected from normal crystalline basement, no estimate of the present day basin and trough thicknesses is possible.

The lower crust in the Capricorn Orogen is characterised by high velocities and, by inference, dense rocks. Wellman (1978) attributed the denser crust in the orogen to higher metamorphic grades. Horwitz & Smith (1978) favoured an evolutionary model for the orogen, in which the Pilbara and Yilgarn Cratons were welded into a stable basement by the end of the Archaean and then rifted to form the Capricorn Orogen. From the gravity map (BMR, 1975), they inferred dense lower crust in the orogen, and attributed it to intrusions of basic magmas into the lower crust during the rifting. However, the intrusions could also have occurred if the cratons had not been welded, but had been free to move relative to each other to relieve the stresses which must have built up during tectonism.

Chemical composition of the crust

The seismic velocities in the upper crust throughout the region, excluding those in the Hamersley Basin, range from 6.0 to 6.2 km s^{-1}. Drummond (1979b) suggested that they represent an upper crust of overall acid to intermediate chemical composition and low metamorphic grade. Below the intracrustal boundary at 9-16 km depth throughout the region, the seismic velocity increases to 6.4 km s^{-1}, and 6.55 km s^{-1} under the axis of the Hamersley Basin. Drummond (1979b) attributed the increase in velocity to the metamorphism of the acid to intermediate crust to felsic granulite. A chemical change was ruled out, because more basic rocks would have higher seismic velocities (Christensen & Fountain, 1975).

Underlying the felsic granulite layer at 32 km depth along the northern Yilgarn Craton is the thick, lower crustal layer with seismic velocities of 6.7-7.0 km s^{-1}. Drummond (1979b) suggested that this layer was caused by 'eclogite'-grade metamorphism of rocks with compositions similar to or slightly more basic than the upper crust. Drummond & others (1981) called it, perhaps less ambiguously, garnet granulite. Garnet granulites of acid to intermediate chemical composition readily give seismic velocities of about 7 km s^{-1} at depths greater than 30 km (pressures greater than 10 kbar). Basic garnet granulites often have much higher seismic velocities, and eclogite velocities at pressures of 10 kbar can exceed 8.00 km s^{-1} (Birch, 1961; Christensen, 1965; Manghnani & others, 1974; Christensen & Fountain, 1975). However, Drummond & Shelley (1981) combined the seismic and gravity data, and suggested that some chemical layering was possible in the Yilgarn Craton, with the lower crust more basic than the upper crust.

Acknowledgements

The BMR is indebted to the iron mining companies of the Pilbara, without whose support the seismic survey would not have peen possible. I acknowledge the generous assistance of Goldsworthy Mining Limited, Cliffs Robe River Associates, Hamersley Iron Pty Ltd, and the Mount Newman Mining Company Pty Ltd.

I am grateful to my colleagues at the BMR who assisted in the field work, and also made useful suggestions during the interpretation; in particular, I thank D. M. Finlayson, P. Wellman, J. B. Connelly, J. W. Williams, and especially C. D. N. Collins who made his ray tracing program SEISRAY available to me. The interpretation was performed while I was a full time

postgraduate research scholar at the Research School of Earth Sciences at the Australian National University, and was supervised by Dr K. J. Muirhead. Dr A. L. Hales of the Geosciences Program, University of Texas at Dallas, and formerly Director of the Research School of Earth Sciences, generously made available the ANU data, and, together with Dr J. Cleary, offered useful advice. The postgraduate research was supported by an Australian Public Service Postgraduate Scholarship.

References

BERRY, M. J., 1971—Depth uncertainties from seismic first-arrival refraction studies. *Journal of Geophysical Research,* 76, 6464-8.

BIRCH, F., 1961—The velocity of compressional waves in rocks to 10 kilobars, Part 2. *Journal of Geophysical Research,* 66, 2199-224.

BMR, 1975—Gravity map of Australia, 1:5 000 000. *Bureau of Mineral Resources, Australia, Canberra.*

BRAKEL, A. T., & MUHLING, P. C., 1976—Stratigraphy, sedimentation, and structure in the western and central part of the Bangemall Basin, Western Australia. *Geological Survey of Western Australia Annual Report,* 1975, 70-9.

CHRISTENSEN, N. I., 1965—Compressional wave velocities in metamorphic rocks at pressures to 10 kilobars. *Journal of Geophysical Research,* 70, 6147-64.

CHRISTENSEN, N. I., & FOUNTAIN, D. M., 1975—Constitution of the lower continental crust based on experimental studies of seismic velocities in granulite. *Bulletin of the Geological Society of America,* 86, 227-36.

COMPSTON, W., & ARRIENS, P. A., 1968—The Precambrian geochronology of Australia. *Canadian Journal of Earth Sciences,* 5, 561-83.

DANIELS, J. L., 1975—Gascoyne Province. *In* Geology of Western Australia. *Geological Survey of Western Australia, Memoir* 2, 107-14.

DE LAETER, J. R., 1976—Rb-Sr whole-rock and mineral ages from the Gascoyne Province. *Geological Survey of Western Australia Annual Report,* 1975, 126-30.

DE LAETER, J. R., & BLOCKLEY, J. G., 1972—Granite ages within the Archaean Pilbara Block, Western Australia. *Journal of the Geological Society of Australia,* 19, 363-70.

DE LAETER, J. R., LIBBY, W. G., TRENDALL, A. F., & FLETCHER, I. R., 1980—The older Precambrian geochronology of Western Australia. *In* GLOVER, J. E., & GROVES, D. I. (editors), *Second International Archaean Symposium, Perth, 1980. Extended Abstracts. Geological Society of Australia and I.G.C.P., Archaean Geochemistry Project,* 9-10.

DE LAETER, J. R., LIBBY, W. G., & TRENDALL, A. F., 1981—The older Precambrian geochronology of Western Australia. *In* GLOVER, J. E., & GROVES, D. I. (editors), Archaean Geology. *Second International Archaean Symposium. Geological Society of Australia, Special Publication,* 7, in press.

DRUMMOND, B. J., 1979a—Pilbara Crustal Survey, 1977—Operational Report. *Bureau of Mineral Resources, Australia, Record,* 1979/54 (unpublished).

DRUMMOND, B. J., 1979b—A crustal profile across the Archaean Pilbara and northern Yilgarn Cratons, northwest Australia. *BMR Journal of Australian Geology & Geophysics,* 4, 171-80.

DRUMMOND, B. J., 1979c—Structural relations between the Archaean Pilbara and Yilgarn Cratons, Western Australia, from deep seismic sounding. *M.Sc. Thesis, Australian National University* (unpublished).

DRUMMOND, B. J., & SHELLEY, H. M., 1981—Isotasy and structure of the lower crust and upper mantle in the Precambrian terrains of northwest Australia, from regional gravity studies. *BMR Journal of Australian Geology & Geophysics,* 6, this issue.

DRUMMOND, B. J., SMITH, R. E., & HORWITZ, R. C., 1981—Crustal structure in the Pilbara and northern Yilgarn Blocks from deep seismic sounding. *In* GLOVER, J. E., & GROVES, D. I. (editors) Archaean Geology. *Second International Archaean Symposium. Geological Society of Australia Special Publication,* 7, in press.

DRUMMOND, B. J., MUIRHEAD, K. J., & HALES, A. L., in prep.—Evidence for a seismic discontinuity near 200 km under a continental margin.

FRASER, A. R., 1973—A discussion on the gravity anomalies of the Precambrian Shield of Western Australia. *Bureau of Mineral Resources, Australia, Record,* 1973/105 (unpublished).

GEE, R. D. (compiler), 1979a—Geological map of Western Australia, 1:2 500 000 scale. *Geological Survey of Western Australia, Perth.*

GEE, R. D., 1979b—The geology of the Peak Hill area. *Western Australia Department of Mines Annual Report,* 1978, 99-106.

GEE, R. D., 1979c—Tectonics of the Western Australian shield. *Tectonophysics,* 50, 327-69.

GIESE, P., 1976—Models of crustal structure and main wave groups. *In* GIESE, P., PRODEHL, C., & STEIN, A. (editors), Explosion seismology in Central Europe. Data and results. Crustal and upper mantle structure in Europe. *European Seismological Commission, Monograph,* 1, 196-200.

HALL, W. D. M., & GOODE, A. D. T., 1978—The early Proterozoic Nabberu Basin and associated iron formations of Western Australia. *Precambrian Research,* 7, 129-84.

HAMILTON, P. J., EVENSEN, N. M., O'NIONS, R. K., GLIKSON, A. Y., & HICKMAN, A. H., 1980—Sm-Nd dating of the Talga-Talga Subgroup, Warrawoona Group, Pilbara Block, Western Australia. *In* GLOVER, J. E., & GROVES, D. I. (editors), *Second International Archaean Symposium Perth, 1980. Extended Abstracts. Geological Society of Australia and I.G.C.P., Archaean Geochemistry Project,* 11-12.

HORWITZ, R. C., 1975—Provisional geological map at 1:2 500 000 of the northeast margin of the Yilgarn Block, Western Australia. *CSIRO Minerals Research Laboratories, Report,* FP 10.

HORWITZ, R. C., & SMITH, R. E., 1978—Bridging the Yilgarn and Pilbara Blocks, Western Australia. *Precambrian Research,* 6, 293-322.

MANGHNANI, M. H., RAMANANTOANDRO, R., & CLARK, S. P., 1974—Compressional and shear wave velocities in granulite facies rocks and eclogites to 10 kbar. *Journal of Geophysical Research,* 79, 5427-46.

MOTA, L., 1954—Determination of the dips and depths of geological layers by the seismic refraction method. *Geophysics,* 19, 242-54.

OVERSBY, V. M., 1975—Lead isotopic systematics and ages of Archaean acid intrusives in the Kalgoorlie-Norseman area, Western Australia. *Geochimica et Cosmochimica Acta,* 39, 1107-25.

PIDGEON, R. T., 1978a—3450 m.y. old volcanics in the Archaean layered greenstone succession of the Pilbara Block, Western Australia. *Earth and Planetary Science Letters,* 37, 421-8.

PIDGEON, R. T., 1978b—Geochronological investigations of granite batholiths of the Archaean granite-greenstone terrain of the Pilbara Block, Western Australia. *In* SMITH, I. E. M., & WILLIAMS, J. G. (editors), *Proceedings of the 1978 Archaean Geochemistry Conference, University of Toronto,* 360-2.

RICHARDS, J. R., 1977—Lead isotopes and ages of galenas from the Pilbara region, Western Australia. *Journal of the Geological Society of Australia,* 24, 465-73.

TRENDALL, A. F., 1975—Hamersley Basin. *In* Geology of Western Australia. *Geological Survey of Western Australia, Memoir* 2, 119-43.

WELLMAN, P., 1978—Gravity evidence for abrupt changes in mean crustal density at the junction of Australian crustal blocks. *BMR Journal of Australian Geology & Geophysics,* 3, 153-62.

WILLIAMS, S. J., ELIAS, M., & DE LAETER, J. R., 1978—Geochronology and evolution of the eastern Gascoyne Province and the adjacent Yilgarn Block. *Geological Survey of Western Australia Annual Report,* 1977, 50-6.

WILLIAMS, S. J., WILLIAMS, I. R., & CHIN, R. J., 1979—Explanatory notes on the Mount Phillips 1:250 000 geological sheet. *Geological Survey of Western Australia, Record* 1978/13.

BMR Journal of Australian Geology & Geophysics, 6, 1981, 137-143

Isostasy and structure of the lower crust and upper mantle in the Precambrian terrains of northwest Australia, from regional gravity studies

B. J. Drummond & H. M. Shelley

Published seismic models for the northwest region of Australia are somewhat at variance with proposed isostatic models for the region. Two density models are examined to explain the difference. In one, the thick, low-density crust of the Yilgarn Craton is compensated at depth by a region of high-density upper mantle rocks, and in the other the composition of the Yilgarn Craton is slightly more iron rich (either at the base or to a lesser extent throughout) than the crust of the Pilbara Craton. A compromise model is preferred in which the crust, particularly in the Yilgarn Craton, is chemically stratified with the denser, more basic rocks at the base. In this model the upper mantle under the Yilgarn Craton is denser than that under the Pilbara Craton and isostatic equilibrium is reached at depths greater than the base of the crust.

The differences in the crust or the mantle throughout the region provide more evidence that the cratons had separate evolutionary histories. The upper mantle under the Pilbara Craton may be less dense than that under the Yilgarn Craton because of iron depletion, and may have been the source of iron for the basic volcanics and banded iron formations in the Hamersley Basin, which overlies the Pilbara Craton.

Introduction

Two Archaean cratons, the Pilbara and Yilgarn Cratons, crop out in Western Australia (Gee, 1979a); their outcrop areas in the northwest part of the State are shown in Figure 1 of Drummond (1981, this issue). Following Gee (1979b), a 'block' is taken as the exposed part of a stabilised 'craton'. Brief summaries of the geology are given by Drummond (1979c, 1981) and comprehensive descriptions can be found in Gee (1979b) and GSWA (1975).

The blocks have large granitoid domes between which greenstone belts of sedimentary and volcanic rocks are draped. Sedimentary and volcanic rocks of the late Archaean to lower Proterozoic Hamersley Basin cover the southern part of the Pilbara Craton, except for small Archaean inliers within the basin, e.g. the Sylvania Dome. The northern part of the Yilgarn Craton is overlain by the Proterozoic sedimentary and volcanic rocks of the Nabberu Basin (Hall & Goode, 1978; Gee, 1979b). These, and the younger Proterozoic rocks of the Ashburton Trough and Bangemall Basin, which occupy the Capricorn Orogenic Belt, mask the structural relations between the cratons.

A seismic refraction and gravity survey conducted in 1977 (Drummond, 1979a) aimed to study the structural relations between the cratons by delineating the crustal structure within and between the cratons. In the seismic models of Drummond (1981), the crust of the Pilbara Craton varies between 28 km thick in the north and 33 km thick in the south. In contrast, the northern Yilgarn Craton has a crust between 50 and 55 km thick, and the crust in the intervening Capricorn Orogenic Belt is 40 km thick. A zone with crustal thickness intermediate between that of the Yilgarn Craton and the crust of the Capricorn province lies along the northern edge of the Yilgarn Craton and contains evidence for remelting of the crust and tectonic activity in the Proterozoic.

The velocity in the upper crust is 6.0–6.2 km.s^{-1}, and increases to 6.4–6.55 km.s^{-1} at 10 to 16 km depth throughout the region, and to 6.7–7.0 km.s^{-1} at 32 km depth in the Yilgarn Craton. Drummond (1981) proposed that the velocity increase with depth was due to increasing metamorphic grade related to the increasing pressure and temperature with depth.

The gravity coverage of the area consists of data from regional helicopter gravity surveys with an 11-km grid spacing (Fraser, 1979a, b), some detailed mining company data, and road and helicopter traverses with station spacing of 1–4 km (McCracken, *in* Drummond, 1979a). The Bouguer anomaly gravity map for the region is shown in Figure 1.

Fraser (1979a,b) gave a qualitative description of the short wavelength features of the gravity field. Over the Pilbara Block, gravity highs correlate with greenstone belts and gravity lows with granitoid intrusions. In the Hamersley Basin, gravity lows correlate with granitic Archaean inliers (a, b, c, d, in Figure 1) and anticlines with granitic cores in the Hamersley Basin strata; gravity highs correlate with synclines in the dense basin strata (Fraser, 1979a). Similar correlations can be made in the Yilgarn Craton and Nabberu Basin.

Gravity highs and lows of longer wavelength ring the cratons. Wellman (1978) suggested that they reflect abrupt changes in average crustal density between crustal blocks, and their regional isostatic compensation.

The purpose of this paper is to compare the theoretical gravity signature of the seismic models with the measured gravity field, and, from this, draw conclusions about isostatic compensation and the composition and structure of the lower crust and upper mantle of the region. Some conclusions are then drawn about the evolutionary processes which generated the crust.

Pressure calculations

Wellman (1976) showed that, for Western Australia, isostatic compensation was mainly complete at the base of the crust for 3° x 3° areas. Using the Nafe-Drake velocity/density relationship (*in* Talwani & others, 1959a) (Fig. 2), pressures for unit columns of rock at 52 km depth are 1.59, 1.54, and 1.51 GPa in the northern Pilbara Craton, southern Pilbara Craton, and northern Yilgarn Craton, respectively, for model (a) of Drummond (1979c). These pressures agree with

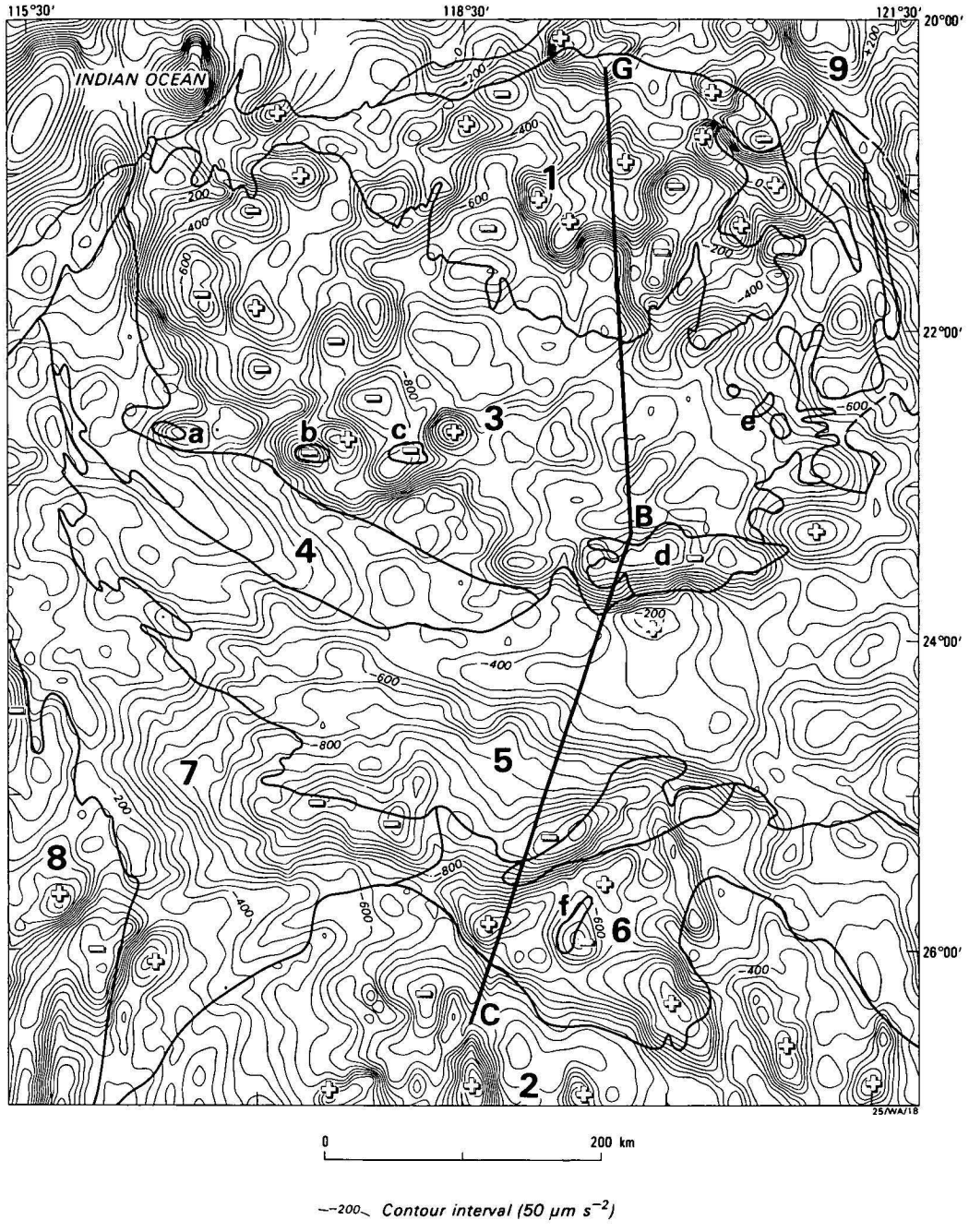

Figure 1. Simple Bouguer gravity map (Bouguer density 2.67 t.m^{-3}) onshore and Free-air gravity map offshore, with geology superimposed. The geological provinces are: 1. Pilbara Block; 2. Yilgarn Block; 3. Hamersley Basin; 4. Ashburton Trough; 5. Bangemall Basin; 6. Nabberu Basin; 7. Gascoyne Province; 8. Carnarvon Basin; and 9. Canning Basin.
The Archaean domes marked in the Proterozoic basins are: a. Wyloo Dome; b. Rocklea Dome; c. Milli Milli Dome; d. Sylvania Dome; e. Rat Hill Anticline; f. Goodwin Dome; and g. Marymia Dome. G. Goldsworthy; B. Newman; C. Meekatharra.

each other to within 5 percent, but the differences between them would result in gravity decreasing by more than 3000 μm.s^{-2} from the northern Pilbara Craton southwards to the northern Yilgarn Craton. The measured decrease is only about 800 μm.s^{-1}, with regional Bouguer anomaly values ranging from about 0 μm.s^{-2} in the north to about 800 μm.s^{-2} in the south. This leaves a discrepancy of about 2000 μm.s^{-2} between the measured gravity and the gravity expected from the seismic model.

The seismic velocity structure in the upper 32 km of the Yilgarn Craton is similar to that of the Pilbara Craton. The differences below 32 km produce a mass deficiency, which generates the gravity difference along the profile. Seismic intercept times for upper mantle P-waves from shotpoints at Newman and Meekatharra, delays in upper mantle P-wave arrivals south of Newman and Tom Price, travel-times northwards and southwards from Meekatharra, and travel-time residuals for teleseismic arrivals from Fiji and the Indonesian Arc all indicate that the crust must thicken considerably between Newman and Meekatharra (Drummond, 1979b, c, 1981; Drummond & others, in prep.). However, the intercept time for upper mantle P-waves from

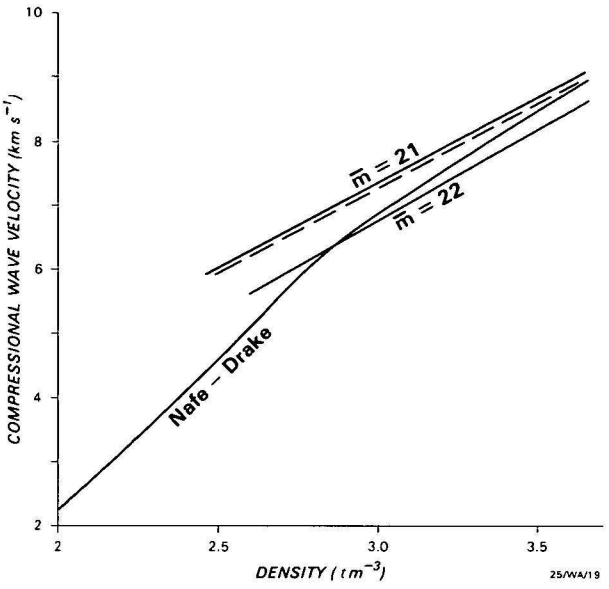

Figure 2. Velocity/density curves of Nafe-Drake (*in* Talwani & others, 1959a) and Manghnani & others (1974) for mean atomic weights of 21 and 22. The dashed line was adopted for the Pilbara Craton.

the blast at Meekatharra recorded southwards is much less than that for similar phases recorded northwards (Drummond, 1979c). This implies that the crust thins south of Meekatharra.

Drummond (1979c, 1981) interpreted seismic first-order velocity discontinuities at all boundaries within the crust. It was recognised that this was probably an oversimplification, and that the velocity and, consequently, density were likely to increase within the crustal layers, and boundaries, especially the crust/mantle boundary, were likely to be transitional. Prodehl (1977) compared the velocity structures under numerous geological provinces in the USA, Europe, Scandinavia, and the Ukraine, and concluded that crust 40–60 km thick is characterised by medium to high seismic velocities and transitional crust/mantle boundaries, and that crust less than 35 km thick is characterised by low seismic velocities and sharper crust/mantle boundaries. If these generalisations are valid, the vertical density gradients should be more prevalent through the thick crust of the Yilgarn Craton than through the thin crust of the Pilbara Craton. Consequently, the density in the lowermost Yilgarn Craton is probably higher than the simple structure described by Drummond (1979c, 1981). However, the effects of this are offset somewhat by the effects that the velocity gradients would have on the depths of the interfaces. Berry (1971) showed that it could be necessary to increase the depths of interfaces by up to 20 percent to account for velocity gradients, and this would regenerate the gravity discrepancy.

The seismic model, based on the available data, stands up to the seismic tests that can be applied, and no simple inadequacies of the model can be found to overcome the mass discrepancy at the southern end of the seismic model.

Two assumptions were made above in calculating the pressure at 52 km depth at the northern and southern boundaries of the Pilbara Craton and at the northern edge of the Yilgarn Craton. The first was that isostasy was complete at the base of the crust, and the other was that a single empirical velocity/density function can be assumed for the whole region. The implications of each of these assumptions on the theoretical calculations for the gravity effect of the seismic model are discussed below.

Compensation below the crust

In the pressure calculations, isostasy was assumed to be complete at 52 km, the base of the thickest crust. However, it may only be complete at greater depths. Very little information is available about the upper mantle structure in the region. Drummond & others (1981) suggested that lateral chemical variations within the upper mantle could account for differences in the upper mantle seismic velocity observed over the Pilbara Craton, but Drummond & others (in prep.) are unable to make any conclusive statement about the structures in the upper mantle above 200 km depth.

Drummond's (1981) seismic model for line GBC (Goldsworthy-Newman-Meekatharra) was tested on the assumption that isostatic equilibrium occurred within the upper mantle. The Nafe-Drake empirical velocity/density relationship (Fig. 2) was used to convert the seismic velocity model into a density model, which is shown as gravity model A in Figure 3. The seismic model is shown for comparison. The calculated gravity profile for the model was generated using the computer program of Milson & Worthington (1977), which utilises the method of Talwani & others (1959b). The measured curve was derived from the contours of the gravity map (Fig. 1); no corrections for regional gradients (Wellman, 1976) were necessary, because the regional gradients along the profile are small compared to the precision with which the curve was fitted.

The short wavelength anomalies in the Pilbara Craton are due to near-surface features such as granitoid domes, greenstone belts, and anticlines and synclines in the Hamersley Basin rocks, and were not accommodated in the gravity model; rather, it is shown that the seismic model can quite easily be made to fit the major features of the gravity field. The general level of the gravity field decreases southwards across the Pilbara Craton. It rises more sharply across the Capricorn Orogen than the seismic model predicts; if the low density Sylvania Dome had been included in the density model, a better match would have been achieved. Note that the high-density lower-crustal layer was moved northwards 30 km relative to the seismic model to match the position of the anomaly.

The thicker crust of the Yilgarn Craton was counterbalanced by a high-density upper mantle root, which extends to 100 km depth. Many other models could have been used for the upper mantle root. The density contrast between the root under the crust of the Yilgarn Craton and the upper mantle under the Pilbara Craton is 0.14 $t.m^{-3}$. The density contrast could be made less and the root made thicker, and the model would still satisfy the measured gravity profile. In addition, if the crust thins to the south of Meekatharra, as may be the case, the root does not need to be as thick or as dense. The northern end of the root must wedge out northwards under the Capricorn Orogen. It could also be modelled as a zone of laterally gradational density contrast (Gendzwill, 1970).

The reversed upper mantle velocity under the Pilbara Craton for a north/south line is 8.34 $km.s^{-1}$ (Drummond, 1979c). Drummond & others (1981) reported

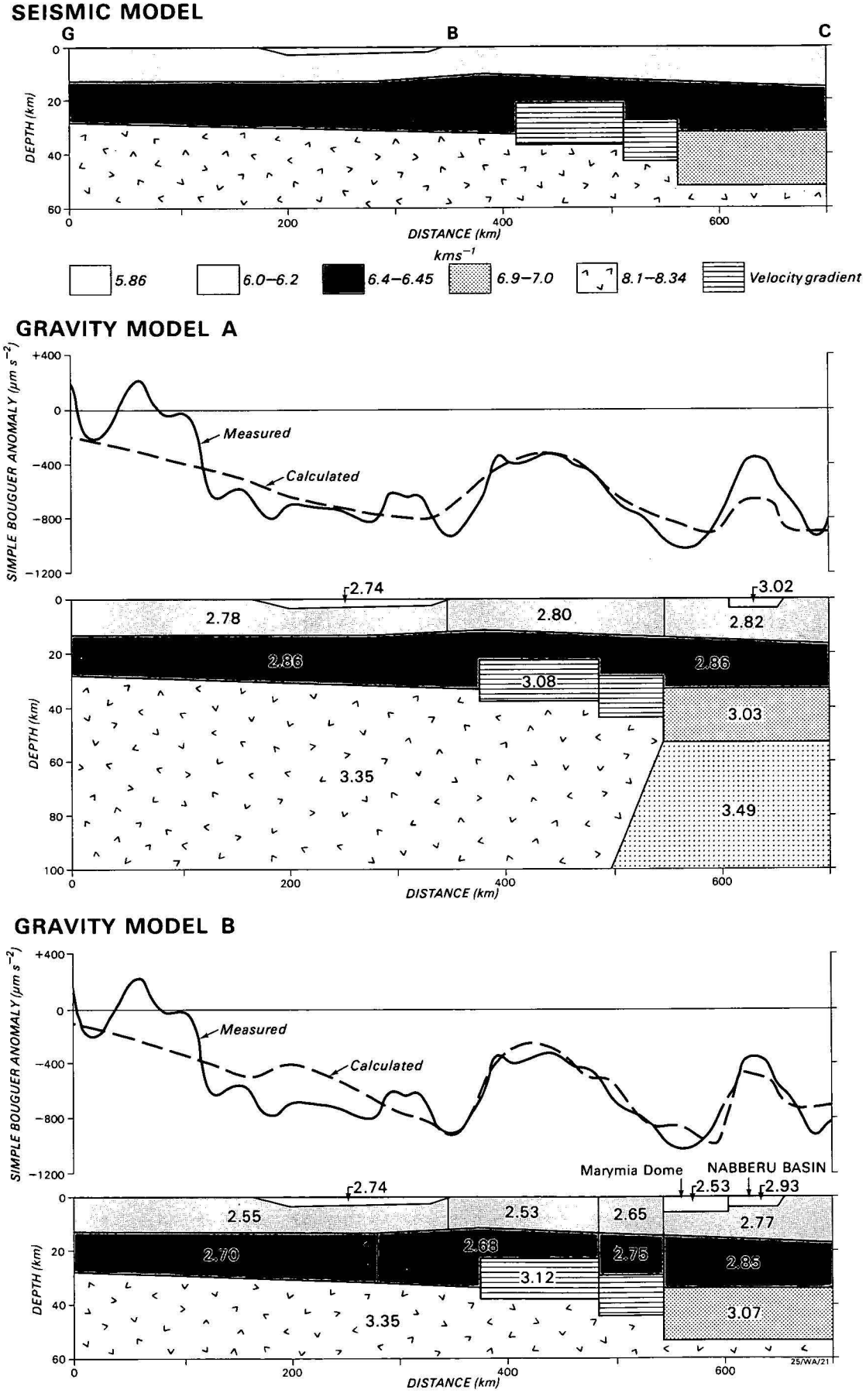
SEISMIC MODEL
G
B
C
DEPTH (km)
DISTANCE (km)
kms⁻¹
5.86
6.0–6.2
6.4–6.45
6.9–7.0
8.1–8.34
Velocity gradient
GRAVITY MODEL A
SIMPLE BOUGUER ANOMALY (μm s⁻²)
Measured
Calculated
2.74
3.02
2.78
2.80
2.82
2.86
2.86
3.08
3.03
3.35
3.49
GRAVITY MODEL B
Marymia Dome
NABBERU BASIN
2.53
2.93
2.55
2.53
2.65
2.77
2.70
2.68
2.75
2.85
3.12
3.07
3.35
25/WA/21

a reversed upper mantle Pn velocity of 7.8 km.s^{-1} along the axis of the Hamersley Basin, which lies approximately northwest/southeast. If the differences in the Pn velocity under the Pilbara Craton indicate upper mantle seismic anisotropy, an average velocity for the Pilbara Craton of 8.07 km.s^{-1} is implied.

Gregson (1978) reported the travel times from the Meekatharra shotpoint, recorded at seismological observatories southwards across the Yilgarn Craton. The unreversed velocity of the upper mantle Pn phase is 8.08 km.s^{-1} (Drummond, 1979c), and is similar to the 8.11 km.s^{-1} measured on a north/south line in the southwest Yilgarn Craton, where the east/west Pn velocity is 8.39 km.s^{-1} (Mathur, 1974). This gives a somewhat tenuous average for the upper mantle velocity under the Yilgarn Craton of 8.25 km.s^{-1}, which is greater than under the Pilbara Craton. It should be stressed that the seismic data only indicate that velocity differences could occur in the upper mantle; the present data are too few to interpret the magnitude of the difference with any confidence.

The second assumption made in calculating the pressures at 52 km depth was that one empirical velocity/density function applies throughout the survey area. Many such functions have been proposed in the past, and Dooley (1976) compared some of them. The variations in the functions are striking.

Birch (1961) defined the mean atomic weight of a rock as $\bar{m} = \Sigma(x_i/m_i)^{-1}$ where m_i and x_i are, respectively, the mean atomic weight and proportion of constituent oxide i. Most common rocks have mean atomic weights of between 20 and 22. Birch (1961) showed that the velocity/density function for rocks was dependent on their mean atomic weight. The element on which the mean atomic weight is most dependent is iron: high iron content correlates with high mean atomic weight. The variations in the published empirical velocity/density functions probably reflect variations in rock chemistry.

Manghnani & others (1974) measured the velocities and densities of 17 granulite facies and 15 eclogite facies rocks, and compared these with other published data. They derived velocity/density curves at 10 kbar (Fig. 2) which were similar to those of Birch (1961).

These curves indicate that the density of rocks, for a given seismic velocity, is dependent on the mean atomic weight—rocks with a seismic velocity of, say, 8.0 km.s^{-1} and $\bar{m} = 21$ have a lower density than those with the same velocity and $\bar{m} = 22$. If the upper mantle under the Yilgarn Craton is more iron rich than that under the Pilbara Craton, the density under the Yilgarn Craton will be higher, irrespective of whether the seismic velocity is greater under the Yilgarn Craton.

The effect of different velocity/density curves with isostatic compensation at the base of the crust

The crustal thickness varies throughout northwest Australia, so that, if isostatic equilibrium is complete at the base of the thickest crust, rather than in the upper mantle, the thin crust of the Pilbara Craton must have a lower density than the thick crust of the Yilgarn Craton. However, the seismic velocities to 32 km depth are similar throughout the region, so that the differences in density must be generated by differences in mean atomic weight.

Manghnani & others (1974) analysed the seismic velocities for the crust in the United States. They found that a mean atomic weight of 22 fitted the data from most regions, but a value of 21 was a better fit to the data from the east Basin and Range Province and the northern Colorado Plateau, which have relatively thin crusts (Prodehl, 1977), as in the Pilbara Craton. This is one example of different geological provinces having different mean atomic weights, and therefore different velocity/density functions, with the lowest values of mean atomic weight in areas of thin crust.

A second gravity model (Figure 3, model B) was therefore generated by assuming that the Pilbara and Yilgarn Cratons had different velocity/density functions. For simplicity, the differences were assumed throughout the entire crust, but the crust may be chemically stratified, with the dense, basic rocks restricted to the lower crust. The curve for $\bar{m} = 22$ in Figure 2 was used for the Yilgarn Craton, and the dashed curve was used for the Pilbara Craton. The density values between the cratons were assumed to be intermediate in value.

Corrections for the effects of pressure and temperature on the seismic velocities were made using the pressure derivative of 3×10^{-3} km.s^{-1}kbar^{-1} and the temperature derivative of -4×10^{-4} km.s^{-1}deg^{-1} of Anderson & others (1972), which were favoured by Manghnani & others (1974), and the temperature gradient for the Yilgarn Craton proposed by Jessop & Lewis (1978).

The density model (gravity model B in Figure 3) gives a good fit to the general long-wavelength features of the observed curve. As in model A, the high-density lower-crustal body between the cratons had to be extended 30 km north relative to the seismic model to match the calculated and measured gravity profiles. Note the better fit of the gravity gradient over the Capricorn Orogen compared with gravity model A. A higher density at the base of the crust was assumed than that used in model A, corresponding to a mean atomic weight of 22. A dense, shallow basin was introduced to model the gravity high over the Nabberu Basin, and also a prism of low-density rock corresponding to the Marymia Dome.

Discussion

Within the crust, the gravity models differ from the seismic models only in the northern limits of the dense crustal root in the Capricorn Orogenic Belt. The seismic refraction data (Drummond, 1979c) place the northern limit about 80 km south of Newman, but the resolution of this is limited by the spacing of seismic recording stations, and could be as much as ±20 km. The position of the seismic boundary was, therefore,

Figure 3. The seismic model (Drummond, 1979c) and two gravity models for line GBC. Model A has a root of high-density upper mantle compensating the effects of the thick crust under end C, and in model B different velocity/density functions (see text) were assumed for each end of the line. The calculated and measured curves agree in the principal features, but the short-wavelength effects were not modelled. Both models require a high-density slab representing the Nabberu Basin near end C, and model B requires a low-density prism to represent the Marymia Dome.

set to coincide with the Mount Vernon Fault Zone, which correlates with a major facies change in the Bangemall Basin (Brakel & Muhling, 1976).

The steep gravity gradients at the boundary of the Hamersley Basin and Bangemall Basin in the region of the seismic profile correlate also with the southern boundary of the Sylvania Dome (Fig. 1). The low density basement rocks of the Sylvania Dome, which were not included in the gravity models, probably contribute to the steep gravity gradient. In view of this, and the possible inaccuracy of the boundary in the seismic model, the departure of the gravity models from the seismic model in the region of the Capricorn Orogenic Belt is outside the accuracy of the experiment, and is not significant.

Assuming that the region is in isostatic equilibrium, the seismic model and the gravity field, when considered together, may be indicative of either isostatic compensation being fully achieved deep in the upper mantle or different bulk chemistry in the cratons and isostatic compensation at the crust/mantle boundary. In model B (Fig. 3) the density in the upper crust of the Pilbara Craton (2.55 $t.m^{-3}$) is very low compared with the densities measured in hand samples from the region (Drummond, 1979a), suggesting a compromise between models A and B. We favour a model similar to model A, but with some chemical stratification in the lower crust and the base of the crust in the Yilgarn Craton perhaps reaching $\bar{m} = 22$.

In gravity model A, the depth of compensation was set arbitrarily, and for convenience, at 100 km. Dooley (1977) suggested that the depth of compensation in the Western Australian Shield was in the upper mantle, but he could do no more than to suggest that it was probably below 160 km depth. Unfortunately, the current seismic data cannot be more definitive.

Although a unique structural profile of the crust and upper mantle cannot be derived from the seismic and gravity data, the models in Figure 3 do have implications for theories of evolution of the crust and upper mantle in the region. Gee (1979b) listed four differences between the Pilbara and Yilgarn Blocks from which different evolutionary histories for the cratons can be inferred:

(i) the western Yilgarn Block has large areas of high-grade gneiss terrain, for which there is no equivalent in the Pilbara Block;
(ii) most of the granitoids in the Yilgarn Block are younger than the majority of those in the Pilbara Block;
(iii) the maturity of the clastic sequences within the greenstone belts of the cratons implies that the Pilbara Block developed more towards crustal stability than the Yilgarn Block; and
(iv) the granitoids of the Pilbara Block are near-circular, whereas those of the Yilgarn Block have distinct linear trends.

Drummond & others (1981) added a fifth: the crust of the Pilbara Craton is much thinner than the crust of the Yilgarn Craton.

The arguments presented above for the depths of isostatic equilibrium imply also that the Pilbara region differs from the Yilgarn region either in the chemistry of the crust, which can be regarded as a sixth difference between the cratons, or in the metamorphic grade or chemistry of the upper mantle.

Jordan (1975, 1978) suggested that sub-continental mantle to depths possibly as great as 400 km evolves in parallel with the overlying continental crust. Because the sub-continental mantle becomes less dense than the surrounding mantle, it does not mix with the rest of the mantle, but is transported with the continents during plate motions. The features of the mantle established during the formation of the crust are frozen in. The differences in the upper mantle structure or chemistry under the cratons in northwest Australia may therefore indirectly imply different evolutionary processes for the cratons. This is an alternative sixth difference between the cratons.

The upper mantle under the Pilbara Craton may be less dense than that under the Yilgarn Craton, because of iron depletion. The upper mantle would, therefore, be implicated as the reservoir which provided the iron for the large volumes of basic volcanics and banded iron formations of the Hamersley Basin.

Acknowledgements

We thank the iron ore companies of the Pilbara for their willing co-operation during the field work and are grateful to our colleagues at BMR for their useful discussions and suggestions for field work; in particular, we thank P. Wellman and D. M. Finlayson.

This work was undertaken when one of us (BJD) was a full time research scholar at the Research School of Earth Sciences, Australian National University, under the auspices of an Australian Government Public Service Postgraduate Scholarship. We are indebted to Professor K. Lambeck and Dr K. J. Muirhead of RSES for their support and advice.

References

ANDERSON, D. L., SAMMIS, C., & JORDAN, T., 1972—Composition of mantle and core. *In* ROBERTSON, E. C. (editor), The nature of the solid Earth. *McGraw Hill, New York,* 41-66.

BERRY, M. J., 1971—Depth uncertainties from seismic first-arrival refraction studies. *Journal of Geophysical Research,* 76, 6464-8.

BIRCH, F., 1961—The velocity of compressional waves in rocks to 10 kilobars, Part 2. *Journal of Geophysical Research,* 66, 2199-224.

BRAKEL, A. T., & MUHLING, P. C., 1976—Stratigraphy, sedimentation, and structure in the western and central part of the Bangemall Basin, Western Australia. *Geological Survey of Western Australia Annual Report,* 1975, 70-9.

DOOLEY, J. C., 1976—Variation of crustal mass over the Australian region. *BMR Journal of Australian Geology & Geophysics,* 1, 291-6.

DOOLEY, J. C., 1977—Implications of Australian seismic and gravity measurements for the structure and composition of the upper mantle. *BMR Journal of Australian Geology & Geophysics,* 2, 1-5.

DRUMMOND, B. J., 1979a—Pilbara Crustal Survey, 1977: Operational Report. *Bureau of Mineral Resources, Australia, Record,* 1979/54 (unpublished).

DRUMMOND, B. J., 1979b—Structural relations between the Archaean Pilbara and Yilgarn cratons, Western Australia, from deep seismic sounding. *M.Sc. Thesis, Australian National University* (unpublished).

DRUMMOND, B. J., 1979c—A crustal profile across the Archaean Pilbara and northern Yilgarn cratons, northwest Australia. *BMR Journal of Australian Geology & Geophysics,* 4, 171-80.

DRUMMOND, B. J., 1981—Crustal structure of the Precambrian terrains of northwest Australia from seismic refraction data. *BMR Journal of Australian Geology & Geophysics,* this issue.

DRUMMOND, B. J., SMITH, R. E., & HORWITZ, R. C., 1981—Crustal structure in the Pilbara and northern Yilgarn blocks from deep seismic sounding. *In* GLOVER, J. E., & GROVES, D. I. (editors), Archaean Geology: Second International Archaean Symposium. *Geological Society of Australia Special Publication,* 7, in press.

DRUMMOND, B. J., MUIRHEAD, K. J., & HALES, A. L., in prep.—Evidence for a seismic discontinuity near 200 km depth under a continental margin.

FRASER, A. R., 1979a—Reconnaissance gravity survey in northwest Western Australia, 1969. *In* FRASER, A. R., & PETTIFER, G. R., Reconnaissance gravity surveys in Western Australia and South Australia, 1969–1972. *Bureau of Mineral Resources, Australia, Bulletin,* 196 Part B, 13-25.

FRASER, A. R., 1979b—Reconnaissance gravity survey in central and southwest Western Australia, 1971–1972. *In* FRASER, A. R., & PETTIFER, G. R., Reconnaissance gravity surveys in Western Australia and South Australia, 1969–1972. *Bureau of Mineral Resources, Australia, Bulletin,* 196, Part C, 27-45.

GEE, R. D. (compiler), 1979a—Geological map of Western Australia, 1:2 500 000 scale. *Geological Survey of Western Australia, Perth.*

GEE, R. D., 1979b—Structure and tectonic style of the Western Australian shield. *Tectonophysics,* 58, 327-69.

GENDZWILL, D. J., 1970—The gradational density contrast as a gravity interpretation model. *Geophysics,* 35, 270-5.

GREGSON, P. J., 1978—Mundaring Geophysical Observatory, Annual Report, 1977. *Bureau of Mineral Resources, Australia, Record,* 1978/73 (unpublished).

GSWA, 1975—Geology of Western Australia. *Geological Survey of Western Australia, Memoir,* 2.

HALL, W. D. M., & GOODE, A. D. T., 1978—The early Proterozoic Nabberu Basin and associated iron formations of Western Australia. *Precambrian Research,* 7, 129-84.

JESSOP, A. M., & LEWIS, T., 1978—Heat flow and heat generation in the Superior Province of the Canadian Shield. *Tectonophysics,* 50, 55-77.

JORDAN, T. H., 1975—The continental tectosphere. *Reviews of Geophysics & Space Physics,* 13, 1-12.

JORDAN, T. H., 1978—Composition and development of the continental tectosphere. *Nature,* 274, 544-8.

MATHUR, S. P., 1974—Crustal structure in southwestern Australia from seismic and gravity data. *Tectonophysics,* 24, 151-82.

MANGHNANI, M. H., RAMANANANTOANDRO, R., & CLARK, S. P., 1974—Compressional and shear wave velocities in granulite facies rocks and eclogites to 10 kbar. *Journal of Geophysical Research,* 79, 5427-46.

MILSON, J., & WORTHINGTON, G. A., 1977—Computer programs for rapid computation of gravity effects of two-dimensional and three-dimensional bodies. *Computers & Geosciences,* 3, 269-81.

PRODEHL, C., 1977—The structure of the crust-mantle boundary beneath North America and Europe as derived from explosion seismology. *In* HEACOCK, J. C., The Earth's crust. *American Geophysical Union Geophysical Monograph,* 20, 349-69.

TALWANI, M., SUTTON, G. H., & WORZEL, J. O., 1959a—A crustal section across the Puerto Rico Trench. *Journal of Geophysical Research,* 64, 1545-55.

TALWANI, M., WORZEL, J. L., & LANDISMAN, J., 1959b—Rapid gravity computations for two-dimensional bodies with application to the Mendocino submarine fracture zone. *Journal of Geophysical Research,* 64, 49-59.

WELLMAN, P., 1976—Regional variation of gravity, and isostatic equilibrium of the Australian crust. *BMR Journal of Australian Geology & Geophysics,* 1, 297-302.

WELLMAN, P., 1978—Gravity evidence for abrupt changes in mean crustal density at the junction of Australian crustal blocks. *BMR Journal of Australian Geology & Geophysics,* 3, 153-62.

BMR Journal of Australian Geology & Geophysics, 6, 1981, 145-151

Australasian mid-Tertiary larger foraminiferal associations and their bearing on the East Indian Letter Classification

George C. H. Chaproniere

Eight larger foraminiferal associations are found in northwest Australia; some can be recognised in other areas of Australia, New Zealand, Papua New Guinea, and Irian Jaya. Correlation with the East Indian Letter Classification can be made for some associations, but there is difficulty with others, owing to the absence of diagnostic forms. Planktic faunas are present in some of the associations, enabling direct correlation with the tropical planktic zonal scheme. In those non-diagnostic associations containing *Cycloclypeus* or *Lepidocyclina (Nephrolepidina)*, correlation with the East Indian Letter Classification can be achieved using biometric methods. The Tertiary *e* stage–Tertiary *f* stage boundary is placed within the N.6-7 zonal interval.

Introduction

Eight associations of larger foraminiferids have been recognised in the North West Cape area (Figs. 1, 2). Most can be recognised in Ashmore Reef No. 1 well (Figs. 1, 3) and some in the Batesford Limestone (Figs. 1, 4) (Chaproniere, 1975). Their recognition also in Irian Jaya and Papua New Guinea demonstrates their validity as biologic entities. The associations have a limited stratigraphic range in all sections (Figs. 2, 3, 4), and there are at least two successive associations in each section. Those from North West Cape and Ashmore Reef No. 1 well are in a similar order (Figs. 2, 3); those from the Batesford Limestone show a similar relationship, but are in a different order (Fig. 4).

Because it has been argued that the distribution of these assemblages is facies controlled (Chaproniere, 1975), their usefulness for biostratigraphic correlation may be limited. However, accurate time-correlation can be achieved in some associations by detailed biometric studies (Chaproniere, 1980), even between areas as widely separated as Batesford (Victoria) and North West Cape (Western Australia), suggesting that gene flow was maintained within the Australian region. For biostratigraphic convenience, the associations have been abbreviated to numbers prefixed by the letters LF (= larger foraminiferids), and are summarised in Table 1. Table 1 also gives their correlation with both the planktic foraminiferal scheme of Blow (1969), as modified for local usage by Chaproniere (1981), and the letter stage classification of Adams (1970).

Even though it is unusual for larger foraminiferal faunas to be associated with good planktic foraminiferal assemblages, several such associations occur in both Australia and New Zealand, and have formed the basis for this paper and for Chaproniere (1980). Such faunal relationships have permitted a better understanding of the correlation between the planktic and letter classification schemes, at least within the Australasian region. Furthermore, for the first time, the Tertiary *e*–Tertiary *f* stage boundary can be correlated with the tropical planktic foraminiferal zonal scheme.

Stratigraphic details

Detailed descriptions of the sections which are the basis for this paper are given in Chaproniere (1975, 1976), and all necessary lithostratigraphic and biostratigraphic details are summarised in Figures 2, 3, and 4. Figure 5 gives the stratigraphic ranges of the larger foraminiferids used in Table 1, for northwestern Australia.

Correlation with the East Indian Letter Classification

Adams (1970), in a discussion of the East Indian Letter Classification, listed typical assemblages for each letter stage, and noted problems with the definition of the stage boundaries. In the North West Cape area, the majority of the faunas contain only a few of the taxa regarded as typical of the Tertiary lower *e* to lower *f* stages. It is difficult, therefore, to locate exactly

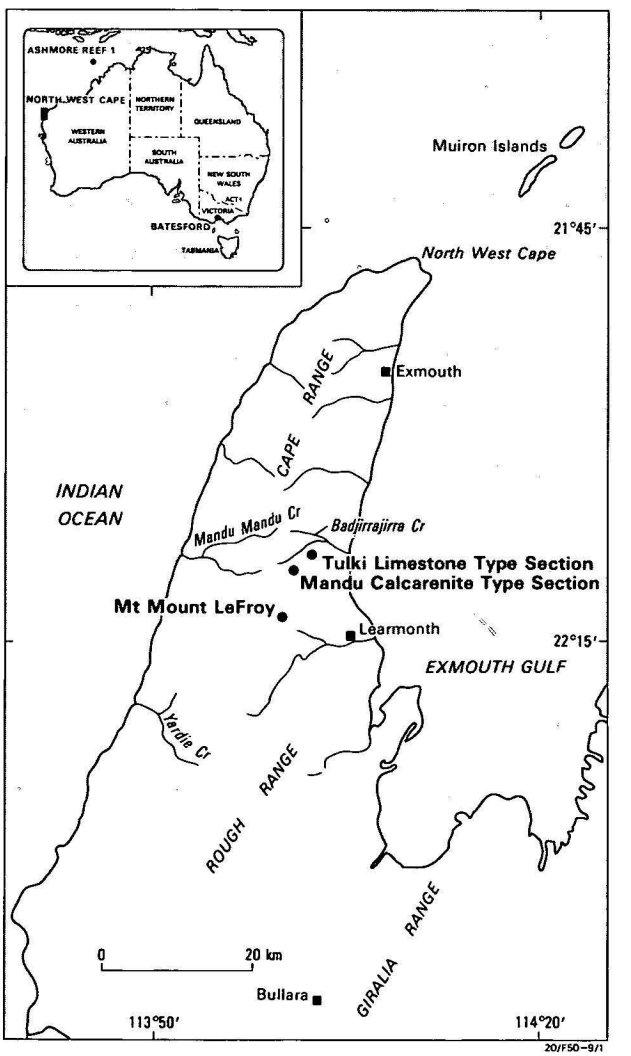

Figure 1. Locality map.

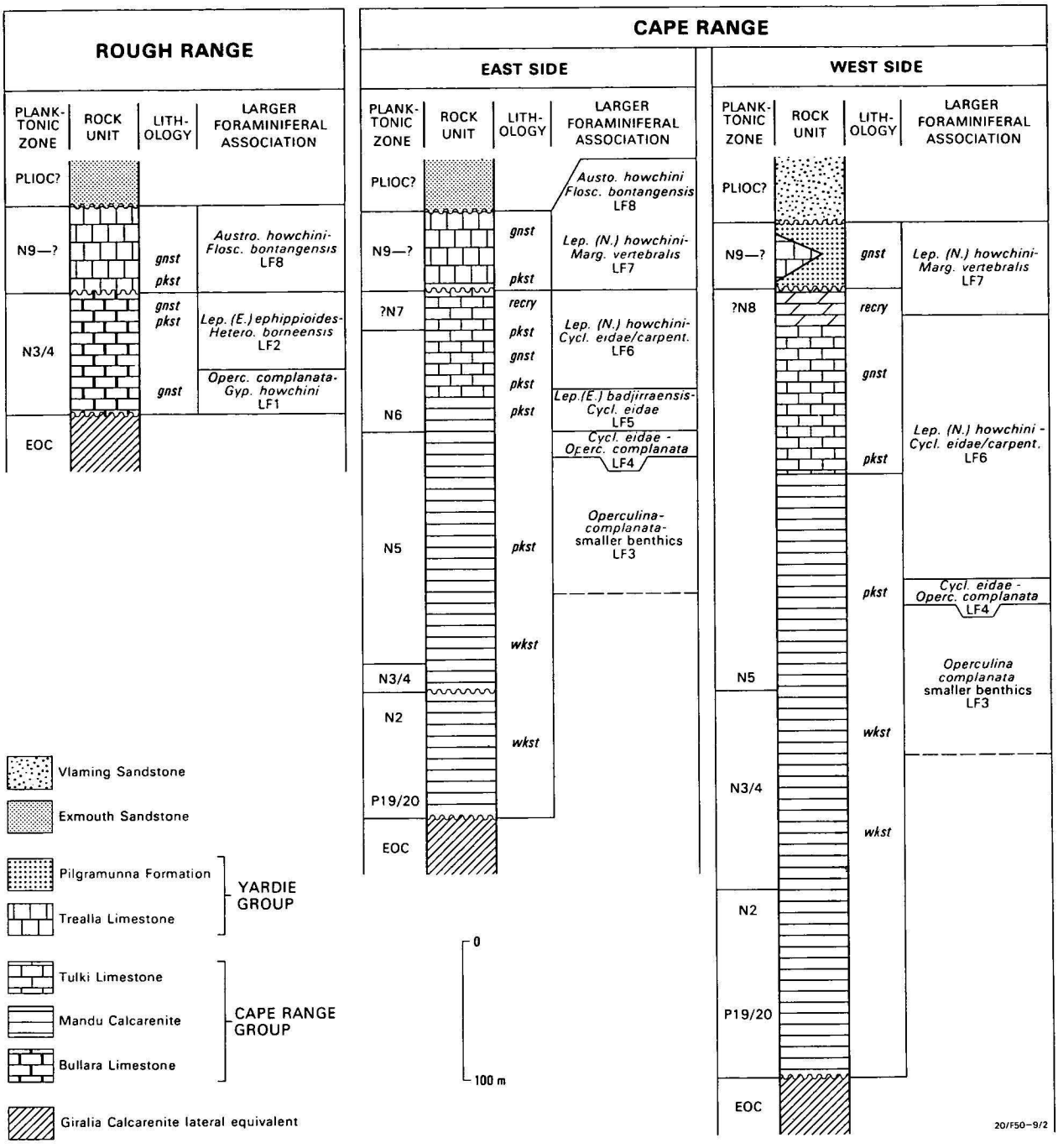

Figure 2. Composite stratigraphic sections from three localities in the North West Cape area, showing the relationship between the planktic and larger foraminiferal biostratigraphic schemes (modified after Chaproniere, 1975).

the position in the Letter Classification of most of the associations.

Furthermore, the difficulties are increased by different workers not having uniform concepts of some of the key species. Many of the specific names for *Lepidocyclina (Nephrolepidina)* used by Adams (1970) have been applied to a great variety of morphotypes by many different authors using differing criteria (see those figured by Ellis & Messina, 1965). Adams (1965) indicated his intention to describe fully, in a later paper, the species on which his study was based. At present it is almost impossible to have a clear picture of any of these species, and they are difficult to equate to those of the present study, which uses taxa based on biometric criteria (Chaproniere, 1980). In addition, of the numerous species of *Cycloclypeus* described by Tan (1932) for this same interval of time, only two are used here, and these are based on the usage of MacGillavry (1962) (see Chaproniere, 1980); critical species such as *C. eidae* Tan, *C. posteidae* Tan, and *C. indopacificus* Tan (as used by Adams, 1970) are difficult to recognise using Tan's (1932) criteria (see MacGillavry, 1962; Drooger, 1955), and almost certainly Adams (1965, 1970) has a concept of those species different from that of other workers and that used by the present writer.

All these factors have made very difficult any attempt to refer the associations described above to the Letter Classification. However, it is fairly certain that the LF.2 association is Tertiary lower *e* (based on the

presence of *Heterostegina borneensis* van der Vlerk, *Lepidocyclina (Eulepidina) ephippioides* Jones & Chapman, *L. (Nephrolepidina) sumatrensis* (Brady)—*parva* Oppenoorth morphotype, and *Austrotrillina striata* Todd & Post), that LF.5 is Tertiary upper *e* (based on the presence of *L. (E.) badjirraensis* Crespin with *Cycloclypeus eidae* Tan—*sensu* MacGillavry, 1962, *Miogypsina (Miogypsinoides) dehaarti* van der Vlerk and the *L. (N.) howchini* Chapman & Crespin group—*sumatrensis* (Brady) morphotype), and that LF.8 is Tertiary lower *f* (based on the presence of *Flosculinella bontangensis* (Rutten) with *Austrotrillina howchini* (Schlumberger)).

The other associations are difficult to place within this time range. The lowest assemblages from New Zealand contain elements that are typical of both Tertiary lower and upper *e* stages. *L. (Nephrolepidina) orakeiensis orakeiensis* (Karrer) is similar to *L. (N.) sumatrensis* (*parva* type), but is slightly more advanced; this form occurs with *Heterostegina borneensis* and either *Miogypsina (M.) globulina* (Michelotti) or *M. (M.) intermedia* Drooger. *H. borneensis* is typical of the Tertiary lower *e* stage and has only been questionably recorded from the Tertiary upper *e* stage (Adams, 1970). *Miogypsina (Miogypsina)*, on the other hand, first appears in the Tertiary upper *e* stage, and

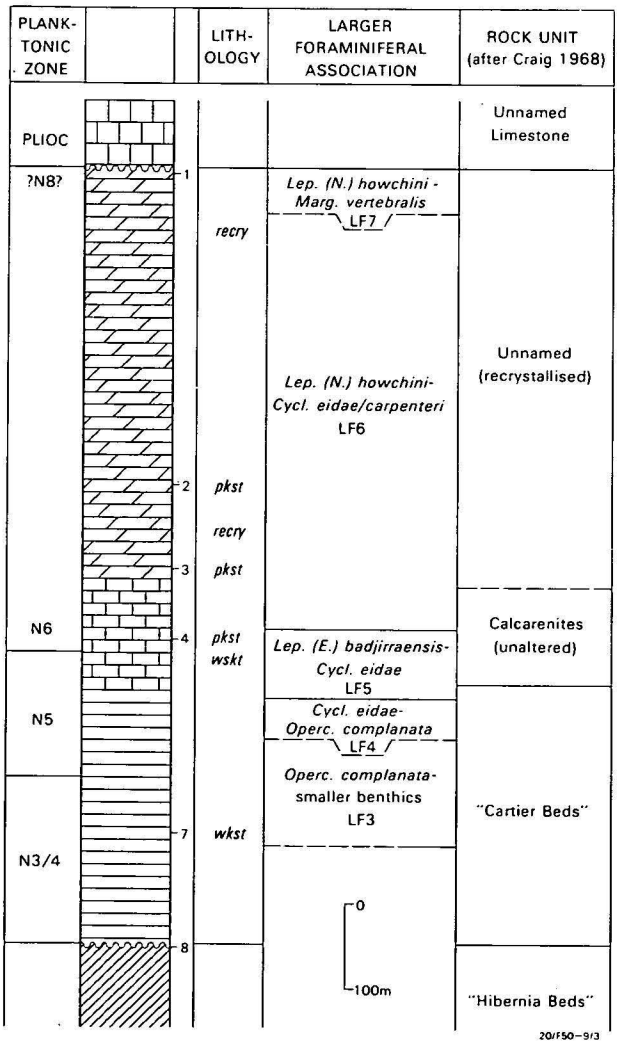

Figure 3. Stratigraphic summary of the Oligo-Miocene section in Ashmore Reef No. 1 Well (modified after Chaproniere, 1975, 1981).

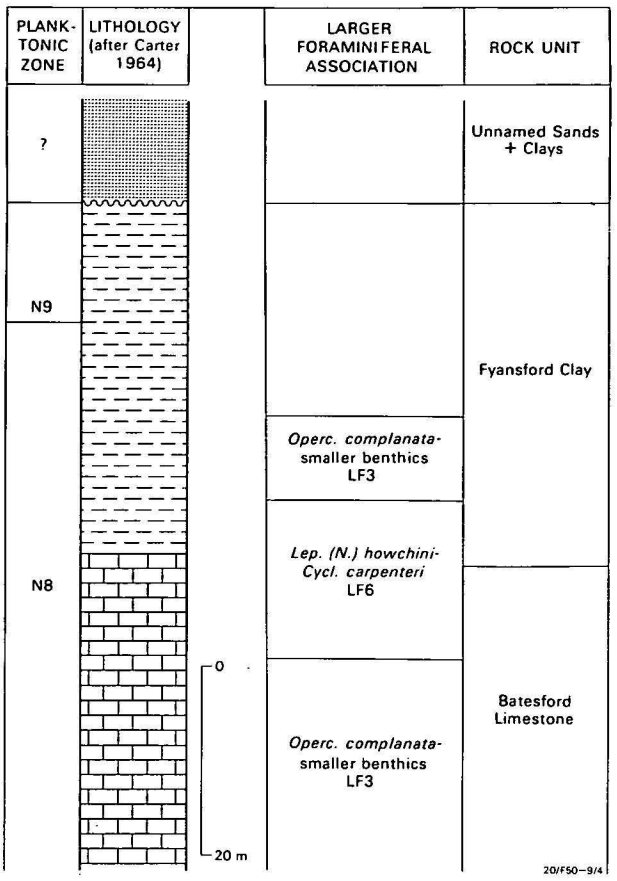

Figure 4. Stratigraphic summary of the Batesford Limestone, Batesford, Victoria (modified from Carter, 1964, fig. 15, and after Chaproniere, 1975).

has not been recorded from assemblages that would otherwise be clearly referable to the Tertiary lower *e* stage (Adams, 1970). The overlap between *H. borneensis* and *Miogypsina (Miogypsina)* occurs in two assemblages containing planktic foraminiferids; one containing *M. (M.) globulina*, contains a Zone N.3/4 fauna, and the other, with *M. (M.) intermedia*, contains a Zone N.5 fauna. Clarke & Blow (1969) place the Tertiary lower *e*–upper *e* stage boundary at the base of Zone N.4 of Blow (1969), while Adams (1970) places it within Zone N.4 (Fig. 6); both these assignments probably correlate to within the upper parts of Zone N.3/4 of Chaproniere (in Shafik & Chaproniere, 1978).

Thus, it would seem that the planktic and larger foraminiferal data suggest that the New Zealand faunas are from the Tertiary lower–upper *e* stage boundary, and that the boundary itself covers the planktic interval from high in Zone N.3/4 to low in Zone N.5. Biometric methods as outlined by Chaproniere (1980) would seem to be the best way to resolve the position of those non-diagnostic faunas, which contain species amenable to such treatment, within the Letter Classification scheme. However, some contain very long ranging forms and cannot, at present, be precisely placed.

The LF.1 and LF.3 associations are based on a long-ranging species, *Operculina complanata* (Defrance); LF.1 also contains *Lacazinella* sp. cf. *L. wichmanni* (Schlumberger). This form, as noted by Chaproniere (1976), is almost certainly reworked from Eocene sediments. In northwestern Australia the LF.1 association conformably underlies the typically

LARGER FORAMINIFERAL ASSOCIATION		ASSOCIATED LARGER FORAMINIFERIDS	PLANKTONIC ZONE			E.I. LETTER STAGE	AGE
			AUSTRALIA		NEW ZEALAND		
			NW	E			
LF8	*Austrotrillina howchini - Flosculinella bontangensis*	*Marginopora vertebralis, Sorites* sp., *Peneroplis* sp.,'*Borelis pygmaeus, Operculina complanata, O. venosa, Cycloclypeus (Cycloclypeus)* sp. cf. *C. carpenteri, Gypsina globulus, G. howchini, G. mastaelensis,* and *Lepidocyclina (Nephrolepidina)* sp. cf. *L. howchini*	N9-?N12			lower T*f*	Middle Miocene
LF7	*Lepidocyclina (Nephrolepidina) howchini - Marginopora vertebralis*	*Austrotrillina howchini, Borelis pygmaeus, Operculina complanata, O. venosa, Cycloclypeus (Cycloclypeus)* sp. cf. *C. carpenteri, Miogypsina (Lepidosemicyclina)* sp. cf. *M. thecideaeformis, Amphistegina quoyi, Borodinia septentrionalis, Gypsina globulus, G. howchini, G.mastaelensis; Cycloclypeus (Katacycloclypeus)* sp. cf. *C. annulatus* is very rare.	N9-?N12			lower T*f*	Middle Miocene
LF6	*Lepidocyclina (Nephrolepidina) howchini - Cycloclypeus (Cycloclypeus) eidae / carpenteri*	*Operculina complanata, Miogypsina (Lepidosemicyclina) thecideaeformis, Amphistegina quoyi, Gypsina globulus, G. howchini, Heterostegina suborbicularis, Miogypsina (Miogypsinoides) dehaarti, Borodinia septentrionalis, Carpenteria alternata,* and *C. proteiformis*	N6-N8	N8	N10-12	lower T*f*	Early Miocene
LF5	*Lepidocyclina (Eulepidina) badjirraensis - Cycloclypeus (Cycloclypeus) eidae*	*Operculina complanata, Amphistegina quoyi, Gypsina globulus, Carpenteria alternata,* and *Lepidocyclina (Nephrolepidina) howchini*	N5-N6			upper T*e*	Early Miocene
LF4	*Cycloclypeus (Cycloclypeus) eidae - Operculina complanata*	*Gypsina globulus, Carpenteria alternata,* and juvenile *Lepidocyclina (Eulepidina) badjirraensis*	N5-N6			upper T*e*	Early Miocene
LF3	*Operculina complanata* - smaller benthic foraminiferid	Juvenile *Cycloclypeus (Cycloclypeus) eidae* and juvenile *Lepidocyclina (Eulepidina) badjirraensis*	N5	N8		T*e* to T*f*	Early Miocene
LF2	*Lepidocyclina (Eulepidina) ephippioides - Heterostegina Borneensis*	*L. (Nephrolepidina) sumatrensis* and *Amphistegina bikiniensis, Operculina complanata, Gypsina globulus, G. howchini, Austrotrillina striata, Sorites* sp., *Borelis pygmaeus,* and *Halkyardia* sp. cf. *H. minima. Miogypsina (M.)* spp., and *L. (N.) orakeiensis* in N.Z.	N3/4		N3/4-N5	lower T*e*	Late Oligocene
LF1	*Operculina complanata - Gypsina howchini*	Rare specimens of *Lacazinella* sp. cf. *L. wichmanni,* probably reworked from the underlying lateral equivalents of the Giralia Calcarenite, are also present	N3/4			T*e*	Late Oligocene

20/F50-9/8

Table 1. Summary of the larger foraminiferal associations from the Australian area (from Chaproniere, 1975) and their relation to the planktic zonal scheme and the East Indian Letter Classification.

Tertiary lower *e* stage LF.2, and almost certainly correlates with that Letter Stage. LF.3 underlies typical Tertiary upper *e* stage faunas, and so is best equated with that stage. At Batesford, however, the LF.3 association contains a Zone N.8 planktic fauna, and, as noted below, this is equivalent to the Tertiary lower *f* stage.

The LF.4 and LF.6 associations contain either *Cycloclypeus* or *Lepidocyclina (Nephrolepidina),* and so, by using biometric criteria, should be readily correlated with the Letter Stage Classification. As noted above, however, problems of nomenclature impede such correlation. Table 2 lists the species of *Cycloclypeus (Cycloclypeus)* and *L. (Nephrolepidina)* given by Adams (1970) for the Letter Stages Tertiary lower *e* to upper *f*. If biometric criteria were to be used, values for parameters such as pc (the number of chambers in the precyclic stage—see O'Herne & van der Vlerk, 1971; Chaproniere, 1980) would decrease, while Spc_{4+5} (the number of secondary chamberlets of the 4th and 5th precyclic chambers) would increase, for populations of *Cycloclypeus (Cycloclypeus)* from Tertiary lower *e* to Tertiary upper *f* stages.

In a similar way, parameter F (which is a measure of the arrangement of the equatorial chambers—see Chaproniere, 1980) for *L. (Nephrolepidina)* would be seen to increase in value. Within the Australian region, populations from Tertiary lower *e* are dominated by specimens with an intersecting curve arrangement of the equatorial chambers: those from Tertiary upper *e* have a circular to polygonal concentric arrangement, those from Tertiary lower *f*, a stellate arrangement, and those from upper *f*, a similar arrangement as in lower *f*, but with many specimens having a complicated multilepidine embryoconch. At all levels, both phylogenetically primitive and advanced specimens could be expected to be found, but the proportions would gradually change—thus in Adams' (1970) lists, advanced forms (stellate), such as *ferreroi* Provale and *martini* (Schlumberger), occur with primitive types (circular concentric), such as *sumatrensis*, in, for example, Tertiary lower *f* stage (Table 2).

From this information, the LF.4 and LF.6 associations are seen to be time transgressive. Those from the eastern side of Cape Range contain phylogenetically more primitive forms than those from the western side.

Letter stage	*Cycloclypeus (Cycloclypeus)*	*Lepidocyclina (Nephrolepidina)*
Upper T*f*	*carpenteri/guembelianus*	*rutteni, radiata, orientalis, talahabensis*
Lower T*f*	*posteidae, indopacificus*	*ferreroi, sumatrensis, martini, japonica, orientalis*
Upper T*e*	*eidae* group	*inflata, japonica, sumatrensis, verbeeki*
Lower T*e*	*eidae*	*isolepidinoides, parva*

Table 2. Species of *Cycloclypeus (Cycloclypeus)* and *Lepidocyclina (Nephrolepidina)* considered by Adams (1970) to be typical of the late Oligocene and Miocene Letter Stages.
Adams & Frame (1979) have recently demonstrated that *C. carpenteri* and *C. guembelianus* are synonymous.

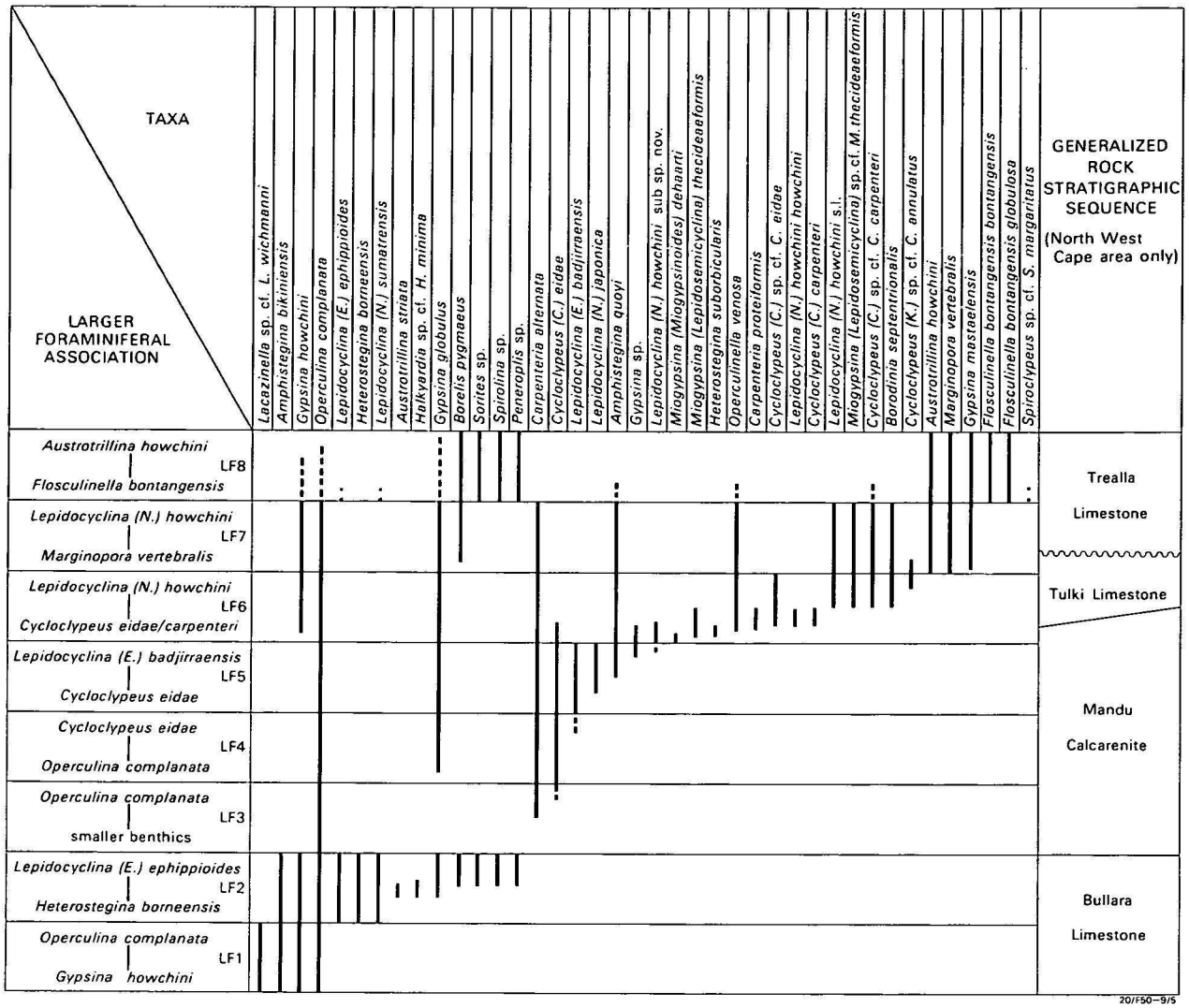

Figure 5. Generalised biostratigraphic range chart of larger foraminiferids in late Oligocene-early Miocene rocks of northwest Australia.
Dashed lines indicate ranges of juvenile or small adult forms; dotted lines indicate reworked specimens.

In addition, both associations occur close to typical Tertiary upper *e* stage faunas on the eastern side, suggesting that there they are best correlated with that stage. In contrast, as will be argued below, those associations from the western side are from levels above the extinction of *Lepidocyclina (Eulepidina) badjirraensis*, and so are best referred to the Tertiary lower *f* stage. The LF.7 association conformably overlies the LF.6, and underlies the LF.8 associations, and is best considered Tertiary lower *f* stage in this region.

The Tertiary *e*–Tertiary *f* stage boundary

The boundary between the Tertiary upper *e* and Tertiary lower *f* stages is difficult to locate, as it is based mainly on the extinction level of both *Spiroclypeus* (which occurs only as reworked specimens higher in the succession within the study area) and *L. (Eulepidina)* (Adams, 1965, 1970).

There is good evidence that *L. (E.) badjirraensis* became extinct within the early parts of the zonal interval N.6-7 in northwest Australia. In the North West Cape area and in Ashmore Reef No. 1 well the highest assemblages of *L. (E.) badjirraensis* are phylogenetically very advanced, as based on biometric criteria (Chaproniere, 1980), and are at a similar development to those of *L. (E.) dilatata* (Michelotti) described by Lange (1968) from Greece; in both areas, the majority of specimens have the protoconch almost completely enveloped by the deuteroconch, a stage above which no other is known, and it is difficult to visualise any evolutionary advancement beyond it.

One of the most persistent and widespread evolutionary trends throughout the larger foraminiferids is the gradual reduction with time of the coiled stage prior to the development of radial growth, and in the lepidocyclines it is taken to its ultimate by the almost total envelopment of the protoconch by the deuteroconch; in *Nephrolepidina*, peculiar multilepidine embryoconchs dominate assemblages prior to the extinction of that group. Thus, in the writer's opinion, it is safe to conclude that soon after the highest known stratigraphic occurrence of *L. (Eulepidina) badjirraensis* in Badjirrajirra Creek on the eastern side of Cape Range, and at a level just above core 3 in Ashmore Reef No. 1 well, this subgenus became extinct.

Further evidence to support this conclusion lies in the presence of identical smaller benthic foraminiferal faunas at levels within the Mandu Calcarenite, both on the eastern and western sides of Cape Range (*L. (E.)*

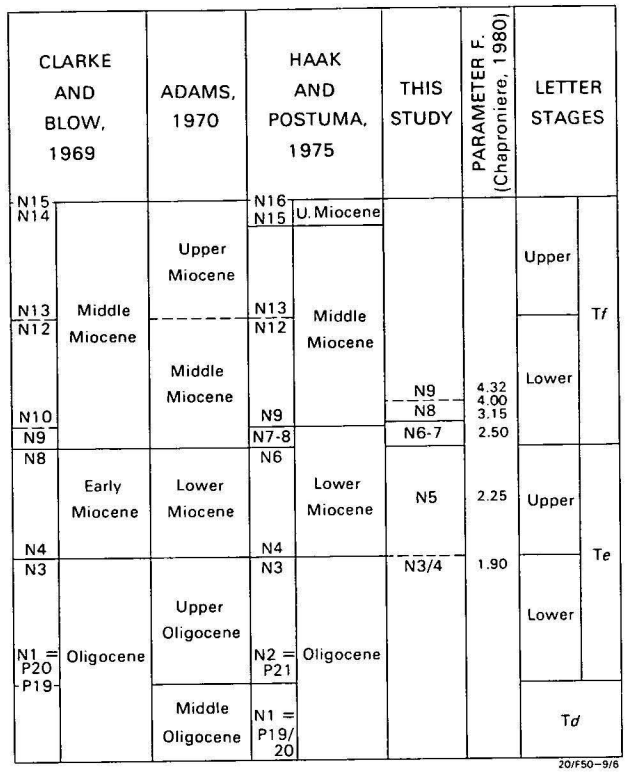

Figure 6. Comparison of relations between the Letter Stages and planktic foraminiferal zonal scheme given by other workers and as used in this paper. Some values for parameter F for *Lepidocyclina (Nephrolepidina)* are also given.

badjirraensis has not been recorded from the latter, which is also younger), suggesting that environmental conditions would not cause the exclusion of this subgenus.

Thus, in the northwest Australian region, the boundary between the Tertiary upper *e* and lower *f* stages can be defined on the extinction level of *L. (E.) badjirraensis* (top of LF.5), an event which occurred within the early part of the zonal interval N.6-7, which is somewhat earlier than that recorded by Adams (1970), Clarke & Blow (1969) and Haak & Postuma (1975).

Although support for the location of the Tertiary *e* —Tertiary *f* stage boundary within the N.6-7 zonal interval for the Australian region can be considered as tenuous, faunas from Irian Jaya and Papua New Guinea give some support to the case argued above. A sample from the basal part of the Moon Volcanics (Pieters & others, in prep.) on the Wesauni River in Irian Jaya contains a good lower Tertiary *f* assemblage (*Flosculinella bontangensis* with *Cycloclypeus* sp. and *Lepidocyclina (N.)* sp. cf. *L. (N.) howchini*) and is overlain by a mudstone with a typical Zone N.8 fauna, containing planktic forms best referred to *Praeorbulina glomerosa* rather than *Orbulina suturalis*. At several localities in the Blucher Range 1:250 000 Sheet area of Papua New Guinea, good Zone N.8 planktic faunas (*Praeorbulina* without *Orbulina*) overlie assemblages typical of the LF.6 association.

These results are in conflict with the statements of Clarke & Blow (1969) and Eames & others (1962) who recorded *L. (Eulepidina)* and other typically Tertiary *e* stage forms with either *Praeorbulina* or *Orbulina suturalis* (Zone N.8 or N.9) in 'Kereruan' stage limestones from Papua. This association was not adequately documented by these workers, and even though the figures given by Eames & others (1962, Pl. V) clearly show *L. (Eulepidina)* and other typical Tertiary *e* stage taxa, no planktic forms can be seen. In addition, unpublished reports of the Australian Petroleum Company indicate that the larger foraminiferids are allochthonous.

Clearly this association needs restudy, but in the light of evidence presented above, the writer believes the record of *L. (Eulepidina)* in Zone N.8 or N.9 doubtful and unlikely. Although accurate assessment of the values for parameter F cannot be made from random thin sections, some indication of the values for this parameter can be achieved (see Appendix 1); evidence suggests that the mean values of parameter F are similar to those of populations from the western side of Cape Range and, thus, of levels above the extinction level of *L. (Eulepidina)*. Moreover, this subgenus is not associated with these faunas. In at least one section (from the headwaters of the Sepik River, Victor Emanual Range) an LF.6 assemblage occurs with a typical Zone N.8 fauna, and is indistinguishable from a similar fauna occurring in the Batesford Limestone of Victoria.

Conclusions

There is no doubt that the Tertiary *e*—Tertiary *f* boundary correlates with levels below the Zone N.8-N.9 boundary (the early-middle Miocene boundary), the position which Clarke & Blow (1969) and Adams (1970) preferred (on evidence available at that time), because of the presence of good Tertiary lower *f* stage faunas with typical Zone N.8 planktic faunas. There is good evidence that this boundary occurs at least within Zone N.8 (see also Haak & Postuma, 1975), and that it even occurs within the zonal interval N.6-7 in the Australian area. The problem of the Tertiary *e* —Tertiary f boundary is made the more difficult in that it is characterised by the extinction level of two taxa *(Spiroclypeus)* and *Lepidocyclina (Eulepidina)*, both of which seem to be excluded from the LF.6 association (an association very widely distributed in the region) on probable environmental grounds (see Chaproniere, 1975).

Acknowledgements

I thank Dr C. G. Adams (British Museum) and Dr D. J. Belford (Bureau of Mineral Resources) for their advice and criticism and Dr Belford for the samples from Papua New Guinea. C. Pigram (Irian Jaya Geological Mapping Project) provided the material from Irian Jaya.

References

ADAMS, C. G., 1965—The foraminifera and stratigraphy of the Melinau Limestone, Sarawak and its importance in Tertiary correlation. *Quarterly Journal of the Geological Society of London*, 121, 283-338.

ADAMS, C. G., 1970—A reconsideration of the East Indian Letter Classification of the Tertiary. *Bulletin of the British Museum, Natural History (Geology)*, 19, 87-137.

ADAMS, C. G., & FRAME, P., 1979—Observation on *Cycloclypeus (Cycloclypeus)* Carpenter and *Cycloclypeus (Katacycloclypeus)* Tan (Foraminiferida). *Bulletin of the British Museum, Natural History (Geology)*, 32, 3-17.

BLOW, W. H., 1969—Late middle Eocene to Recent planktonic foraminiferal biostratigraphy. *Proceedings of the 1st International Conference on Planktonic Microfossils, Geneva,* 1, 199-421.

CARTER, A. N., 1964—Tertiary foraminifera from Gippsland, Victoria, and their stratigraphic significance. *Geological Survey of Victoria Memoir* 23, 1-154.

CHAPRONIERE, G. C. H., 1975—Palaeoecology of Oligo-Miocene larger Foraminiferida, Australia. *Alcheringa,* 1, 37-58.

CHAPRONIERE, G. C. H., 1976—The Bullara Limestone, a new rock-stratigraphic unit from the Carnarvon Basin, Western Australia. *BMR Journal of Australian Geology & Geophysics,* 1, 171-174.

CHAPRONIERE, G. C. H., 1980—Biometrical studies of Early Neogene larger Foraminiferida from Australia and New Zealand. *Alcheringa,* 4, 153-181.

CHAPRONIERE, G. C. H., 1981—Late Oligocene to Early Miocene planktic Foraminiferida from Ashmore Reef No. 1 Well, northwest Australia. *Alcheringa,* 5, 103-131.

CLARKE, W. J., & BLOW, W. H., 1969—The inter-relationships of some Late Eocene, Oligocene and Miocene larger foraminifera and planktonic biostratigraphic indices. *Proceedings of the 1st International Conference on Planktonic Microfossils, Geneva,* 2, 82-96.

CRAIG, R. W., 1968—Ashmore Reef No. 1 Well completion Report. *Burmah Oil Company of Australia Ltd Report* (unpublished).

DROOGER, C. W., 1955—Remarks on *Cycloclypeus.* Parts I and II. *Proceedings Koninklijke Nederlandse Akademie van Wetenschappen, series B,* 56, 104-123.

EAMES, F. E., BANNER, F. T. BLOW, W. H., & CLARKE, W. J., 1962—Fundamentals of Mid-Tertiary stratigraphical correlation. *Cambridge University Press.*

ELLIS, B. F., & MESSINA, A. R., 1965—Catalogue of index foraminifera, Vol. 1, Lepidocyclinids and Miogypsinids. *The American Museum of Natural History, New York.*

HAAK, R., & POSTUMA, J. A., 1975—The relation between the tropical planktonic foraminiferal zonation and the Tertiary Far East Letter Classification. *Geologie en Mijnbouw,* 54, 195-198.

LANGE, H., 1968—Die evolution von *Nephrolepidina* und *Eulepidina* im Oligozän und Miozän der Insel Ithaka (Westgriechenland). *Doctoral Thesis Ludwig-Maximilians-Universität zu München.*

MACGILLAVRY, H. J., 1962—Lineages in the genus *Cycloclypeus* Carpenter (foraminifera), Parts I and II. *Proceedings Koninklijke Nederlandse Akademie van Wetenschappen, series B,* 65, 429-458.

O'HERNE, L., & van der VLERK, I. M., 1971—Geological age determinations on a biometrical basis (comparison of 8 parameters). *Societa Paleontologica Italiana, Bollettino* 10, 2-18.

PIETERS, P. E., HARTONO, U., & CHAIRUL AMRI, in preparation—Geology of the Mar 1:250 000 Sheet area. *Irian Jaya Geological Mapping Project Data Record.*

SHAFIK, S., & CHAPRONIERE, G. C. H., 1978—Nannofossil and planktic foraminiferal biostratigraphy around the Oligocene-Miocene boundary in parts of the Indo-Pacific region. *BMR Journal of Australian Geology & Geophysics* 3, 135-151.

TAN SIN HOK, 1932—On the genus *Cycloclypeus* Carpenter. Part 1 and an appendix on the heterostegines of Tjimanggoe, South Bantam, Java. *Wetenschappelijke Mededeelingen Dienst van den Mijnbouw in Nederlandsch-Indie,* 19, 3-194.

Appendix 1. The estimation of parameter F for *Lepidocyclina (Nephrolepidina)* in random thin-sections.

Chaproniere (1980) proposed parameter F for *L. (Nephrolepidina),* and indicated that, of all the parameters used in biometric studies of the taxon, this proved to be the most accurate for correlation. That study was based on oriented thin-sections of individual specimens, as accurate measurements could not be made from random thin-sections. Subsequent work has shown that if sufficient random thin-sections are examined, an estimation of the value of parameter F can be obtained. This is due to the form of the equatorial layer in vertical sections which are not centred, that is, in sections which cut the test tangentially, at a distance from the embryoconch. Centred vertical sections (which cut through the embryoconch), show a gradual increase in the height of the equatorial chambers, as seen in Figure 7D, regardless of the arrangement of those chambers in equatorial section. Uncentred vertical sections, however, give information as to the arrangement of the equatorial chambers. Examples are given in Figures 7A-C. Figure 7A illustrates a form where F = 1 or 2, that is, where the equatorial chambers have either an intersecting curve or a circular concentric arrangement; in this case the height of the equatorial chambers gradually increases towards the test periphery and is similar to that of Figure 7D. Figure 7B illustrates a form where F = 3, that is, where the equatorial chambers are in a polygonal concentric arrangement; in this case the height of the equatorial chambers rapidly increases and then remains constant towards the periphery. Figure 7C illustrates a form where F = 4 or 5, that is, the chambers are a stellate arrangement; in this case the height of the equatorial chambers fluctuates, giving an undulating effect as the rays intersect the plane of the section. Thus, by estimating the numbers of the various categories present, a value for parameter F can be estimated. Illustrations of the various arrangements of the equatorial chambers are given by Chaproniere (1980, fig. 12).

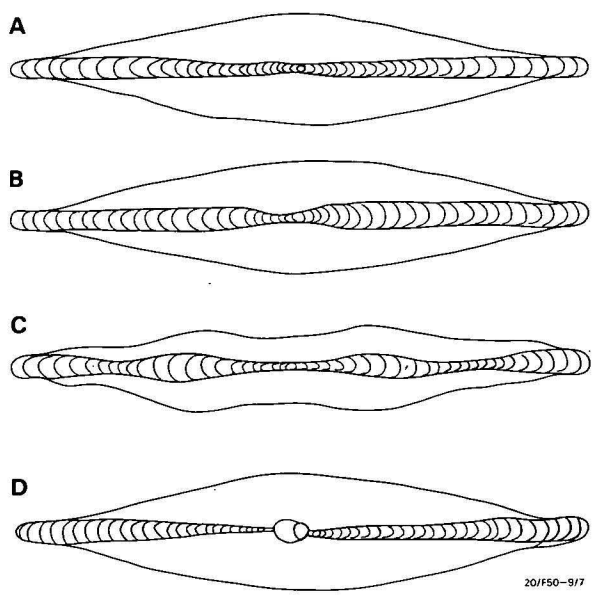

Figure 7. Diagrammatic off-centred vertical sections of *Lepidocyclina (Nephrolepidina)*, to illustrate a method by which values for parameter F can be estimated.
In A, F = 1 or 2; B, F = 3; C, F = 4 or 5; D, median section through embryoconch, from which no information on the values of F can be obtained.

BMR Journal of Australian Geology & Geophysics, 6, 1981, 153-159

Sedimentary cycles in the Surat Basin and global changes of sea level

N. F. Exon[1] *& D. Burger*

Six sedimentary cycles, each hundreds of metres thick, have been recognised in the Surat Basin. The Jurassic cycles (nos. 1-4) typically started with high-energy deposition of coarse sediments, and ended with labile sand, silt, and mud. The environments are thought to have been braided streams, followed by meandering streams, swamps, lakes, and deltas. After a period of non-deposition or erosion, followed by a phase of high-energy deposition, the first Cretaceous cycle (no. 5) ended with marine mud; the second (cycle 6) started with paralic silt and sand and ended with shallow marine silt.

The cycles are thought to be the result of global sea-level changes, characterised by rapid falls of sea level followed by slow rises, which, respectively, lowered and raised the base of erosion in the Surat Basin. During the Jurassic, the open sea lay several hundred kilometres to the east, and the sea only occasionally entered the basin, via the 'Brisbane' and 'Toowoomba' Straits. In the Cretaceous, the sea level was relatively higher and eustatic falls and rises of sea level led to alternating marine regressions and transgressions. The six Surat Basin cycles correspond in time to nine global sea-level oscillations. We think that some of the latter may have been too slight to be identified in the basin. There is also evidence that local isostatic movements may have exaggerated the impact of some global cycles and obscured that of others.

Introduction

The Jurassic and Cretaceous sediments of the Surat Basin were first described by Jensen (1926), who split the 2500-m thick sequence into two major parts: the Jurassic Walloons, and the marine Cretaceous. Reeves (1947) described the geology of the region north of Roma and established many of the rock units which are still used to subdivide the Surat Basin sequence. Whitehouse (1952, 1954) was the first to discuss the depositional environments of the Surat Basin sediments. Commenting on the volume and extent of the Jurassic sandstones, Whitehouse (1952) asked where they came from, and where the bulk of the non-sandy material from the source areas went to. He postulated that the Jurassic sandstone bodies 'formed on great plains by streams coming in from all directions, just as the great alluvial plains of the Channel Country of the Lake Eyre Basin are formed today. These streams came partly over the level Pre-Cambrian craton, partly down from the sandy terrain of the Drummond Range, and partly from other mountain blocks. It is postulated further that these streams went through the sagging basins to the deep sea'.

We are in general agreement with this reconstruction and consider that the main exit to the ocean was via the 'Toowoomba' and 'Brisbane Straits' (Figure 1). Most of the sediment was probably derived from the adjacent basement blocks, and from the sediments of the Bowen Basin to the north. However, Martin (1980) used the radiometric dating of micas in the Precipice Sandstone to argue for a westerly source in Precambrian areas such as the Willyama Block. A period of andesitic volcanism in the Albian and Cenomanian provided the fresh lithic (labile) sands deposited throughout the Eromanga and Surat Basins (Exon & Senior, 1976).

Whitehouse (1952, 1954) commented on three periods of important fluvial activity, marking the commencement of deposition of the Clematis Sandstone in the Triassic, and the Precipice and Gubberamunda Sandstones in the Jurassic. He noted that these units are coarse and siliceous, strongly current-bedded, and commonly very porous, and contrasted the sediments to those typical of his Walloon Coal Measures (our

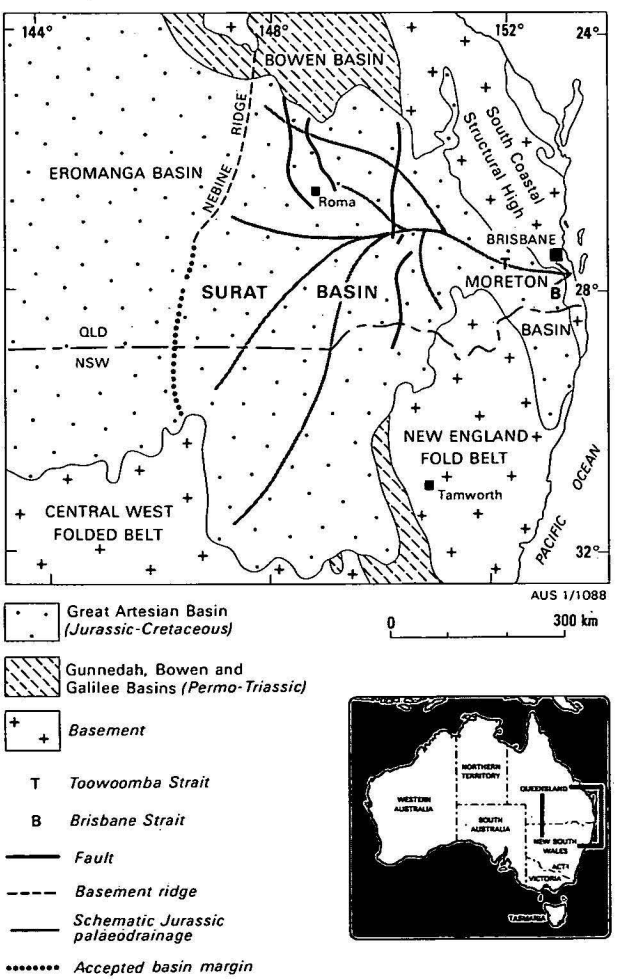

Figure 1. Regional setting of the Surat Basin.
In earliest Jurassic times the Nebine Ridge may not yet have formed a structural divide.

[1] **Present address: CCOP/SOPAC, C/- Mineral Resources Department, Suva, Fiji.**

Eurombah-Westbourne sequence), which are montmorillonitic fissile mudstones and calcareous feldspathic sandstones with some coal. He pointed out that the Walloons were deposited in basins showing no evidence of the removal of detrital material.

It is clear that Whitehouse (1952) had a general concept of cyclicity in mind as he wrote about the two types of sedimentary sequences: 'thick, coarse, current-bedded, siliceous sandstone formations . . . and calcareous shales'. This twofold development he called the 'characteristic pattern in the Mesozoic in Queensland', and he went on to explain that 'when waters passed freely through the basin, alkalis and alkaline earths were borne away in solution and non-calcareous sandstones and kaolinitic clays developed; when there was ponding and retention of dissolved salts, limestones, calcareous sandstones, and other kinds of clays were formed'.

Exon (1976), in his synthesis of Surat Basin geology, defined four cycles of Jurassic sedimentation and one Jurassic-Cretaceous cycle (cycles 1 to 5 of Figure 2), each of which was hundreds of metres thick, and which 'represented deposition in turn from braided streams, from meandering streams, and finally from swamps, lakes and deltas'. We now recognise four Jurassic and two Early Cretaceous cyclic units in the basin. The stratigraphic nomenclatures of Reeves and Whitehouse are shown in Table 1, with the more detailed subdivisions of Day (1964) and Exon (1976), the last being used in this paper. The individual rock units described by Exon (1976, 1980) are shown in Figure 2.

Sedimentary cycles

Six sedimentary cycles have been identified in the Surat Basin (Figure 2). The rocks of each cycle are generally 270 m to 600 m thick, and each cycle spans 10 to 20 million years. One exceptionally thick cycle is the Hutton-Walloon sequence (cycle 2, maximum 1000 m), and further work may prove this to contain two sub-cycles. The Mooga-Doncaster sequence (cycle 5) is also very thick (maximum 840 m) and may be regarded as consisting of at least two sub-cycles, the Mooga-Nullawurt and Minmi-Doncaster intervals.

Jurassic cycles

Cycles 1 to 4 started with a phase of high-energy deposition, and their basal sandstones commonly rest on a scoured surface of the underlying sequence. Lower-energy deposition associated with finer-grained labile sandstone and siltstone became predominant later, and labile sandstone, siltstone, mudstone, and coal are characteristic of the upper part of each cycle. As Whitehouse (1952) noted, the clean sandstone at the base of each cycle is non-calcareous, whereas the labile sandstone and siltstone of the upper part of each cycle are commonly highly calcareous.

The ideal cycle seems to have involved deposition in turn by braided streams, by meandering streams, and finally in swamps. lakes, and deltas, but the effects of these modes of deposition varied from cycle to cycle. The initial burst of energy was only great enough to produce extensive braided stream deposits, characterised by planar cross-bedding, in the first and fourth cycles (Fig. 2). Meandering streams, characterised by trough cross-bedding, deposited most of the sands. Swamp, lake, and delta deposits are characterised by muds and parallel bedding, but streams meandering through the depositional areas laid down sands in trough cross-bedded units. Coals are best developed in the upper parts of the second and fourth cycles, but thin coal stringers also occur in the first and third cycles.

The Jurassic sea did not rise high enough to inundate the Surat Basin completely, and the sediments deposited were almost entirely nonmarine, but there is evidence from palynology to indicate brief recurrent influxes of the sea into the area (Fig 3). For instance, Evans (1966a) and Reiser & Williams (1969) reported spinose acritarchs (phytoplankton) of the genera *Micrhystridium* and *Veryhachium* in multitudes from oolitic beds in the upper Evergreen Formation. This indicates brackish-marine coastal conditions prevailing at the end of cycle 1. Contemporaneous swarms are also known from immediately to the east, in the Moreton Basin (McKellar, 1978b). Acritarchs of the above genera have been reported in much lesser abundance from the Walloon Coal Measures further south in the Moreton Basin (Burger, in Exon & others, 1974), and in the correlative Birkhead Formation of the north-eastern Eromanga Basin at the top of cycle 2 (Evans, 1966b; Burger & Kemp, 1972).

The indications of brackish-marine conditions in the Moreton Basin support Whitehouse's idea of the existence of a corridor to the open sea further east. Marine influence appears to have been greatest during cycle 1, the Evergreen Formation being largely deltaic on well-log evidence (Porter, 1979). At the end of cycle 2 this corridor must have extended into the northeastern Eromanga Basin, but the fact that no significant numbers of acritarchs have been reported from the Surat Basin probably means that the corridor was narrow and may have been closed at times.

Cretaceous cycles

Immediately prior to the onset of the Cretaceous, the fifth cycle commenced with the high-energy, braided stream deposits of the Mooga Sandstone. Meandering stream and lacustrine environments dominated deposition of the Bungil Formation. The sea was relatively higher than in the Jurassic, and this probably explains why the basin was inundated several times (Fig. 2). The first (minor) marine transgression within this cycle is associated mainly with the upper part of the Kingull Member and the Nullawurt Sandstone Member of the formation. The latter member contains a marine shelly macrofauna mixed with freshwater fossils (Day, 1964, 1969), and palynofloras from it and the underlying Kingull Member include increased numbers of spinose acritarchs and a few marine phytoplankton, as shown in Figure 3 (Burger, 1973, 1974, 1980).

The first major marine Cretaceous transgression at the end of cycle 5 commenced with a distinct transgressive phase, which is marked by the appearance of abundant dinoflagellates, and reasonably diverse foraminiferal faunas and shelly macrofaunas in nearshore sands and silts of the Minmi Member (Day, 1967, 1969; Haig, 1979). The peak of the transgression is associated with the offshore muds of the Doncaster Member (Wallumbilla Formation). It marks the highest rise of sea level recorded in the Mesozoic of Australia, when most of Queensland, much of South Australia, and large tracts of New South Wales and the Northern Territory were inundated.

Geological age	*Reeves (1947)*	*Whitehouse (1954)*	*Day (1964)*	*Exon (1976)*	*Lithology*
Early-Middle Albian				Griman Creek Formation	Labile sst, siltst, mudst
				Surat Siltstone	Siltst, mudst, sst
				Wallumbilla Formation Coreena Member	Siltst, mudst, sst
Aptian	Rolling Downs Formation	Roma Formation	Roma Formation	Doncaster Member	Mudst (siltst)
		BLYTHESDALE GROUP	Blythesdale Formation Minmi Member	Bungil Formation Minmi Member	
	Transition Stage	Transition Beds	Nullawurt Sandstone Member	Nullawurt Sandstone Member	Mudst, siltst, sst
Neocomian			Kingull Member	Kingull Member	
	Mooga Sandstone	Mooga Sandstone	Mooga Sandstone Member	Mooga Sandstone	Qtz sst (siltst, mudst)
Late Jurassic	Fossil Wood Stage	Fossil Wood Beds	Orallo Formation	Orallo Formation	Labile sst, siltst, mudst
	Gubberamunda Sandstone	Gubberamunda Sandstone	Gubberamunda Sandstone	Gubberamunda Sandstone	Sst (conglom, siltst)
				INJUNE CREEK GROUP Westbourne Formation	Siltst, mudst, sst
				Springbok Sandstone	Labile sst, siltst, mudst
Middle Jurassic	Lower Walloon Coal Measures	Walloon Coal Measures		Walloon Coal Measures	Mudst, siltst, labile sst
				Eurombah Formation	Sst (conglom, siltst, mudst)
		BUNDAMBA GROUP			
	Hutton Sandstone	Marburg Formation		Hutton Sandstone	Sst (siltst, mudst)
Early Jurassic	Boxvale Sandstone	Boxvale Sandstone			
	Shale	Evergreen Shales		Evergreen Formation	Siltst, mudst, sst
	Bundamba Sandstone	Precipice Sandstone		Precipice Sandstone	Qtz sst (siltst, mudst)
	UNCONFORMITY			UNCONFORMITY	

Table 1. Age and nomenclature of rock units in the Surat Basin (classification of arenites according to Crook, 1960).

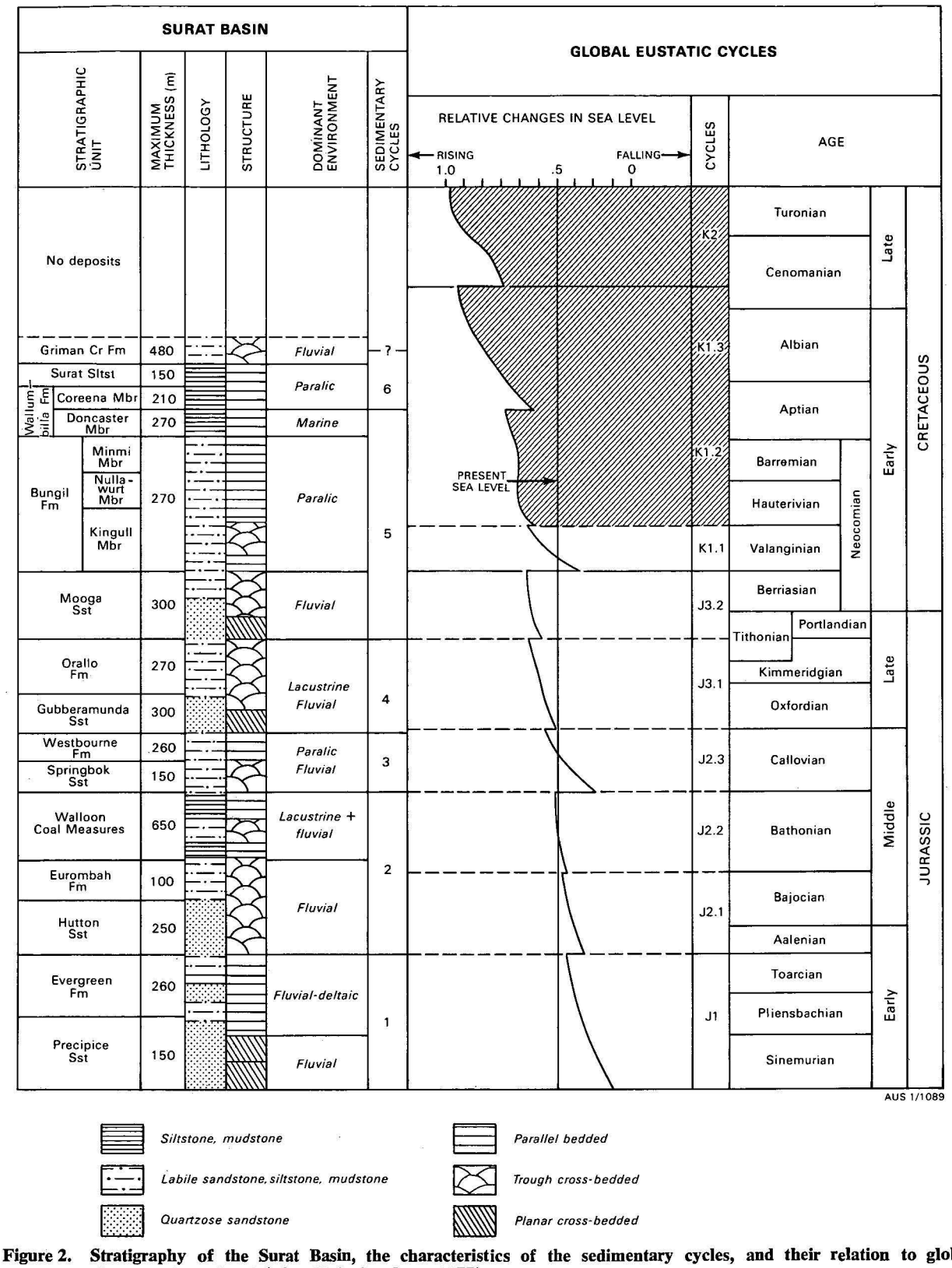

Figure 2. Stratigraphy of the Surat Basin, the characteristics of the sedimentary cycles, and their relation to global changes of sea level (after Vail & others, 1977).
In Vail & others' summary the global curve in the hatched interval lacks detail.

The sixth and final cycle started with a marine regression, during which paralic silts and sands of the basal Coreena Member were deposited. During the subsequent transgression, shallow marine silts of the upper part of this member were laid down. This transgression was brief and restricted; dinoflagellate microfloras from the member were still reasonably species-diverse, but the macrofauna was already distinctly impoverished (Day, 1969).

The sandstone, siltstone, and mudstone of the Griman Creek Formation were deposited as the sea slowly receded from the Surat Basin, making it diffi-

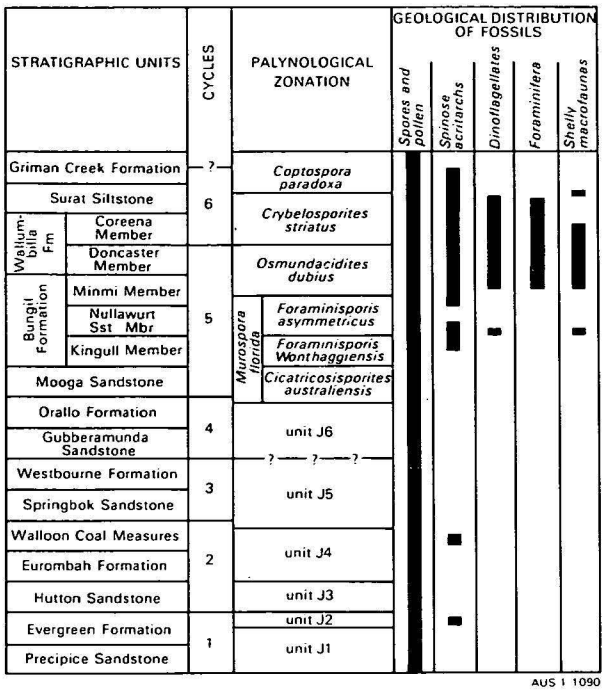

Figure 3. Relation in time of palynological zones to sedimentary cycles in the Surat Basin, and geological distribution of major fossil groups.

cult to delineate the end of cycle 6. Haig (1973) reported the last occurrence of foraminifera from the Surat Siltstone, and only brackish water microfossils (acritarchs) persisted in the overlying Griman Creek Formation (Fig. 3). The corridor to the east was cut off, and only a narrow area, perhaps a valley floor, of brackish and nearshore environments remained, opening to the northwest (Burger, 1980).

Origin of the cycles

The Surat Basin cycles (except the last) started with a phase of high-energy deposition, preceded in some cycles by erosion. Initially, Exon (1976) attributed such phases to periodic changes in climatic, tectonic, or eustatic conditions. Recurrent high rainfalls or rapid local uplifts around the basin margins would indeed result in increased run-off, and erosion of the hinterland. It is now doubted, however, whether recurrent uplifts were important, since at that time the area was fairly stable tectonically, with the hinterland probably undergoing steady rather than episodic uplift.

There is no evidence in the palynological record of periodic changes in climate, which might have generated higher rainfalls. We have no reason to believe that Australia moved through different climatic zones at the time, since Creer (1970) has shown that the Australian Plate was relatively stationary during the Jurassic and Early Cretaceous. At present, the possible impact of the climate, from whatever cause, on the Surat Basin cycles cannot be evaluated. It is possible that isostatic movements of the region, for instance such as those generated by movements of the Australian Plate over local mantle hot-spots, may have had some effect, but no evidence exists at present to confirm this.

We have reason to assume that these cycles stem from world-wide causes. Sea-level movements in rhythm with the Mooga-Kingull and Minmi-Doncaster 'subcycles' within our cycle 5 have been recently identified in the Eromanga Basin (Morgan, 1978), Carpentaria Basin (Burger, study in progress), and Carnarvon Basin (Wiseman, 1969). Following Vail & others' (1977) scheme of eustatic sea-level movements for the Jurassic and Cretaceous, Exon (1980) suggested that these were the underlying causes of the Surat Basin sedimentary cycles, as the global movements occurred at intervals approximating those of the Surat Basin cycles. Also, faunal and palynological evidence indicates that the upper parts of our cycles 3, 5, and 6 correspond in time to high eustatic sea levels in many parts of the world (Cooper, 1976; Vail & others, 1977).

Vail & others (1977) distinguished six eustatic cycles (J1, J2.1, J2.2, J2.3, J3.1, and J3.2) in the Jurassic, and three cycles (K1.1, K1.2, and K1.3) in the Early Cretaceous. They presented a curve of relative changes in sea level, which is reproduced in Figure 2 together with the authors' age determinations of their cycles. It should be noted that the curve in the interval of cycles K1.2 and K1.3 lacks detail, and that, therefore, their age determinations in this interval cannot be accurately compared with those from the Surat Basin shown in Table 1.

Correlation of cycles

Correlation of the Surat Basin cycles with the global cycles is based on the following considerations. The acritarchs from the Evergreen Formation have not been sufficiently investigated to serve as age indicators for cycle 1, but Reiser & Williams (1969), De Jersey (1971), and McKellar (1978a), on palynological grounds, dated the Precipice Sandstone of this cycle and its correlative Helidon Sandstone to the east as Rhaetian or Early Jurassic, and probably pre-late Liassic. For this reason we think that cycle 1 coincides with the Early Jurassic global cycle J1, and not with the Middle Jurassic cycles J2.

The first appearance of a spore species of continent-wide distribution, *Contignisporites cooksonae* (Balme) in the uppermost Walloon Coal Measures, indicates that the upper part of the Injune Creek Group, i.e. cycle 3, is not older than Callovian (see Balme, 1957; De Jersey & Paten, 1964; Evans, 1966a). It appears very likely, therefore, that cycle 2 is older than global cycle J2.3, and we take it to coincide with global cycles J2.1 and J2.2. We correlate cycle 4, which is associated with the youngest Jurassic palynological interval unit J6 (as defined by Burger & Senior, 1979), with global cycle J3.1, and this means that our cycle 3 would correspond to global cycle J2.3.

The lower part of cycle 5 is associated with the *Murospora florida* zone, which commences in the latest Jurassic (Burger, 1973). Faunal evidence dates the Doncaster Member at the top of the cycle as late Aptian, and, from the sea-level curve, it is probable that cycle 5 substantially corresponds to global cycles J3.2, K.1.1, and K1.2. A slight discrepancy in the position of the Aptian-Albian boundary, as compared with Table 1, may be attributed to the lack of detail in Vail & others' scheme.

Within cycle 5 we distinguish a lower sub-cycle ending with the Kingull Member, which is of Valanginian-Hauterivian age and thus may correspond to the top of global cycle K1.1. A substantial fall of the sea level shown in the curve at the beginning of this cycle has had no apparent effect on the Surat Basin. We think that such effects may have been blurred by local tectonic warping. The Kingull Member contains

swarms of acritarchs only in the east; towards the west it is nonmarine (Burger, 1980). Apparently, an arm of the sea extended briefly into the Basin via the 'Toowoomba' or 'Brisbane' Straits. The main marine transgression is distinctly of northwestern origin (Burger, 1973, 1980). Palynological evidence indicates that straits were most probably not cut off until much later, so that the change of direction might perhaps be attributed to a slight tilt of the basin floor to the west.

The Coreena Member at the base of cycle 6 contains early Albian shelly faunas, and this cycle may correspond approximately to the lower part of global cycle K1.3. The top of the cycle is ill-defined, and the youngest sediments preserved are associated with the *Coptospora paradoxa* zone/unit K2a, of middle Albian age. It is difficult to fit the local events into the global picture. The simplified curve given by Vail & others (1977) does not adequately represent eustatic movements at the end of the Early Cretaceous; Cooper (1976) indicated that there were two main eustatic fluctuations of sea level during the Albian.

Conclusions

Cyclic sedimentation in the Surat Basin during the Jurassic and Early Cretaceous was caused primarily by eustatic sea level movements. Vail & others (1977) produced curves which show that, within a global cycle, an initial rapid fall of sea level was followed by a slow rise (see Fig. 2). We envisage the following scenario developing in the course of a typical cycle. A sudden fall of sea level would result in a lowering of the regional base level of erosion. There would be a period of erosion or non-deposition while streams cut back from the sea. Widespread scouring indicates that there are small gaps at the base of some of our cycles, and evidence from stratigraphic drilling has shown that hiatuses representing the removal of 50 m or more of sediment occur below the Precipice Sandstone of cycle 1 and below the Mooga Sandstone of cycle 5 (Exon, 1980; also unpublished data). Following an initial phase of non-deposition or erosion, high-energy deposits would be accumulating while the sea level was still low. Coarse sands were laid down over vast areas without observable time lags, so that the landscape must have had little local relief. A subsequent decrease in energy of deposition would parallel a rise of sea level, and the end of a cycle would be characterised by valley-floor, nearshore, or marine deposits. Steady sinking of the basin would prevent the system from becoming imbalanced, and would allow the entire cycle to be repeated.

Our cycles do not correlate one to one with the global cycles, since nine global cycles span the period of our six (Fig. 2). This probably is partly due to the low amplitude of some sea-level oscillations. Local effects, such as slight tectonic movements, may also have exaggerated the impact of some global cycles and muffled those of others. We believe that global cycles J2.1 and J2.2 correspond in time to our cycle 2, which includes the very thick and lithologically varied Hutton-Walloon sequence. The drop in sea level at the base of global cycle J2.2 may well have been too slight to be easily identified regionally. Global cycles J3.2, K1.1 and K1.2 correspond in time to our cycle 5, and can be correlated with the two subcycles: Mooga-Nullawurt and Minmi-Doncaster. Slight (isostatic?) movements of the basin may have blurred the effects of the apparently major eustatic movements at the beginning of global cycle K1.1.

According to the curves given by Vail & others (1977) the sea level was, on average, low during the Jurassic, so that an initial fall of sea level must have been followed by a protracted interval of widespread erosion or non-deposition before the first coarse sands were laid down. At the present time, there are no obvious gaps known in the palynological record at the bases of our cycles to indicate sedimentary breaks, except for cycle 1, but certain intervals still lack detailed fossil documentation. During the Early Cretaceous, there was a general eustatic rise of sea level, during which phases of low sea level resulted in nonmarine to brackish-nearshore deposition and phases of high sea level to offshore, open marine conditins.

References

BALME, B. E., 1957—Spores and pollen grains from the Mesozoic of Western Australia. *CSIRO Fuel Research, Coal Research Section,* T.C. 25.

BURGER, D., 1973—Palynological zonation and sedimentary history of the Neocomian in the Great Artesian Basin, Queensland. *In* GLOVER, J. E., & PLAYFORD, G. (editors), Mesozoic and Cainozoic palynology; Essays in honour of Isabel Cookson. *Geological Society of Australia Special Publication* 4, 87-118.

BURGER, D., 1974—Palynology of subsurface Lower Cretaceous strata in the Surat Basin, Queensland. *Bureau of Mineral Resources, Australia, Bulletin* 150, 27-42.

BURGER, D., 1980—Palynological studies in the Lower Cretaceous of the Surat Basin, Australia. *Bureau of Mineral Resources, Australia, Bulletin* 189.

BURGER, D., in preparation—A basal Cretaceous dinoflagellate suite from northeastern Australia.

BURGER, D., & KEMP, E. M., 1972—Notes on the Carboniferous to Cretaceous palynology of the Buchanan, Muttaburra, Tangorin and Hughenden 1:250 000 Sheet areas, Queensland. *Bureau of Mineral Resources, Australia, Record* 1972/99 (unpublished).

BURGER, D., & SENIOR, B. R., 1979—A revision of the sedimentary and palynological history of the northeastern Eromanga Basin, Queensland. *Journal of the Geological Society of Australia* 26, 121-32.

COOPER, M. R., 1977—Eustacy during the Cretaceous: its implications and importance. *Palaeogeography, Palaeoclimatology, Palaeoecology,* 22 1-60.

CREER, K. M., 1970—Review and interpretation of palaeomagnetic data from the Gondwanic continents. *2nd International Gondwana Symposium, Proceedings and Papers,* 55-72.

CROOK, K. A. W., 1960—Classification of arenites. *American Journal of Science,* 258, 419-28.

DAY, R. W., 1964—Stratigraphy of the Roma-Wallumbilla area. *Geological Survey of Queensland Publication* 318.

DAY, R. W., 1967—Marine Lower Cretaceous fossils from the Minmi Member, Blythesdale Formation, Roma-Wallumbilla area. *Geological Survey of Queensland Publication* 335.

DAY, R. W., 1969—Marine Lower Cretaceous of the Great Artesian Basin. *In* CAMPBELL, K. S. W. (editor), Stratigraphy and palaeontology: essays in honour of Dorothy Hill. *Australian National University Press, Canberra,* 140-73.

DE JERSEY, N. J., 1971—Early Jurassic miospores from the Helidon Sandstone. *Geological Survey of Queensland Publication* 351 (*Palaeontological Papers* 25).

DE JERSEY, N. J., & PATEN, R. J., 1964—Jurassic spores and pollen grains from the Surat Basin. *Geological Survey of Queensland Publication* 322.

EVANS, P. R., 1966a—Mesozoic and stratigraphic palynology in Australia. *Australasian Oil & Gas Journal,* 12(6), 58-63.

EVANS, P. R., 1966b—Palynological studies in the Longreach, Jericho, Galilee, Tambo, Eddystone & Taroom 1:250 000 Sheet areas, Queensland. *Bureau of Mineral Resources, Australia, Record* 1966/61 (unpublished).

EXON, N. F., 1976—Geology of the Surat Basin in Queensland. *Bureau of Mineral Resources, Australia, Bulletin* 166.

EXON, N. F., 1980—The stratigraphy of the Surat Basin, with special reference to coal deposits. *Coal Geology*, 1(3), 57-69.

EXON, N. F., & SENIOR, B. R., 1976—The Cretaceous of the Eromanga and Surat Basins, Queensland. *BMR Journal of Australian Geology & Geophysics*, 1, 33-50.

EXON, N. F., REISER, R. F., CASEY, D. J., & BRUNKER, R. L., 1974—The post-Palaeozoic rocks on the Warwick 1:250 000 Sheet area, Queensland and New South Wales. *Bureau of Mineral Resources, Australia, Report* 140.

HAIG, D., 1973—Lower Cretaceous Foraminiferida, Surat Basin, southern Queensland: a preliminary stratigraphic appraisal. *Queensland Government Mining Journal*, 74, 44-52.

HAIG, D., 1979—Cretaceous foraminiferal biostratigraphy of Queensland. *Alcheringa*, 3, 171-87.

JENSEN, H. I., 1926—Geological reconnaissance between Roma, Springsure, Tambo and Taroom. *Geological Survey of Queensland Publication* 277.

MARTIN, K. R., 1980—Early Jurassic sedimentation in the Surat Basin. *Coal Geology*, 1(3), 71-81.

MCKELLAR, J. L., 1978a—Palynostratigraphy of samples from GSQ Eddystone 1. *Queensland Government Mining Journal*, 79, 424-34.

MCKELLAR, J. L., 1978b—Biostratigraphy of Early Jurassic miospore assemblages from the Leyburn area, southwestern Moreton Basin. *Queensland Government Mining Journal* 79, 517-25.

MORGAN, R., 1980—Eustasy in the Australian Early and Middle Cretaceous. *Geological Survey of New South Wales Bulletin* 27.

PORTER, C. R., 1979—Fluvio-deltaic deposition in Lower Jurassic sediments of the Surat Basin, Queensland. *The APEA Journal*, 19(2), 37-49.

REEVES, F., 1947—Geology of Roma district, Queensland, Australia. *American Association of Petroleum Geologists Bulletin*, 31, 1341-71.

REISER, R. F., & WILLIAMS, A. J., 1969—Palynology of the Lower Jurassic sediments of the northern Surat Basin, Queensland. *Geological Survey of Queensland Publication* 399.

VAIL, P. R., MITCHUM, R. M., & THOMSON, S., 1977—Seismic stratigraphy and global changes of sea level, Part 4: Global cycles of relative changes of sea level. *In* PAYTON, C. E. (editor), Seismic stratigraphy-applications to hydrocarbon exploration. *American Association of Petroleum Geologists Memoir* 26, 83-97.

WHITEHOUSE, F. W., 1952—The Mesozoic environments of Queensland. *Australasian Association for the Advancement of Science Report* 29, 83-106.

WHITEHOUSE, F. W., 1954—The geology of the Queensland portion of the Great Artesian Basin. Appendix G *in* Artesian water supplies in Queensland. *Department of the Co-ordinator General of Public Works, Queensland Parliamentary Papers*, A, 56-1955.

WISEMAN, J. F., 1979—Neocomian eustatic changes—biostratigraphic evidence from the Carnarvon Basin. *The APEA Journal*, 19, 66-73.

BMR Journal of Australian Geology & Geophysics, 6, 1981, 161-179

The influence of geology on the location, design and construction of water supply dams in the Canberra area

E. J. Best[1]

The design and construction of safe and economic dams depends upon many factors, not least of which is an accurate assessment of the geology of the dam site and reservoir area. During the past 80 years, geological factors have caused the failure of, or serious damage to, at least 150 large dams throughout the world. Since 1945, ten possible sites for large water supply dams in the Canberra area have been geologically investigated; of these, three sites were selected for the design and construction of dams. In each case, the site selected, the type of dam constructed, and the layout of the engineering structures were decided upon only after detailed geological investigations. Geological mapping was carried out continuously during the construction of all three dams, and variations from the expected conditions were encountered at each site. Examples are given of problems caused by geological factors which arose at each site, together with the measures adopted to overcome the difficulties. Despite these problems, each of the dams was constructed at a cost very close to the original contract price, and no significant stability problems have occurred during their operation. The thorough geological investigations carried out at these sites have contributed significantly to the economic and safe construction of the three dams.

Introduction

After much discussion and argument around the turn of the century, the site of the Federal Capital of Australia was finally narrowed down to the Yass-Canberra area by the Seat of Government Act of 1908. This Act stated, among other things, that the territory to be acquired by the Commonwealth 'shall include the catchment area of the water supply; such water must be of sufficient magnitude to place the question of volume at all seasons, and purity, beyond doubt'.

When the Commonwealth Surveyor, Mr C. B. Scrivener, was asked to propose the limits of the Australian Capital Territory in 1909, he suggested that the Territory should comprise the whole of the catchments of the Molonglo, Queanbeyan and Cotter Rivers. Subsequent negotiations with the NSW Government excluded the catchments of the Molonglo and Queanbeyan Rivers to the east of the Goulburn-Cooma railway line, and included instead the catchments of the Gudgenby, Naas, and Paddys Rivers. The boundary of the Australian Capital Territory was therefore determined largely by consideration of adequate water supply catchments (Fig. 1). The final agreement with the NSW Government provided that the rights of NSW to use and control water of the Queanbeyan and Molonglo Rivers upstream of the ACT boundary 'shall be subject and secondary to the use and requirements of the Commonwealth'. The agreement also provided that 'the State shall not pollute, and shall protect from pollution, the waters of the Queanbeyan and Molonglo Rivers throughout their whole course above the Territory'; in 1976 rehabilitation of the mine waste dumps at Captains Flat was carried out at a cost of $2.5 million.

During the 70 years since Canberra was established, the Cotter River and Queanbeyan River catchments have been developed to cater for the present ACT population of 225 000; in fact, the existing reservoirs can supply up to 400 000 people. Much of this development has occurred during the past 25 years, and in that time twelve potential sites for major dams have been

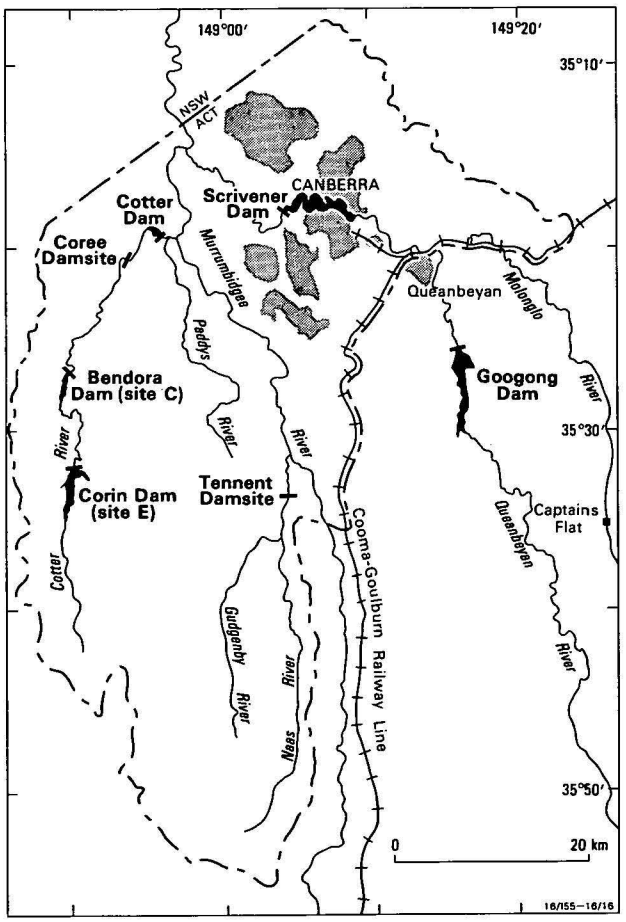

Figure 1. Dam sites in the Canberra area.

[1] **Formerly BMR: now Canberra College of Advanced Education, P.O. Box 1, Belconnen, ACT 2616.**

investigated in the Canberra area; of these, four were selected for the design and construction of dams. Three of these dams were constructed to augment Canberra's water supply (Bendora Dam, Corin Dam and Googong Dam), while the fourth (Scrivener Dam) was constructed to form Lake Burley Griffin, an essential feature of the original design for Canberra. All twelve sites were investigated geologically in varying degrees of detail, and geophysical surveys were carried out at eight of them. Most of this geological and geophysical work was carried out by the BMR, on behalf of the Commonwealth Department of Works (now the Department of Housing and Construction), which was responsible for the implementation of the site investigations and the design of the four dams which were constructed. This paper summarises the main geological results of the water supply dam site investigations, and will thereby illustrate the significant influence that geological features have had on the location, design, and construction of these dams.

Engineering geology of large dams

The development of water supply catchments requires the construction of dams to create storage reservoirs, and the location and design of major dams are invariably influenced to some extent by geological features. In many cases, geological factors such as foundation conditions and the proximity of construction materials are of overriding importance in determining the type of dam constructed at a given site. It therefore follows that a detailed knowledge of the geology of a prospective dam site and its environs is necessary before an informed decision can be made on the most suitable dam design and the estimated cost of construction.

The most important basic geological data required are the distribution and nature of the various rock types present in the area, the weathering profile, and details of the structural geology. These data are obtained by a site investigation program which uses a wide range of data-gathering techniques, such as outcrop mapping, bulldozed trenching to expose bedrock below overburden, diamond core drilling, water pressure testing, geophysical surveys, joint surveys, and laboratory testing of rock samples. The geological and physical data so obtained are then integrated to form a geomechanical model of the site, which provides the design engineer with a reasonably realistic and quantitative basis on which to design the dam and its associated structures. This process of collecting relevant geological data and presenting them in a form which is useful to the engineer is the main function of the engineering geologist.

A large dam has two essential requirements:

(a) It must be reasonably watertight. To achieve this, the dam is either constructed of impermeable material (e.g. concrete) or it incorporates an impermeable membrane in its structure (e.g. an earth core); also, the dam foundations must be made watertight by grouting or other means if necessary.

(b) It must be stable. Movement and deformation of the dam and its foundations cannot be eliminated, but they must be predicted and allowed for in the design.

Types of dam

In designing a dam for a particular site, the engineer has several basic types of dam to choose from. A summary of the layout and characteristics of these basic types is given in Figure 2.

At some dam sites, the most economical design has been a composite of two or more basic dam types. One particular type of composite concrete dam is the multiple arch design, which consists of several cylindrical arches supported by buttresses. This is well-suited to sites with geologically variable foundations—the buttresses are located on strong parts of the foundations, while the arches are located so as to bridge weak zones in the foundations.

Dam foundations

In the dam types listed in Figure 2, there is a progressive decrease in the area of foundations for a given dam height from the earth dam (largest area) to the double curvature arch dam (smallest area). This also means that the bearing pressure which must be supported by the foundations progressively increases from a minimum for the earth dam to a maximum for the arch dam; in other words, the sequence of dam types from (1) to (6) in Figure 2 requires progressively stronger foundations. It therefore follows that foundation geology at a proposed dam site is an important factor in deciding the most economic type of dam for the site.

Construction materials

Dams are constructed from large volumes of naturally-occurring earth materials—broken rock for rockfill and concrete aggregate, sand, gravel, and slopewash or highly weathered regolith for earth core. These construction materials must be obtained from as close to the dam site as possible if the dam is to be economically feasible. Therefore, the location and cost of extraction of construction materials is another important factor in determining the type of dam to be built.

For instance, a site may have highly weathered bedrock which appears to be only suitable for the foundations of an earth dam. However, if there is little suitable earth material close to the site, it may well be cheaper to excavate the foundations to a depth suitable for a concrete dam than to transport earth material over a long distance to the site.

Choice of dam type

In practice, several types of dam will be considered at a site, and estimates of quantities of materials, cost of materials, amount of foundation excavation, type and amount of foundation treatment, and so on, will be prepared for each type. The final choice will be the dam with the lowest estimated construction cost. In general, there are three factors which control this final decision:

(a) topography of the dam site and reservoir area,

(b) strength and variability of the foundations,

(c) availability and suitability of construction materials.

These factors are largely controlled by the geological structure and history of the site, and an informed decision requires a lot of geological data analysis and interpretation, particularly for factors (b) and (c), presented in a manner which the engineer can use in his design calculations.

Site investigation

The geological investigation of a large dam project starts with the initial proposal to dam a river, and continues through until the end of construction. It is

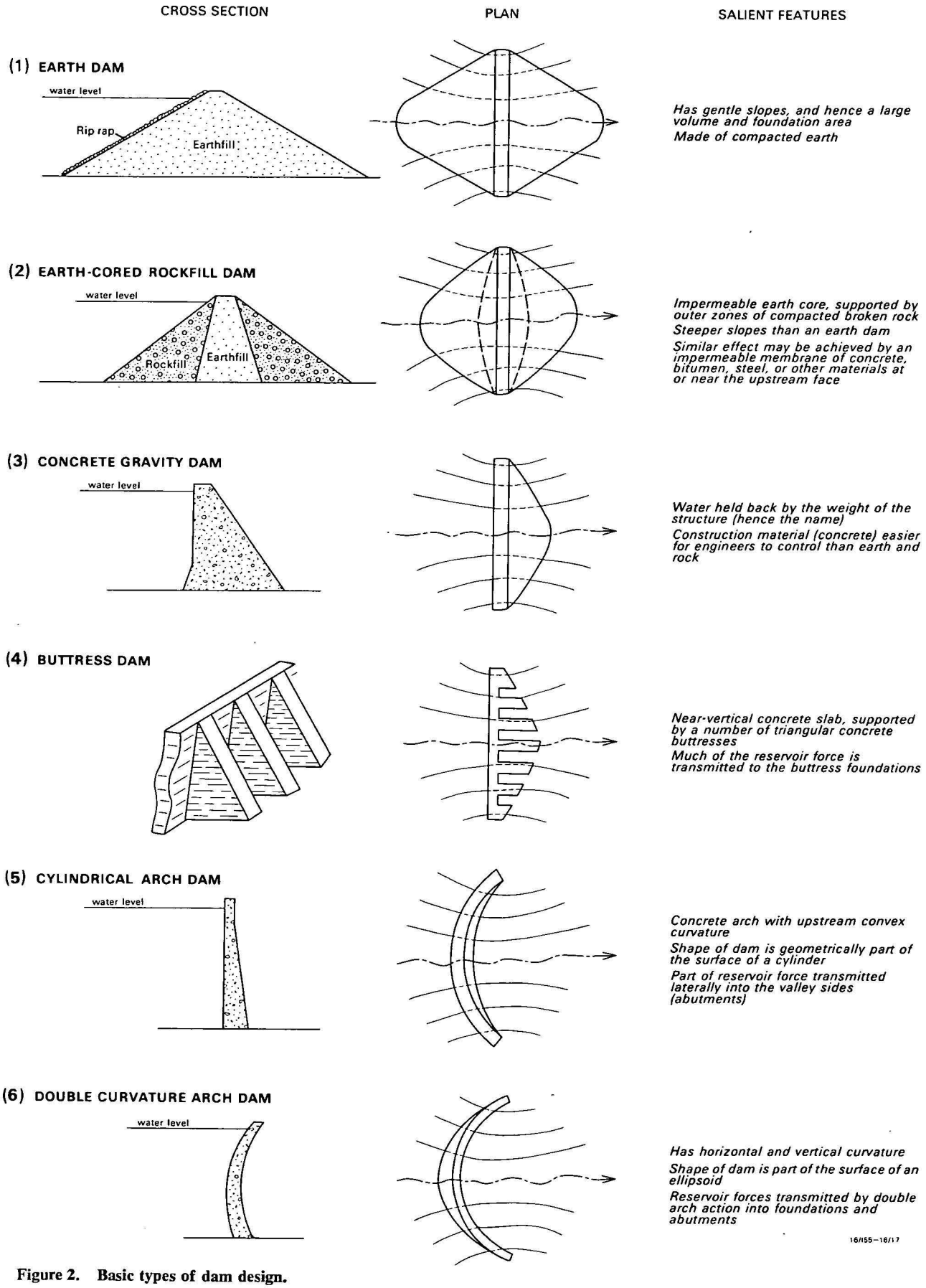

Figure 2. Basic types of dam design.

usually carried out in several phases associated with the sequence of engineering decisions which must be made. Following is a brief description of the general sequence of site investigations.

Preliminary or *reconnaissance* investigation—usually the consideration of several alternative sites.

Feasibility investigation—This is carried out at the site or sites being considered as a result of the preliminary investigation. Its purpose is to determine the type of dam best suited to a site, and its approximate cost.

Design investigation—the evaluation of particular features of the dam type selected, so as to provide the design engineer with information for an economic dam design. The results of these investigations also provide potential contractors for dam construction with information on which they can make realistic estimates of construction costs.

Construction services—the provision of on-site geological services and advice throughout the construction period. This includes detailed geological mapping of all rock exposures created during the construction, particularly those that are eventually to be covered by the engineering structures. Unexpected variations from the anticipated geological conditions may require substantial investigation, and must be recognised as soon as they are exposed; failure to do so can cause costly delays and treatment later in the construction period.

Post-construction investigations—these are necessary if problems occur after the dam has been completed (such as leakage through the foundations). The plans of the 'as constructed' site geology are invaluable in evaluating post-construction problems.

During site investigations, information is required not only from the surface and near-surface bedrock, but also from the rock at depth. The main techniques used in site investigations are as follows.

Geological mapping. The main component of all site investigations is detailed large-scale mapping of natural and artificial exposures of bedrock. The scale of mapping typically ranges between 1:100 and 1:1000.

Costeaning (trenching). The excavation of costeans (or trenches) through the overburden to bedrock provides continuity and extension of surface geological information. Larger areas of bedrock can be exposed by sluicing with high pressure water jets, if the additional expense is warranted.

Diamond drilling. Much useful information is obtained from carefully-planned diamond-drill holes, in which special equipment and techniques are used to ensure that the core obtained is as undisturbed as possible by the drilling process.

Water pressure testing. Quantitative data on the leakage properties of rock can be obtained by conducting water pressure tests in drill holes. Packers are used to isolate a section of drill hole, water is pumped into the section under a known pressure, and the rate of water leakage into the rock is measured. Leakage rates are measured for a range of water pressures, and after appropriate corrections are made to the field data, the results give a good indication of the water tightness and degree of open jointing in the rock at depth.

Geophysical surveys. Drill-hole information is often complemented by geophysical surveys, which provide a means of extrapolating and interpolating drill-hole data, as well as giving useful information on the physical properties of the rock mass (such as moduli of elasticity). The seismic refraction method is invariably used, and in particular cases resistivity and magnetic traverses can give useful additional information.

Investigations for Canberra's water supply dams

First phase (Cotter Dam, Stage 1)

During the early surveys of the Canberra area, it became evident that the Cotter catchment was the obvious location for initial water supply development, and in 1908 a party of surveyors of the Lands Department of NSW carried out a traverse along the entire length of the Cotter River. Six possible dam sites were selected during this survey; one site was near the confluence with the Murrumbidgee River, four sites were in the middle reaches of the river (these were designated Sites A, B, C and D) (Fig. 3) and the remaining site was in the upper reaches of the valley (Site E). Because of its closeness to Canberra, the lowest site was the obvious choice for the first water supply dam, even though water would have to be pumped to the storage reservoirs in Canberra. Thus the Cotter Dam, a concrete gravity structure, 20 m high was constructed at this site between 1912 and 1915. There are no records of the geology of the foundations, but the dam is founded on massive, fresh dacite porphyry. The concrete aggregate for the dam was almost certainly quarried from the same rock type close to the site.

Second phase (Cotter Dam, Stage 2)

During the 1920s, the Federal Capital Commission carried out a survey of the Queanbeyan River catchment, and selected two possible dam sites; one at Googong Station, and the other 10 km upstream at London Bridge. The Googong site was investigated by a number of shallow shafts and adits, and the site was visited in July 1929 by Dr W. G. Woolnough, the Commonwealth Geological Adviser. He reported very favourably on the site, stating that the foundations were nearly ideal from a geological viewpoint, the rock exposed at the site would provide excellent concrete aggregate, and the river deposits would provide abundant sand.

Canberra grew very slowly between 1925 and 1945, and it was not until after the war that consideration was given to augmenting Canberra's water supply. In December 1945, a party of BMR geologists mapped the area of the Cotter valley near dam sites A, B, C and D, after which a report was written summarising the regional geology and setting out the relative advantages and disadvantages of the four sites (Noakes, 1946a). A geological survey was also carried out at site E, from which it was concluded that the site was not as suitable as site B (Noakes, 1946b). As an alternative to constructing a dam at one of these sites, the engineers also assessed the practicability and economics of increasing the storage of the Cotter reservoir by increasing the height of the Cotter Dam. This was the solution finally adopted; and in 1950-51 the Cotter Dam was reconstructed to a height of 26 m, an increase of 6 m.

Third phase (Bendora Dam)

By 1953, it was apparent that the rate of growth of Canberra was steadily increasing, and that a new water

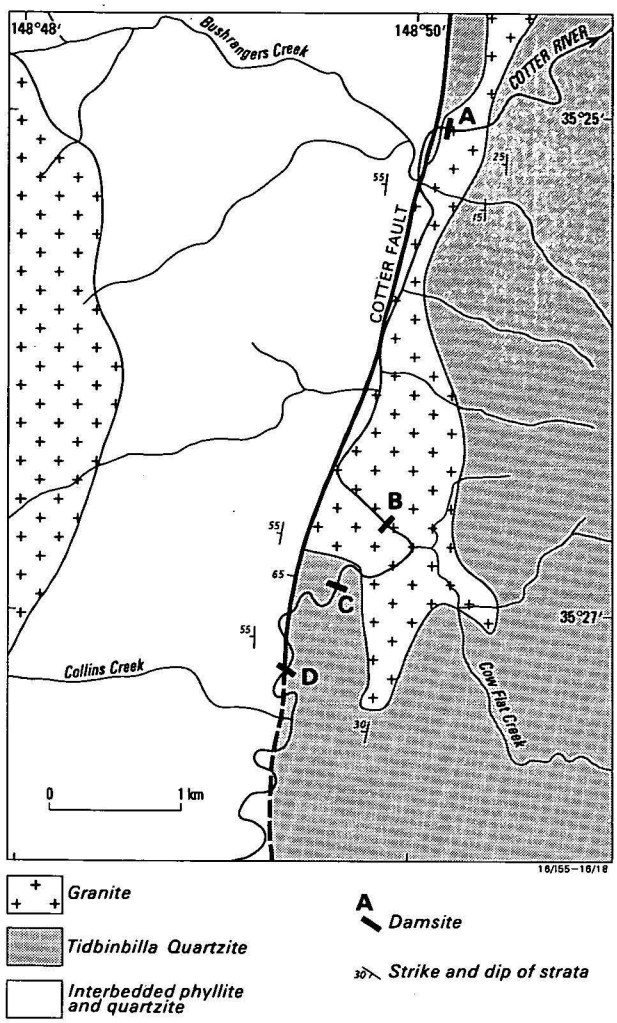

Figure 3. Regional geology of the Cotter valley near dam sites A, B, C, and D.

storage would be required by about 1962. Geological site investigations were therefore carried out at Sites A, B and C on the Cotter River (Site D had been rejected as unsuitable after the 1946 geological survey), and at Googong. Work at Googong showed that the geology was much more complex than had been evident from Woolnough's one-day inspection in 1929, and a major fault was located close to the dam site; the Googong site was therefore eliminated from further consideration at this stage.

The regional geology near Sites A, B, C and D is shown in Fig. 3. The geological work so far had indicated that Site B, located on granite, would be the best site, followed by Site C, which has foundations of gently-dipping quartzite. Site A was considered less suitable because it had foundations of both granite and quartzite, and was very close to a major fault zone (the Cotter Fault). Site D had already been rejected because it straddles the Cotter Fault. Therefore, although geological investigations continued on Sites A, B and C, there was an initial concentration on Site B. Work in 1953 raised doubts about this site, however, as a deep zone of weathered granite was suspected on the east bank (Perry, 1953). This was followed up later by a geophysical survey (Hawkins & Stocklin, 1956) which indicated weathered rock to depths of 20-30 m; Site B was therefore rejected.

Although, at this stage, Site C appeared to be geologically preferable to Site A, it had the disadvantage of having a smaller reservoir capacity than a similar height dam at Site A. In 1955, the Parliamentary Works Committee recommended that the next water supply dam be constructed at Site A, and a program of drilling and costeaning was planned to test the suitability of the site for a double curvature arch dam. These investigations showed that the foundations of the site were not strong enough for an arch dam, but were suitable for a concrete gravity dam, which would be more expensive (Noakes, 1955, 1956). A similar investigation was therefore carried out at Site C, which showed that the foundations were adequate for a double curvature arch dam (Noakes & others, 1957; Foweraker, 1958). Because of the significant difference in the amount of concrete necessary for these two dam types, a geological survey for suitable construction materials was made (Gardner, 1957); this revealed a scarcity of suitable sand for concrete, but more-than-adequate resources of rock for concrete aggregate.

Despite the significant advantage of Site A with respect to the reservoir storage/dam height relationship, a costing by the engineers on the basis of the geological information available showed that an arch dam at Site C would be cheaper than the lower concrete gravity dam necessary at Site A to give the same storage capacity. The final decision was made in 1958 to design and construct a 47-m high, double curvature arch dam with an over-dam spillway at Site C to form Canberra's next water supply storage reservoir.

The dam was constructed during 1960 and 1961, and upon completion was named Bendora Dam; the reservoir has a storage volume of 11.2 x 10^6 m^3, which is 2.5 times that of the Cotter Dam reservoir.

In 1966-67, a 1.5-m diameter pipeline was constructed from Bendora Dam to the Cotter pumping station, so that the water could be reticulated to Canberra under gravity head without the need for pumping (the Bendora reservoir is at a higher elevation than the Canberra storage reservoirs).

Fourth phase (Corin Dam)

It was calculated that the combined storage of Cotter and Bendora would provide water for a Canberra population of 97 000. In 1960, it was predicted that this figure would be reached by 1969, and so work started on investigating sites for the next dam before Bendora Dam had been completed.

Between 1961 and 1963, Site E and Googong dam site were both investigated to assess their suitability for the construction of a dam 60 m high. Investigation techniques included detailed geological mapping, trenching, diamond drilling, water pressure testing, geophysical traverses and laboratory testing of rock samples. The overall geological suitability of both sites was rather similar, and neither site had obvious advantages over the other. At Site E, the foundations consist of folded metasediments with well-developed jointing, and the presence of several major faults was revealed or strongly suspected; it was concluded that the site was suitable for a concrete gravity dam and a rockfill dam (Best & Hill, 1962). At Googong, the dam would be founded on a sequence of well-jointed, dacitic tuffs and flows, with a granite intrusion 60 m downstream and a major fault 60 m upstream of the proposed dam axis. Because of the small area of good foundations, a buttress dam was suggested; alternatively, an earth or rockfill dam would be suited to the larger foundation area

which would include poorer rock conditions (Burton, 1963).

In November 1963, the National Capital Development Commission decided that the next water supply dam would be constructed at Site E on the Cotter River. A feasibility site investigation was started in January 1964 to determine the type of dam best suited to the site. Initially, three types were considered (a buttress dam, a multi-arch dam, and a rockfill dam), and the investigations were directed firstly to obtaining information common to all three types, e.g. distribution of rock types, degree of weathering and jointing. Later, special requirements for each type of dam were investigated, such as spillway sites for a rockfill dam, and buttress foundations for a multi-arch dam. A provisional cost estimate in mid-1964 indicated that the multi-arch and rockfill dam designs would be of comparable cost, and cheaper than a buttress dam.

The usual investigation techniques of diamond drilling, water pressure testing, trenching and geophysics were used, but an innovation for this site investigation was the sluicing of large areas of the proposed foundations with high-pressure water jets, thus exposing the bedrock for geological mapping (Best & Hill, 1967). About 4000 m^2 of bedrock was cleaned down by this technique and geologically mapped at 1:120 scale. Much valuable geological information was obtained, and three major fault zones were exposed in the foundations. The last fault exposed by sluicing was adversely-oriented with respect to the dam foundations, and insufficient time was available to determine the exact location, attitude and nature of the fault at depth; this was a major factor in the decision of November, 1964, to design and construct an earth-cored rockfill dam at the site (Best, 1965).

The design investigation was started as soon as the type of dam had been decided, and continued until August 1965. A problem was immediately encountered in locating foundations for the spillway chute, as a seismic traverse along the proposed line indicated overburden thicknesses of up to 20 metres, subsequently confirmed by a diamond-drill hole, which located bedrock at a depth of 22 m. The area was investigated by 1500 m of seismic traverses before suitable spillway foundations could be located, and even then, the conditions were so restrictive that a more sophisticated engineering design had to be used than was originally intended. The proposed tunnel line and its portals were investigated by sluicing, mapping and diamond drilling, and the adverse fault in the dam foundations was investigated by drilling. The search for an economic quarry for rockfill proved more difficult than anticipated, and several possible areas were drilled before a suitable quarry site was located. Systematic augering and trenching in the Cotter valley upstream of the site located sufficient impermeable core material and sand for filter zones within 1.5 km of the dam site. The investigations ceased in August 1965, and a report of the engineering geology of the site was prepared (Best, 1965). Details of the dam design were finalised a few months later, and in March, 1966, a contract was let for the construction of a 75-m high dam at the site, to be known as Corin Dam. The reservoir started filling in April 1968, 5 months ahead of schedule, but did not fill soon enough to prevent the imposition of severe water restrictions in Canberra during the summer of 1968, which was the worst drought on record in the area. When full, the Corin reservoir contains about 76 x 10^6 m^3 of water which is five times the combined storage of the Bendora and Cotter reservoirs. Since construction, a study has been made of highly acid water emerging from the rockfill of the dam and the outlet tunnel (Haldane & others, 1971) and of erosion below the spillway.

Fifth phase (Googong Dam)

Consideration was being given to the next stage of Canberra's water supply development soon after construction had started at Corin. While Googong was a logical choice, it was decided that alternative sites within the ACT should also be identified and considered. The Naas-Gudgenby catchment was an obvious possible source of water, and the most suitable site, topographically, for a dam is on the Nass River 5 km upstream from its confluence with the Murrumbidgee River; this is known as the Tennent dam site (Fig. 1). Another possibility considered was further control of the Cotter River by creating a large storage reservoir on its lower reaches. This could be done by constructing a large dam, either at the site of the Cotter Dam, or at a site just upstream of the Cotter reservoir known as Coree dam site.

No further work was done at Googong at this stage, as a feasibility investigation had been carried out between 1961 and 1963. At the Cotter Dam, several holes were drilled in 1967 to test the quality of the concrete and the dam foundations; the results were not encouraging, and the proposal to build a 75-m high dam at this site was rejected. At the Tennent and Coree dam sites, however, comprehensive feasibility site investigations were carried out between December 1966 and July 1968, using geological mapping, diamond drilling and seismic refraction surveys.

The foundations at Tennent dam site consist of adamellite, which is fresh in the river bed, but weathered to considerable depths high up on the valley sites (Buchhorn, 1968a). Faulting and associated deep weathering was found on the east bank, and it was concluded that the site is only suitable for an earth or rockfill dam. The investigation included a search for possible sources of construction materials, and it became evident that there would be difficulty in obtaining adequate quantities cheaply, particularly of earth material. The proposed dam would be 68 m high, and would require an auxiliary dam or spillway structure across a topographic saddle on the west bank.

At Coree, a 78-m high dam was proposed, which would require a 24-m high saddle dam on the west bank; there is also a saddle on the east bank, which provides a convenient location for a spillway structure. The investigations at this site revealed strong, massive foundations of acid volcanics, with some faulting and probable folding (Buchhorn, 1968b). It was concluded that the site is suitable for any type of dam, although an arch dam would probably require a large concrete thrust block on the east abutment. The foundations for the saddle dam, however, are deeply weathered, and are probably only suitable for a rockfill or earth dam. Reconnaissance surveys for construction materials located likely sources of earth, rockfill and concrete aggregate, but no large sand deposits were found close to the site.

As soon as all three possible sites had been investigated to give basic data on foundation conditions and construction materials, the Department of Works prepared provisional designs and cost estimates for each site. On comparing these costs with the additional

population which would be supported by the proposed reservoirs, it was clear that the Googong proposal would have the lowest cost per head, followed by the Tennent project, with the Coree proposal the most expensive. Googong also had other advantages; it is located on a catchment which is meteorologically different to the Cotter and Naas catchments (which would increase the reliability of the overall water supply system for Canberra), and the water could also be used to help regulate changes in the water level of Lake Burley Griffin. It was therefore decided, in late 1969, that Canberra's next water storage dam be constructed at Googong.

A feasibility investigation was carried out during 1970 and 1971 to determine the type of dam best suited to the site. A design concept was prepared for an earth-cored rockfill dam in which the spillway would be excavated on the right (north) bank, with the excavated rock providing all of the rockfill required for the dam; this was thought likely to be the most economic design. Other types of dam were still considered, and the investigtion also incorporated a search for construction materials, including rockfill, away from the dam site. The investigation included detailed geological mapping, 17 drill holes, totalling 714 m, joint surveys, and 4100 m of seismic traverses, mostly in the spillway area. The reports of the investigation (Saltet, 1971; Taylor & Pettifer, 1972) concluded that the site was suitable for the construction of the proposed rockfill dam, and that construction materials were available at, or close to, the site. An arch dam was also considered possible, but the foundation treatment necessary would probably make it more costly than the rockfill design.

The decision to construct a rockfill dam at Googong was made in mid-1972, and a design investigation commenced in August 1972. A further 16 holes were drilled, totalling 599 m, and a core-orienting device was used in 10 of these holes to provide detailed information on joint set orientations in the proposed diversion tunnel and spillway excavation. Eight costeans, totalling 710 m, were excavated to provide continuous bedrock exposure in critical areas. The proposed rockfill design with a combined spillway/rock quarry was verified as being geologically feasible (Simpson, 1974), and the accumulated geological data were used extensively in drawing up the design and specifications for the construction of the dam and the excavation of the spillway and diversion tunnel.

Googong Dam was constructed between March 1975 and November 1977. The reservoir has a storage capacity of 109 x 10^6 m^3 which, together with the water from Bendora and Corin, is sufficient for a population of about 400 000.

Summary of pre-construction site investigations

The site investigation techniques listed earlier have been used to varying degrees in all investigations for dam sites in the Canberra area since 1955. A summary of the use of these methods at the various stages of site investigations is given in Table 1.

The influence of geology on dam construction—some examples

Bendora Dam

The main features of the foundation geology and the dam layout are shown in Figure 4. The concrete thrust blocks on each abutment are designed to distribute the lateral arch forces of the dam over a larger area of rock, thereby reducing the imposed stresses to acceptable values which can easily be withstood by the quartzite bedrock. A concrete-lined spillway apron and stilling basin were constructed to protect the downstream foundations from erosion by the overflow water. The concrete buttress and key wall are particular structures designed to overcome adverse geological features exposed in the right abutment.

The dam foundations consist of a sequence of bedded quartzite which dips to the west at between 17° and 25°. The quartzite contains a number of prominent sedimentary breccia beds, and an interbed of silicified ashstone 3 m thick; these provided very useful

Site investigation technique	*Phase*	*Bendora*	*Corin*	*Googong*	*Tennent*	*Coree*
Diamond drilling (no. of holes; total length)	P	0	6; 244 m	4; 222 m	3; 117 m	5; 242 m
	F	13; 508 m*	15; 915 m	18; 714 m	—	—
	D		27; 1026 m	16; 599 m	—	—
	Total	13; 508 m	48; 2185 m	37; 1535 m	—	—
Water pressure testing (no. of holes; total length)	P	0	6; 244 m	4; 222 m	3; 102 m	5; 242 m
	F	12; 460m*	12; 760 m	18; 697 m	—	—
	D		3; 60 m	11; 394 m	—	—
	Total	12; 460 m	21; 1064 m	33; 1313 m	—	—
Seismic refraction traverses (total length)	P	480 m	610 m	2350 m	1100 m	1660 m
	F	0	4100 m	4100 m	—	—
	D	0	1500 m	0	—	—
	Total	480 m	6210 m	6450 m	—	—
Costeaning (total length)	P	0	335 m	75 m	0	0
	F	290 m*	430 m	850 m	—	—
	D		2010 m	710 m	—	—
	Total	290 m	2775 m	1635 m	—	—
Sluicing (total area)	P	0	0	0	0	0
	F	0	3700 m^2	0	—	—
	D	0	650 m^2	0	—	—
	Total	0	4350 m^2	0	—	—

Site investigation phases: P = Preliminary, F = Feasibility, D = Design. * = F + D

Table 1. Summary statistics for site investigation techniques used in Canberra water supply dam site investigations 1955-1975.

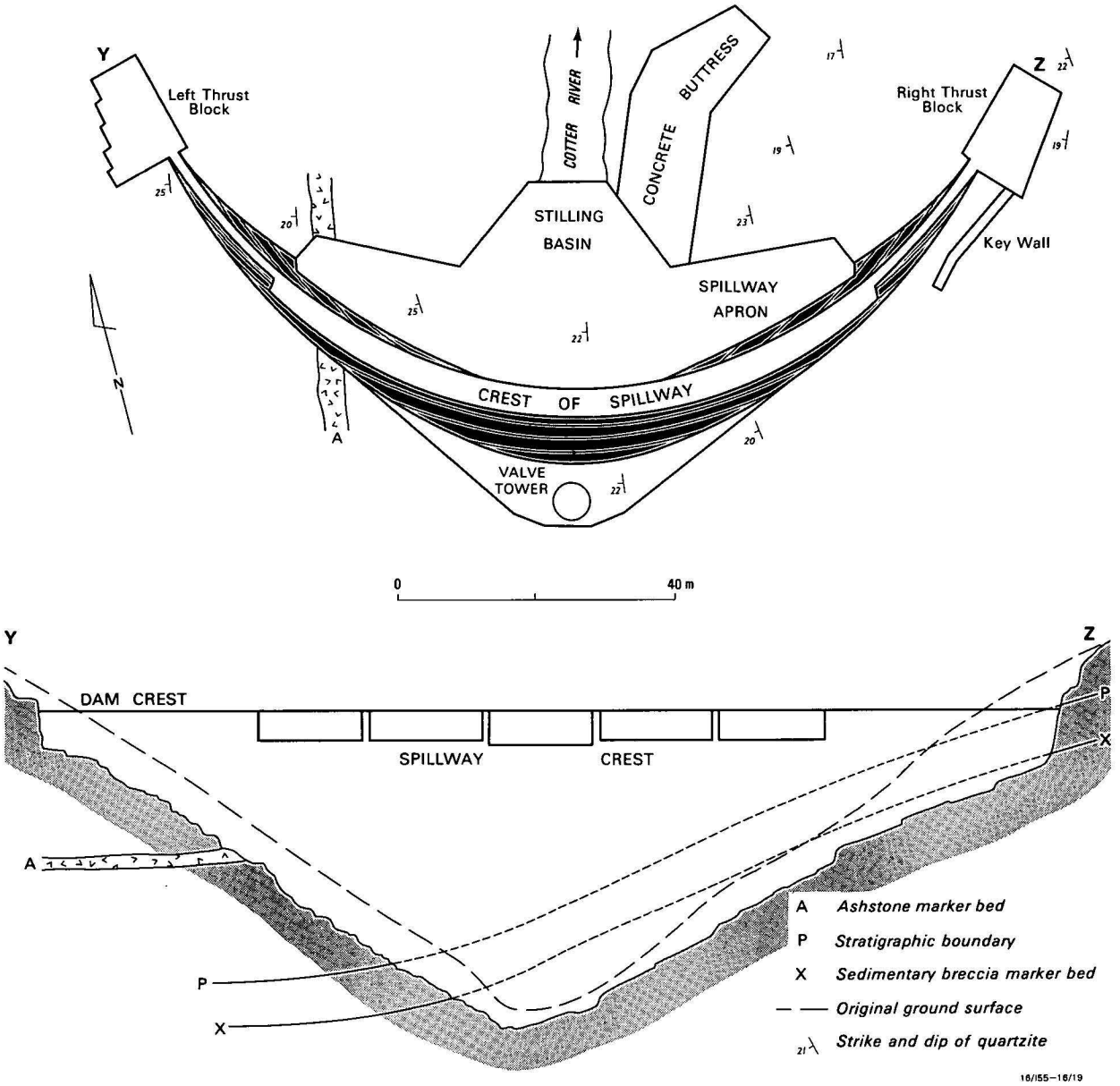

Figure 4. Bendora Dam site, showing generalised foundation geology and layout of engineering structures.

marker beds for the detailed geological mapping of the site.

Bedding plane joints are well-developed throughout the sequence. In the western foundations, the beds dip into the hillside, and no major problems were encountered during excavation of the foundations. On the eastern side of the river, however, the beds dips towards the river at a lower angle than the ground surface, yet at a sufficiently high angle for sliding of rock along major bedding planes to be possible. The excavation for the right thrust block aggravated this potential instability by undercutting the uphill beds (Figure 4, just downhill from Z), and there was concern that a rockslide could occur just upstream from the thrust block, which would endanger the dam wall. The area downstream of the right bank spillway apron was also considered to be potentially unstable, and it was thought that vibration of the rock during large spillway flows could trigger off rockslides, if suitable precautions were not taken.

Stability of right thrust block

Excavation of foundations for the right thrust block showed that the quartzite was open-jointed to depths of up to 10 metres. The progressive geological mapping showed that most of the open joints terminated at the sedimentary breccia marker bed (Bed X), joints in the quartzite below Bed X being generally tight.

Later excavation of the dam foundations just downhill of the thrust block revealed a major open vertical joint with an aperture of 3 to 5 cm, underlain by a 15 cm thick clayey seam of crushed rock parallel to bedding. The opening up of the vertical joint could have been caused by sliding of the rock downhill along the bed of crushed rock, and it was possible that such movement could occur again, especially if the crushed seam became saturated after filling of the reservoir. Further detailed mapping showed that the clayey seam was sedimentary breccia Bed X which had been locally crushed or sheared. In view of the poor quality of Bed X and the open jointing of the overlying rock, it

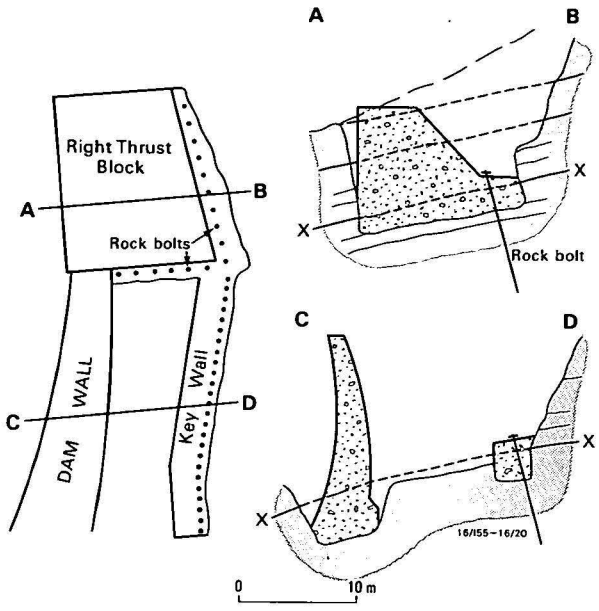

X-----X *Sedimentary breccia marker bed*

Figure 5. Treatment to stabilise potential slip plane in right thrust block excavation, Bendora Dam.

was decided that the right thrust block foundations be excavated down to the base of the quartzite bed immediately below Bed X, or deeper (see section in Figure 4).

However, while the above measures ensured good foundations for the thrust block itself, the deep excavation increased the instability of rock uphill of the thrust block and dam wall. If the shearing of Bed X persists in the up-dip direction, then the frictional resistance of the bed may well be insufficient to resist the weight force of the overlying quartzite beds, particularly in the area where Bed X would be saturated after filling of the reservoir. Considerable geological mapping and laboratory testing indicated that Bed X was not extensively sheared, and did not deteriorate in the short term when saturated with water. It was also shown that the freeze-thaw mechanism contributed significantly (and possibly entirely) to the opening of vertical joints in the quartzite. Despite this evidence, the possibility of sliding of rock along Bed X could not be completely ruled out, and so preventative measures were taken.

The measures adopted are shown in Figure 5. A trench 3 m wide, 2-3 m deep, and 23 m long was excavated into the rock below the general foundation surface (which is a prominent bedding plane below Bed X). This trench was then filled with concrete to form a key wall, which was built up to a level about 1 m above Bed X. The resistance of this key wall was considerably increased by anchoring it to the foundations at a depth of 6 m with 25 tensioned rock bolts, installed at a spacing of 90 cm. The key wall also extends around the upstream sides of the thrust block, and a further 16 rock bolts were installed. Under these conditions, the angle of friction of Bed X will need to decrease to 7.5° before there is any danger of sliding; the estimated angle of friction of the crushed rock when saturated is 19°, so the precautionary measures incorporate a factor of safety of 2.6, even assuming the worst conditions for Bed X.

Stability of spillway beds

During the feasibility/design investigation at Site C, a prominent quartzite exposure on the right bank immediately downstream of the proposed spillway apron was mapped. Apart from the prominent bedding plane jointing typical of the site, the quartzite in this area is transected by a conjugate set of steeply dipping joints. Several of the bedding plane joints are developed along thin sedimentary breccia beds which dip at 17° to 23° towards the river, and near river level these beds have been preferentially eroded to form several overhanging cliffs. The mapping revealed obvious downhill movement of blocks of quartzite along bedding planes, and loosening of the bedrock to a depth of 4 m was apparent. This large area of unstable rock would obviously become more unstable during operation of the proposed overflow spillway, unless substantial treatment was carried out to stabilise the area. An alternative spillway design on the left abutment was considered by the engineers, but a cost analysis showed that it would be cheaper to stabilise the right bank quartzite beds.

About 550 m^2 of bedrock downstream of the right spillway apron was stabilised during construction. The exposed bedrock surface was mapped, and the five most prominent bedding plane surfaces were identified. (A, B, C, D and E in Figure 6). A number of major conjugate joints were also accurately located during the geological mapping, but these have been omitted from Figure 6 for reasons of clarity. The specifications for stabilisation of these blocks of quartzite were as follows.

(a) Clean out all open fissures and fill them with concrete.
(b) Wash the sub-surface fissures and seal them with cement grout injected at low pressure.
(c) Anchor the surface blocks of quartzite to good rock at depth by installing tensioned and grouted rock bolts.
(d) Construct a concrete buttress at the foot of the rock slope to support all quartzite beds below bedding plane C, and protect the rock slope from further erosion and undercutting.

All of the 175 rock bolts installed were individually located by the site geologist. Most of the bolts were oriented perpendicular to the bedding plane surfaces so that all surface beds are tied to deeper beds as shown in the section of Figure 6; in this way, all of the loose bedding slabs were progressively 'clamped' together to form a coherent slab, which is supported by the concrete buttress and also tied to rock below plane E by rock bolts. Some of the rock bolts were oriented so as to tie rock together across a few major near-vertical joints; these bolts had a declination of 60° and were directed perpendicular to the joint strike. The approximate position of the major joints treated in this way can be inferred from the pattern of rock bolts shown in Figure 6.

Corin Dam

The general arrangement of Corin Dam and its associated structures is shown in Figure 7, together with a nominal dam cross section to show the main features of the dam design. No attempt has been made to show the foundation geology because of the variability of the lithology, and the complexity of folding and faulting at the site. In summary, the foundations consist of a sequence of interbedded quartzite, silicified sandstone, and laminated siltstone, which has

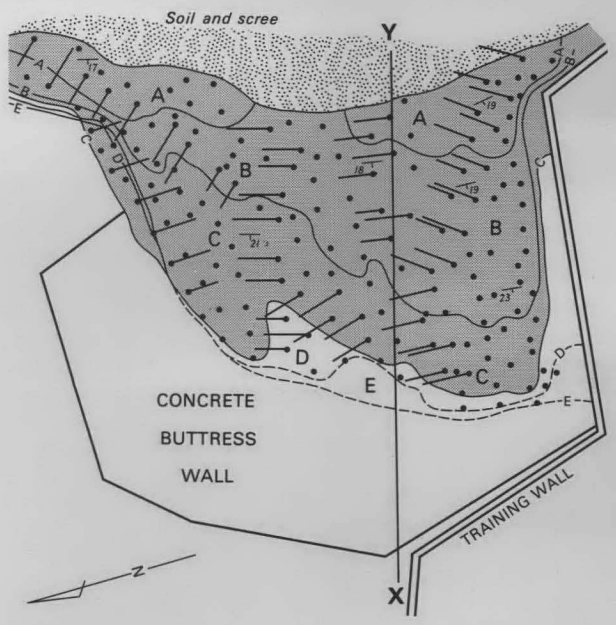

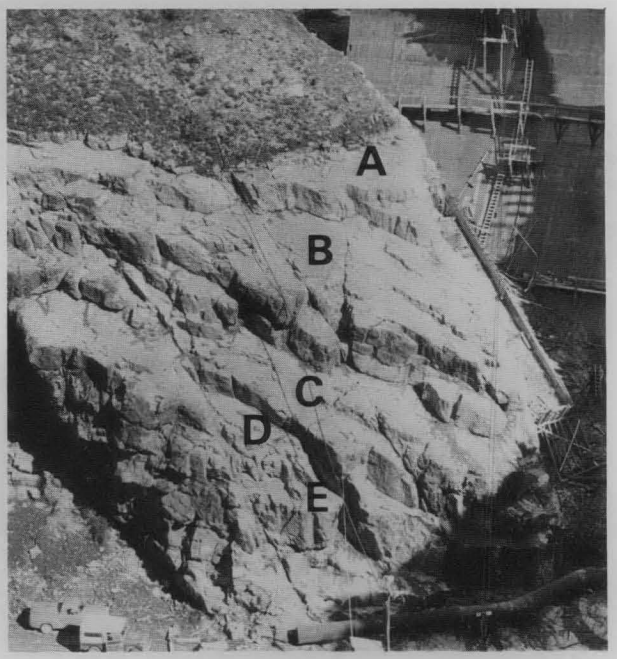

Figure 6. Treatment of unstable rock downstream of right spillway apron, Bendora Dam.

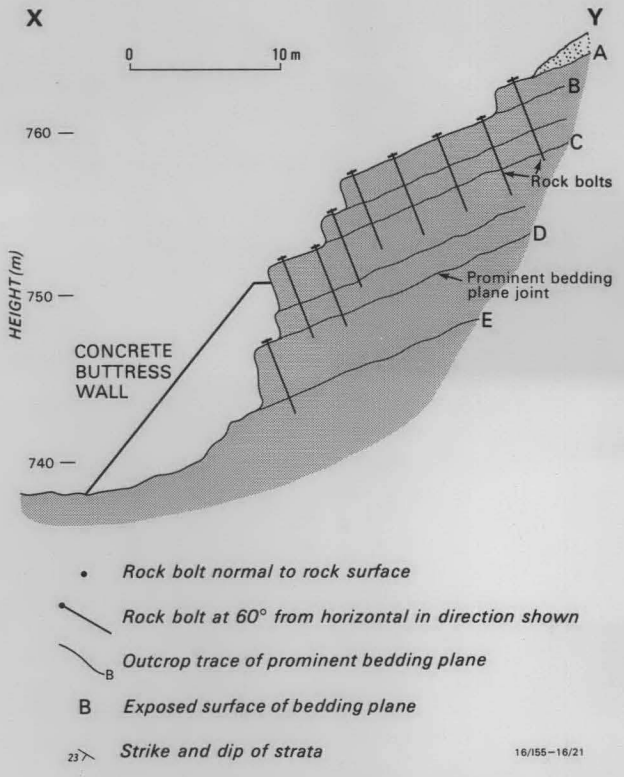

been tightly folded and considerably faulted. The regional strike is north-west, and bedding dips are generally steeper than 45°.

The dam itself is made up of three zones; the impermeable core zone (zone 1), the filter zone (zone 2) and the rockfill zone (zone 3). The upstream and downstream rockfill zones are each subdivided into four zones which increase in coarseness from the filter zone outwards; zone 3a was placed and compacted in 45-cm layers, 3b in 90-cm layers, 3c in 1.8-m layers, and 3d is a protective layer of very coarse rockfill placed on both faces of the dam. This progressive grading of the material in a rockfill dam is an important design feature to prevent migration of fine grained material from the core zone, which could lead to failure of the impermeable membrane.

Location of dam

The site for Corin Dam was originally selected because of the pronounced widening of the Cotter valley immediately upstream, which results in a large reservoir storage capacity; downstream of Corin Dam, the Cotter River flows in a narrow, youthful valley with overlapping spurs and steep valley sides (Fig. 8).

This sudden change in the physiography of the Cotter valley is a direct result of variations in the regional geology. Downstream of Corin Dam, the Cotter River flows over a sequence of folded, north-westerly striking metasediments. This sequence is terminated just west of the river by the Cotter Fault, a major structural feature which has controlled the overall course of the Cotter River, and to the west of the fault there is a sequence of westerly-dipping phyllites and quartzites. Upstream of the dam site, however, faulted blocks of quartz porphyry occur to the east of the main Cotter Fault (Oldershaw, 1965), and the preferential weathering and erosion of this zone of porphyry (which is up to 600 m wide) have resulted in the development of a comparatively broad and straight valley floor. The valley sides are generally as steep as those downstream from the dam site, but the extra width of the valley floor has effectively doubled the storage capacity of an equivalent dam located in the adjoining downstream tract of the Cotter River.

Location of construction materials

Core material. The faulted blocks of quartz porphyry have also provided suitable core material close to the dam site. Weathered granitic rocks usually form good core zone material: the weathered feldspars provide the clay binder which makes the material impermeable, while the residual quartz grains give the weathered material strength and rigidity. A program of augering and trenching during the design investigation was carried out in areas where the quartz porphyry was

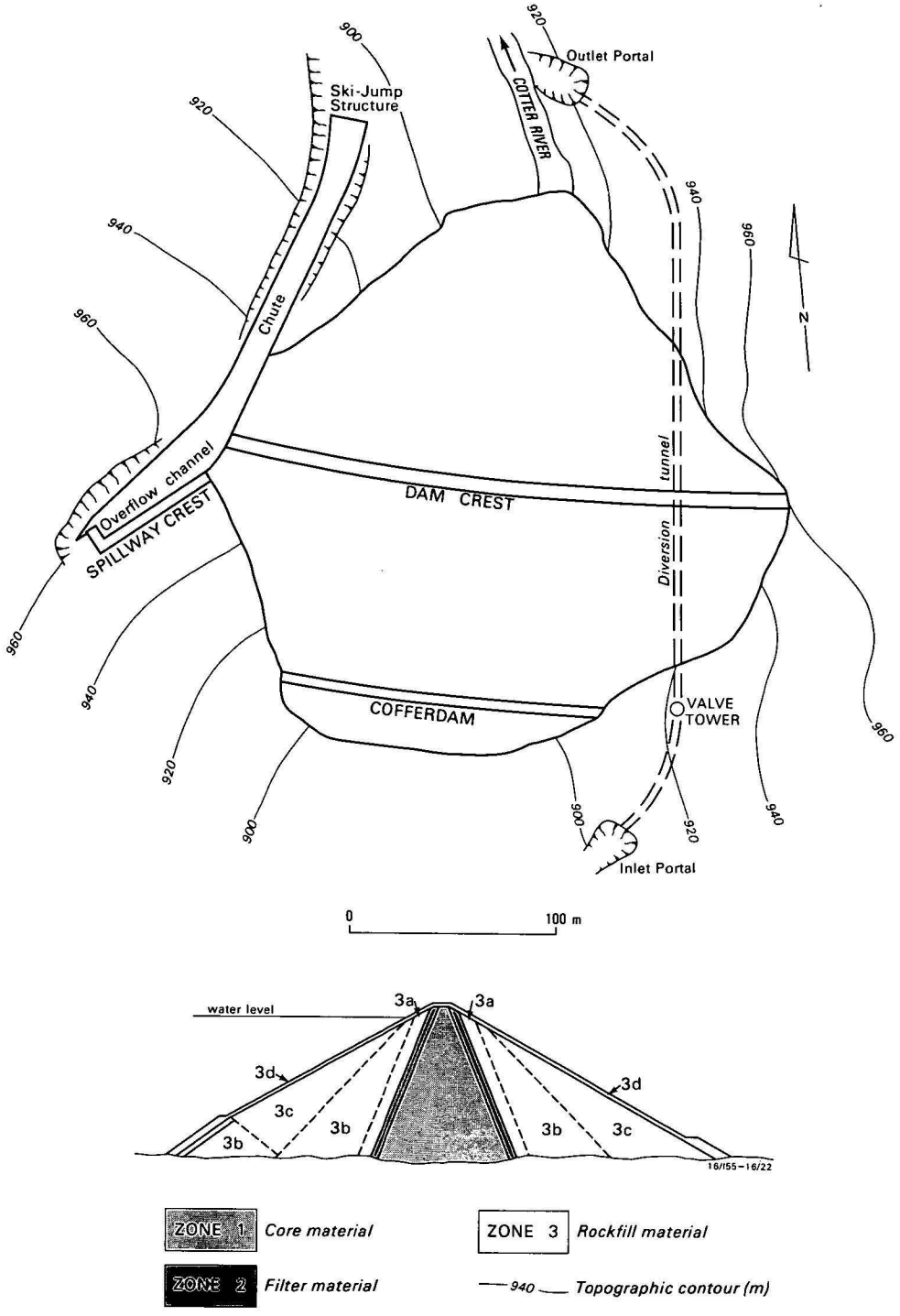

Figure 7. Design layout of Corin Dam.

exposed, and a spur of deeply weathered (up to 40 m) porphyry was located 1300 m upstream from the dam site (Figs. 8 and 9). Engineering tests proved its suitability for use as core material, and the bulk of the 262 000 m^3 required for the impermeable core was obtained from this site.

Filter material. The presence of the quartz porphyry in the valley floor upstream of the dam site was also significant in providing a cheap source of filter material for the dam. The broad valley floor on the porphyry, together with a slight but significant decrease in river gradient on the less resistant porphyry, resulted in the deposition of substantial volumes of alluvium in the valley within 1.5 km of the dam site (Fig. 9). A total of 89 000 m^3 of filter material was placed in the dam, and most of this was obtained from an extensive alluvial deposit 500-800 m upstream of the dam site.

Rockfill material. Rockfill material for a dam must fulfil certain requirements of strength, size range, and shape. In particular, the material must not contain more than a specified proportion of fine-grained fragments, and must not disintegrate or slake during long term saturation. In the context of Corin Dam, the rockfill had to be composed essentially of sandstone or quartzite, with only a small proportion of siltstone interbeds allowable.

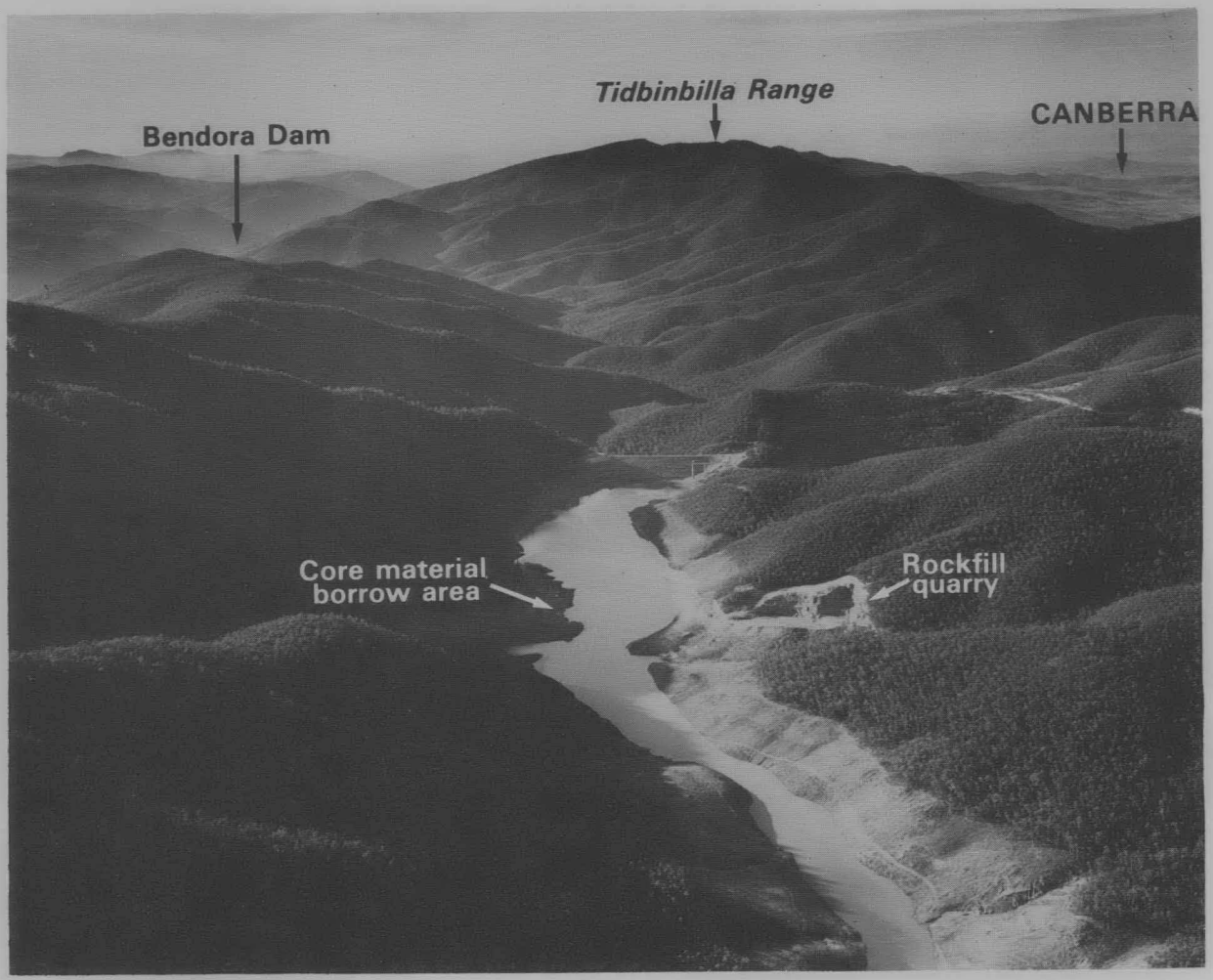

Figure 8. Aerial view of middle reaches of the Cotter Valley immediately upstream of Corin Dam (News and Information Bureau photograph NDC 1113/22).

During the feasibility investigation, a number of prominent outcrops of sandstone were noted close to the site, and one of these (R1 in Fig. 9) was investigated by a diamond-drill hole. It was concluded that a suitable source of rockfill would be present close to the site. This was also the opinion of outside consultants, who stated that the area R2 in Figure 9 would probably be a suitable quarry site.

Once the decision had been taken to construct a rockfill dam, R2 was investigated by diamond drilling, which revealed the presence of siltstone interbeds scattered throughout the sandstone sequence. It became evident that the siltstone/sandstone ratio was too high for suitable rockfill, and so investigations moved to site R3. These showed that sites R1 and R3 combined could just provide sufficient rockfill material; however, as the sandstone sequence dips at 80° and would have to be quarried to depths of up to 75 m, the waste rock/rockfill ratio would be high, giving a high cost per unit volume for the rockfill.

The search was then extended up the Cotter valley, and a promising site was located 1.5 km upstream (R4 in Fig. 9). A prominent cliff of quartzite 45 m high was found, exposed at the end of a westerly trending spur between two tributary creeks of the Cotter River. The quartzite dipped east at only 15°, and mapping along the spur to the east revealed a sudden change in bedding attitude to 75° west, suggesting a syncline which would bring the prospective quartzite back to the surface. Bulldozed trenching and diamond drilling confirmed the synclinal structure, and further detailed geological investigations showed that this would be an ideal location for the rockfill quarry.

A simplified plan and cross-section of the rockfill quarry is shown in Figure 10. The massive quartzite, which originally cropped out in the cliff, is overlain by a sequence of sandstone with siltstone interbeds, which in turn is overlain by laminated siltstone. The massive quartzite is underlain by a sequence of well-bedded quartzite, occurring as beds ranging from 5 cm to 75 cm thick. Only the laminated siltstone sequence was unsuitable for rockfill, and this was removed from the site before quarrying for rockfill commenced. The proportion of siltstone in the upper beds of the interbedded sequence was sufficiently high for excess fines to be formed, but mixing with good quality rock reduced the volume of material rejected from the quarry to an insignificant amount.

As expected, the quarry produced rock of adequate durability and grading for use as rockfill. However, the engineering properties of the rockfill and the economics of quarrying were considerably enhanced by particular geological features of the quarry area.

1. The three rock sequences quarried had different ranges in spacing of bedding planes, and this greatly facilitated provision of suitable rock for the four

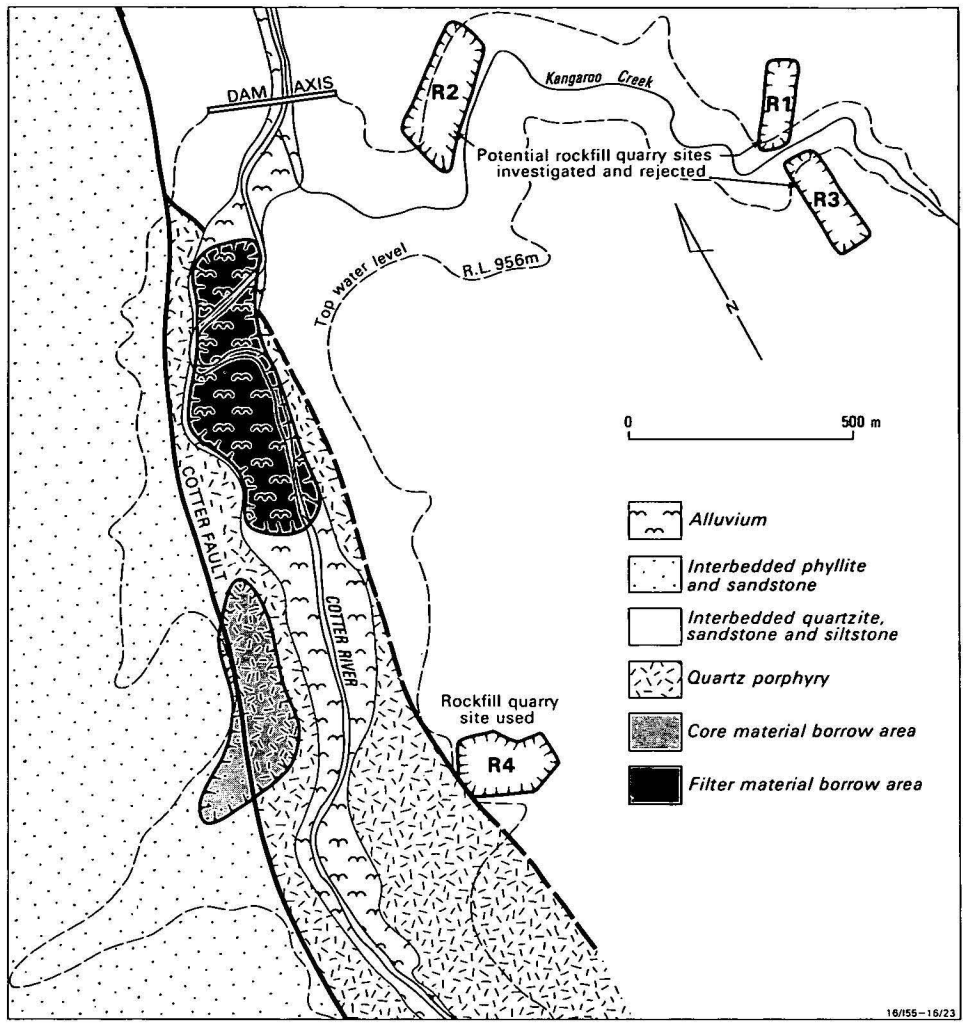

Figure 9. Sources of construction materials for Corin Dam.

rockfill zones in the dam. The interbedded sandstone and siltstone provided material for zone 3b and to a lesser extent 3a; the massive quartzite provided rock for zones 3c and 3d; and the well-bedded quartzite was used for most of zone 3a and some of zone 3b.

2. The folding and faulting of the rock sequence had formed well-developed joint sets, even at depth, and this resulted in very good and economical rock fragmentation during blasting. No secondary blasting was necessary during the entire quarrying operation.
3. The absence of a dominant joint set resulted in the formation of irregular, roughly equidimensional rock fragments, which are ideal for rockfill.
4. The folding of the geological succession was very convenient for quarrying operations, because benches could be developed so as to expose the different rock sequences in the same quarry face. This enabled working of the most suitable rock sequence to provide rockfill for any particular zone of the dam at any time. It also allowed easy mixing of good rock with the marginal quality rock from the top of the interbedded sequence to produce suitable rockfill.

The total volume of solid rock quarried was 789 500 m^3 which, when placed and compacted in the dam, produced 1 039 400 m^3 of rockfill. This gives a bulking factor of 1.32, which is indicative of the high quality of the rockfill.

Stability of spillway crest

The spillway crest is a concrete structure which controls the overflow level of the reservoir. It is constructed on the lip of a concrete-lined excavation in rock, called the overflow channel, which directs the water down a concrete chute into the river valley downstream of the dam (Fig. 7). The force of water flowing over the crest exerts a considerable overturning moment on the crest structure; this is resisted by the installation of a number of steel cables, anchored to the bedrock, which effectively tie the crest structure to solid rock at depth.

The overflow channel is a large excavation into bedrock, with a maximum vertical depth below original bedrock surface of 25 m on the uphill side. It was obviously desirable to design the walls of the excavation at as steep an angle as possible so as to minimise the amount of rock to be removed. A joint survey of the spillway area, carried out during the site investigation, revealed the presence of six joint sets in the rock; however, a stereographic analysis of joints (Fig. 11) indicated that none of these sets was unfavourably oriented with respect to a steep rock face on the uphill side of the proposed excavation. The overflow channel

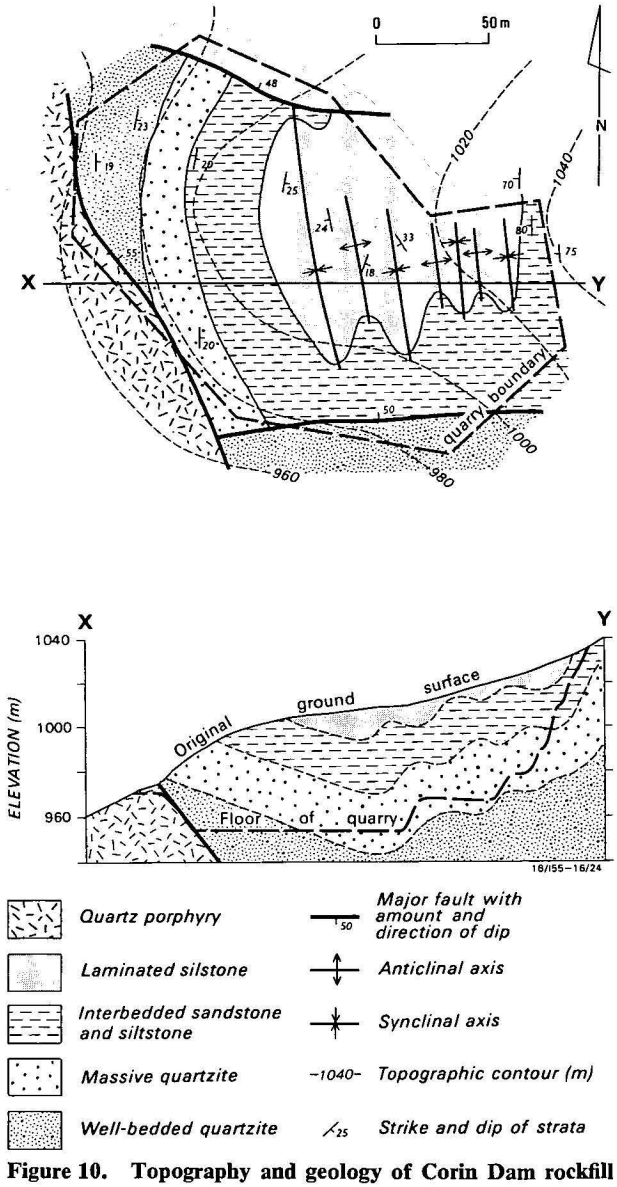

Figure 10. Topography and geology of Corin Dam rockfill quarry.

excavation was therefore designed with walls at an angle of 65°.

Excavation of the spillway channel went ahead according to the design, and no rock slope stability problems were encountered. However, when the contractor blasted the rock on the downhill side of the excavation to form the spillway crest foundations, considerable overbreak of rock occurred at the lip of the excavation along two thirds of the length of the crest area. The overbreak was caused by one of the joint sets being unusually well-developed in this particular area of the spillway. Although the downhill wall of the excavation was only 5 to 7 metres high, the well-developed joint set was adversely oriented with respect to the rock slope, and the situation would obviously be aggravated by the forces imposed by the spillway crest structure. A detailed joint survey of the crest area was therefore carried out to provide a basis for stabilising the crest and its foundations.

The joint set causing the problem was Set 4 in Figure 11, which dips at 30° to the north. It is present in bedrock over a large area of the western abutment, but in the spillway crest area the joints of this set are more closely spaced and much more continuous than elsewhere (Fig. 12). This condition was not apparent during the original joint survey of scattered outcrops of weathered surface outcrops.

The original design for the spillway crest structure is shown in Figure 13, along with the modified design necessary to overcome the foundation instability. There were 3 stages in the stabilisation of the spillway crest:

1. Installation of 137 rock bolts, each 4 m long, along the wall of the excavation—these replaced the grouted anchor bars of the original design.
2. Placement of a concrete slab on the irregular rock surface of the crest foundation, followed by the installation of 46 rock bolts, each 6 m long, on a 2-m grid spacing.
3. Installation of 26 post-tensioned cables, each 11 m long and tensioned with a force of 498 MN (50 tons). In the original design, these cables were vertical, and would therefore not contribute to the stability of the jointed rock. However, by re-orienting the cables to an angle of 65° (i.e. roughly perpendicular to the adversely-oriented joint set), the stability of the crest and its foundations was considerably enhanced.

This particular example is typical of the problems which arise during a major construction project as a result of the geological variability of rock, particularly at depth below the surface. While the remedial work resulted in extra cost (due mainly to extra materials and the 3-stage construction of the concrete crest), the recognition, investigation and evaluation of the problem was quickly carried out and there was no costly delay in the overall construction schedule. The problem could not have been predicted from the information available before construction started.

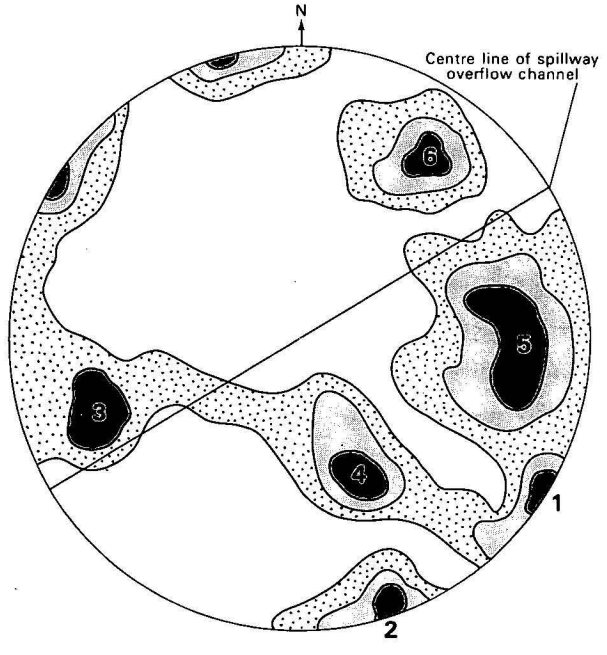

Figure 11. Stereographic plot of joint survey from the spillway area, Corin Dam.

Figure 12. Corin Dam spillway crest foundations, showing overbreak along well-developed 30° joint set.
The arrows in the top photograph identify some of the prominent joint faces.

A detailed account of all geological aspects of the construction of Corin Dam is given in Best (1969).

Googong Dam

Googong Dam is an earth-cored rockfill dam 62 m high, containing 801 000 m^3 of fill material. The general arrangement of the dam and spillway is shown in Figure 14, together with the foundation geology. A critical feature of the design was that rock from the excavation for the spillway channel and energy dissipation basin should provide all of the rockfill for the dam.

The geology in Figure 14 gives only a general picture of the distribution of rock types. The dam foundation and the spillway excavations contained several major faults and many shear zones, which required careful evaluation as construction proceeded. In particular an extensive clay seam exposed in the right abutment foundations posed a potential threat to the stability of part of the dam foundations.

Rockfill quarries

The design layout of the spillway approach channel and the energy dissipation pool formed two quarries for rockfill, known as the upper and lower quarries respectively. The site investigation predicted that 500 000 m^3 of suitable rockfill would be produced from these two quarries, which was 75 000 m^3 less than required; it was anticipated that this balance would be obtained from zones of better quality rock in the excavation for the spillway chute.

In the upper quarry, the lenses of sediment posed greater problems than anticipated. It was intended that

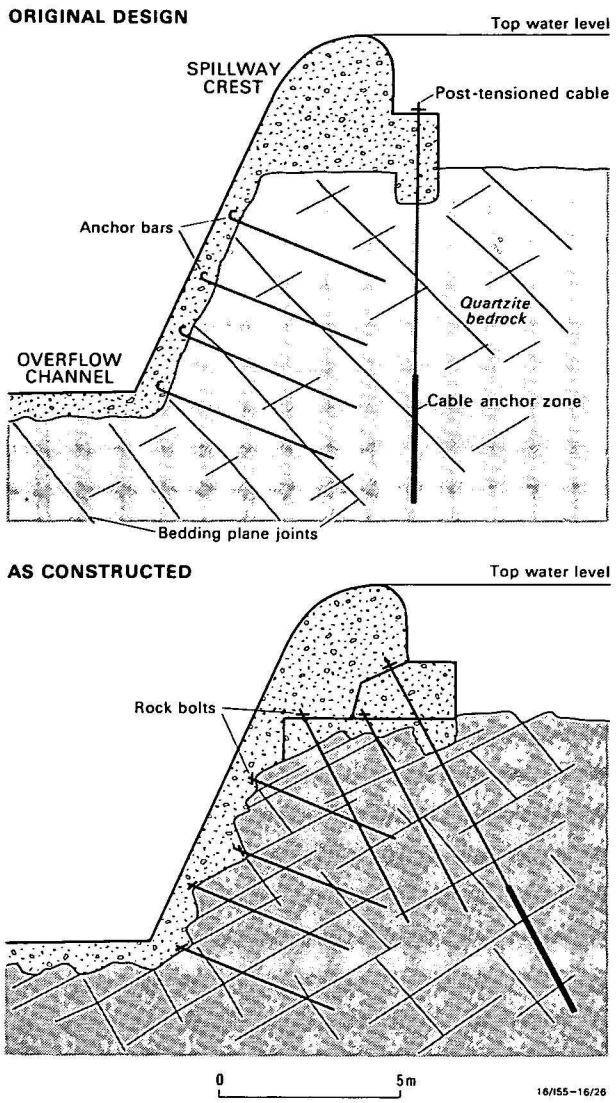

Figure 13. Sections through the spillway crest, showing the original design and design as constructed.

the working face of the quarry be oriented perpendicular to the strike of the sediments, so that the poorer quality sediments could be mixed with good quality dacite to form a satisfactory rockfill material. However, the contractor found difficulty in working this way, and had to excavate benches parallel to the sediments. As a result, thick lenses of sediments had to be excavated and discarded. An additional problem was that the excavated dacite had a high proportion of fines which reduced the bulking factor from an expected 1.30 to 1.25. The net result of these problems was that the upper quarry produced considerably less rockfill than predicted. It was obvious that, even using the most optimistic assumptions for the lower quarry, there would not be enough rockfill within the design limits of the spillway excavation, and so the upper quarry was extended by working a deeper bench in the floor of the approach channel. This extension beyond the original design limit of the quarries produced 11% of the total rockfill for the dam.

Clay seam in dam foundations

Cleaning down of the right bank dam foundations revealed a major seam, 10-50 cm thick and filled with clay and weathered rock, exposed for 130 m in the core zone foundations (Fig. 15). It has a downhill dip component ranging between 15° and 40°, and so the stability of the large volume of rock overlying the seam had to be carefully considered. The following steps were taken to investigate the properties of the seam and the overlying rock.

1. An uplift gauge was installed to monitor rock movement during grouting.
2. The area was accurately surveyed and a geological map at 1:200 scale was prepared, from which a three-dimensional model was constructed.
3. The nature and position of the seam at depth was investigated by drilling.
4. A joint survey was carried out on the overlying rock.
5. The clay material was analysed; it was found to consist of 80-90% crushed quartz and plagioclase with about 10% montmorillonite.
6. Laboratory tests were carried out to determine the likely friction angle of the seam, and the weight density of the overlying rock.

The quantitative data obtained from these investigations were then used in stability analysis calculations for a wide range of environmental conditions, such as hydrostatic forces in the rock and the effect of earth tremors. The factor of safety of the seam was generally found to be greater than 1.0, but a combination of high hydrostatic pressure and an intensity VI earth tremor (recurrence interval of at least 1500 years) would be sufficient to cause failure given certain simplistic assumptions necessary in the analyses. The actual factor of safety against sliding would be increased by factors such as side constraints and non-planar surfaces, and once the dam was constructed, the weight of the embankment against the foundations would also have a considerable stabilising influence. Despite this, it was considered prudent to adopt special measures over and above the standard procedures for foundation treatment.

1. Consolidation grouting (normally only carried out in core zone foundations) was extended into the rockfill zone foundations to consolidate the potentially unstable rock above the clay seam.
2. Water testing of grout holes intersecting the seam was not carried out, as the water could cause uplift of the overlying rock and could reduce the cohesion of the seam material.
3. During grouting of rock overlying the seam, a careful watch was kept for surface leaks and sudden increases in grout consumption; either of these circumstances could indicate that rock uplift was taking place.
4. Excavation of clayey and crushed rock in the outcrop trace of the seam was rigorously carried out, and the seam exposure was carefully sealed off with concrete.

In view of the above investigations and remedial measures, it is concluded that the rock overlying the seam is stable and it is not expected to cause problems during the life of the dam.

A detailed account of geological aspects of the construction of Googong Dam is given in Goldsmith (1979).

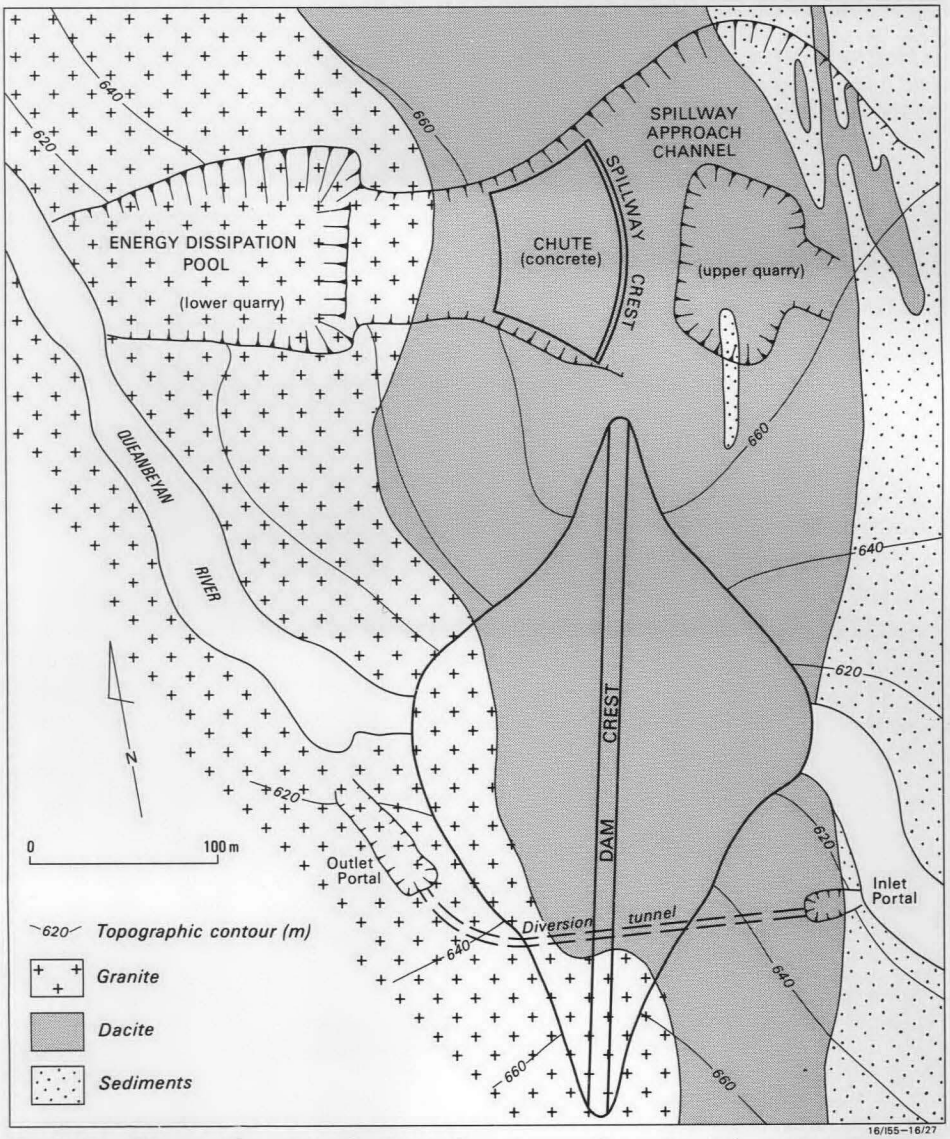

Figure 14. Googong Dam area, showing geology, topography, and engineering layout.

Figure 15. Clay seam in right bank of Googong Dam foundations.

Discussion

In this paper, I have shown the significant role of geology during the main phases of the development of Canberra's water supply dams:

1. the selection of the most suitable site for each dam;
2. the design of the most economic dam at each selected site; and
3. the economic and safe construction of each dam.

I have also described at least one example of geologically-based problems which arose during construction of each dam, and these are by no means the only such problems which occurred. However, the overall success of the investigation and construction of these dams is shown by the fact that no significant stability problems have occurred, and that the actual construction cost of each dam was very close to the original contract price.

When designing a large dam, the engineer has two prime objectives:

1. the dam must be stable and successfully fulfil its function throughout its projected life; and
2. the dam and its associated structures must be constructed as economically as possible.

Of course, there is a dilemma here, because the two objectives act against each other; ensuring stability by over-design increases the cost, while cost-cutting methods, if taken to extremes, will lead to an unsafe structure. The optimum design and construction of a dam is therefore a delicate balance, and the geology of the dam site and reservoir area is a very important part of this balance.

On a world-wide scale, it is clear that the objective of constructing stable dams is not always achieved. During the period 1900-1965, about 1 percent of the 9000 large dams in service throughout the world have failed, and another 2 percent have suffered serious accidents; significantly, in more than half of these 'incidents', the failure or damage could be related to geological causes (Stapledon, 1976). The magnitude of the problem can be illustrated by quoting brief details of some recent failures.

Malpasset Dam, France— a 60-m high double curvature arch dam which failed in 1959 with the loss of 400 lives. The cause of failure was uplift and sliding of a section of the rock foundations (Jaeger, 1963; Londe 1967).

Vajont Dam, Italy— a 265-m high double curvature arch dam. In 1963, some 260 million m^3 of rock slid into the reservoir just upstream of the dam, and more than 2000 lives were lost in the flood caused by the displaced water which overtopped the dam (Muller, 1963). The dam itself did not give way, so this was a reservoir failure rather than a dam failure.

Baldwin Hills Storage Basin, U.S.A.— this structure failed in 1963, after 12.5 years of service, with the loss of 5 lives and $15 million damage. The cause of failure was subsidence and erosion, owing to movement along fault planes (James, 1968).

Teton Dam, U.S.A.— a 92-m high earth dam with a volume about 7 times that of Corin Dam. Failure occurred in 1976 with the loss of 11 lives and damage estimated at about $400 million. The investigating committee concluded that failure was probably caused by a combination of inadequate sealing of bedrock in a critical part of the dam foundations, and inadequate protection of the core material against internal erosion (U.S. Department of the Interior, 1977).

It might be expected that progressive advances in dam design and construction techniques would result in a lower incidence of failures. However, this does not appear to be the case, and there are two main reasons:

1. With any technological advance, there are always likely to be unforeseen factors which can produce unexpected problems. For example, when Malpasset Dam was constructed, drainage of foundations to reduce hydrostatic pressures downstream of arch dams was not considered necessary (Malpasset was one of the first dams constructed to the then-new double curvature thin arch design); the subsequent failure was caused by hydrostatic uplift in the foundations.
2. As the obvious and easy dam sites around the world are used up, future dam construction will be necessary at progressively more difficult and geologically complex sites, which increases the probability of foundation problems arising. It is therefore clear that if dam failures and accidents are to be minimised in future, the role of geology must be maintained or enhanced during the investigation, design construction, and monitoring of dams.

Geology is no less important in helping to achieve the engineer's other objective of constructing a dam as economically as possible. There are hundreds of case histories of dams costing much more than the original contract price, and unexpected geological features are often the cause of expensive problems. In many cases, these unexpected problems could have been identified and avoided by a more thorough geological investigation. It is possible to over-investigate a site, but I doubt that it has ever been done. In many cases, dam sites are under-investigated and the resultant extra cost of construction is far greater than the additional expense that would have been necessary to carry out a thorough investigation.

Geology has always had a significant influence on the location, design and construction of dams. If safe and economic dams are to be constructed in the future, then recognition of this influence must be increased on the world-wide scale.

Acknowledgements

This paper is a very brief summary of some of the work carried out by the Engineering Geology and Engineering Geophysics Sections of BMR during the past 35 years. Most of the major contributors to the investigations described are identified in the list of references. However, many other BMR personnel, too numerous to mention individually, have been involved to various degrees in the work, and their contributions are gratefully acknowledged.

I thank the Director of BMR for the opportunity to spend 5 months' study leave there in 1980, during which time this paper was written.

References

BEST, E. J., 1965—Geological report on the feasibility and design investigation of Corin damsite, Cotter River, A.C.T. *Bureau of Mineral Resources, Australia, Record* 1965/200 (unpublished).

BEST, E. J., 1969—Geological report on site investigation and construction of Corin Dam, Cotter River, A.C.T. *Bureau of Mineral Resources, Australia, Record* 1969/111 (unpublished).

BEST, E. J., & HILL, J. K., 1962—Geological investigation of damsite E, upper Cotter River, A.C.T. *Bureau of Mineral Resources Australia, Record* 1962/140 (unpublished).

BEST, E. J., & HILL, J. K., 1967—Site investigation techniques used at Corin damsite, Cotter River, A.C.T. *Proceedings of the 5th Australia-New Zealand Conference on Soil Mechanics and Foundation Engineering*, 1-8.

BUCHHORN, D. A., 1968a—Geological investigation of Tennent damsite, Gudgenby River, A.C.T. *Bureau of Mineral Resources, Australia, Record* 1968/88 (unpublished).

BUCHHORN, D. A., 1968b—Geological investigation of Coree damsite, Cotter River, A.C.T. *Bureau of Mineral Resources, Australia, Record* 1968/98 (unpublished).

BURTON, G. M., 1963—Googong damsite, Queanbeyan River, N.S.W. Report of investigations May 1961-August 1963. *Bureau of Mineral Resources, Australia, Record* 1963/68 (unpublished).

FOWERAKER, J. C., 1958—Geological report of damsite C, upper Cotter River, A.C.T. *Bureau of Mineral Resources, Australia, Record* 1958/16 (unpublished).

GARDNER, D. E., 1957—Investigation of sources of aggregate and sand, damsite C, upper Cotter River. *Bureau of Mineral Resources, Australia, Record* 1957/55 (unpublished).

GOLDSMITH, R. C. M., 1979—Geological report on the construction of the Googong Dam, Queanbeyan River, N.S.W. *Bureau of Mineral Resources, Australia, Record* 1979/83 (unpublished).

HALDANE, A. D., CARTER, E. K., & BURTON, G. M., 1971—The relationship of pyrite oxidation in rockfill to acid water at Corin Dam, A.C.T., Australia. *Proceedings of 1st International Congress of the International Association of Engineering Geology, Paris, 1970.*

HAWKINS, L. V., & STOCKLIN, A., 1956—Seismic survey of the eastern abutment of damsite B, upper Cotter River, A.C.T. *Bureau of Mineral Resources, Australia, Record* 1956/124 (unpublished).

JAEGER, C., 1963—The Malpasset report. *Water Power,* February 1963.

JAMES, L. B., 1968—Failure of Baldwin Hills Reservoir, Los Angeles, California. *Geological Society of America, Engineering Geology Case Histories,* No. 6, 1-11.

LONDE, P., 1967—Panel discussion. *1st Congress of the International Society of Rock Mechanics, Proceedings,* III, 449-453.

MULLER, L., 1963—The rock slide in the Vajont valley. *Rock Mechanics and Engineering Geology,* 2, 149-212.

NOAKES, L. C., 1946a—Damsites in the upper Cotter valley between Bushrangers and Collins Creeks. *Bureau of Mineral Resources, Australia, Record* 1946/12 (unpublished).

NOAKES, L. C., 1946b—Damsite E, upper Cotter River. *Bureau of Mineral Resources, Australia, Record* 1946/26 (unpublished).

NOAKES, L. C., 1955—Proposed diamond drilling at damsite A, upper Cotter River, A.C.T. *Bureau of Mineral Resources, Australia, Record* 1955/68 (unpublished).

NOAKES, L. C., 1956—Upper Cotter damsite investigations, damsite C; progress geology report and proposed drilling programme. *Bureau of Mineral Resources, Australia, Record* 1956/98 (unpublished).

NOAKES, L. C., FOWERAKER, J. C., BURTON, G. M., 1957—Second progress report, damsite C, upper Cotter River, A.C.T. *Bureau of Mineral Resources, Australia, Record* 1957/17 (unpublished).

OLDERSHAW, W., 1965—An investigation of the Cotter and other faults near the Corin damsite, upper Cotter River, A.C.T. *Bureau of Mineral Resources, Australia, Record* 1965/86 (unpublished).

PERRY, W. J., 1953—Geological survey of upper Cotter damsites A and B. *Bureau of Mineral Resources, Australia, Record* 1953/108 (unpublished).

SALTET, J. A., 1971—Googong damsite, Queanbeyan River, N.S.W., feasibility investigations 1970 and 1971. *Bureau of Mineral Resources, Australia, Record* 1971/52 (unpublished).

SIMPSON, G. B., 1974—Googong damsite, Queanbeyan River, N.S.W. geological investigation 1972 and 1973. *Bureau of Mineral Resources, Australia, Record* 1974/100 (unpublished).

STAPLEDON, D. H., 1976—Geological hazards and water storage. *Bulletin of the International Association of Engineering Geology,* 14, 249-262.

TAYLOR, F. J., & PETTIFER, G. R., 1972—Googong damsite spillway, seismic refraction survey, 1971. *Bureau of Mineral Resources, Australia, Record* 1972/2 (unpublished).

U.S. DEPARTMENT OF THE INTERIOR, 1977—Failure of Teton Dam: a report of findings.

BMR Journal of Australian Geology & Geophysics, 6, 1981, 181-185

The determination of suspended-sediment loads in the southern Great Barrier Reef: field techniques

Barry G. West & Peter J. Davies

A mechanical system for collecting samples of suspended sediment in the water column at various stages of a tidal cycle, together with measurement of tidal current velocities, has provided quantitative data on suspended-sediment load transport in a modern coral reef environment. This is the first time that an experiment of this nature has been conducted in such an environment. Suspension load in the water column was monitored over One Tree Reef in the southern Great Barrier Reef by erecting sampling towers at various sites. Suspension loads were collected by siphon action at selected levels of the flooding tide and by a float-activated siphon system at selected levels of the falling tide. Suspended calcium carbonate in the samples was determined by complexometric titration. Water movement was monitored by fluorescein dye casts and arrays of bidirectional current meters. The results show large suspension-load fluxes, which fluctuate with the tidal cycle. Suspended-sediment transport into lagoons and over leeward margins is an important sedimentological process.

Introduction

Studies to identify the biological and abiological processes involved in the growth of coral reefs have been conducted by BMR in the southern Great Barrier Reef since 1976. Significant processes that are dominant on reefs which have grown to a stabilised sea level position are sedimentation of extensive rubble banks, intertidal and subtidal sand sheets, lagoon infill, and leeside sand accumulations. Monitoring of these growth processes has never, to our knowledge, been attempted previously in coral reef environments.

Any quantitative estimate of sediment flux demands (1) that transported-sediment loads be measured on both the rising and the falling tide, and (2) that water velocity and direction be accurately measured at short time intervals for long durations. Suspension-load monitoring in the field can be achieved by continuous or spot sampling. However, in coral reef waters, the high ratio of suspended organic matter to particulate carbonate makes continuous monitoring by turbidometric or densitometric methods impractical. Spot sampling the water column is, therefore, the only sure method of differentiating organic and particulate carbonate components of the total suspension load. Monitoring of water velocity requires expensive and sophisticated field equipment and generates vast amounts of data, the interpretation of which is necessary in the field for the planning of subsequent experiments.

Equipment for monitoring suspended-sediment loads was constructed in BMR and was used on One Tree Reef during March and April 1979. Over this period, tidal ranges encountered were 0.3 m to 3.0 m for springs and 1.2 m to 1.9 m for neaps. Water depths at the sampling sites ranged from zero to 0.5 m at low tide, and 1.5 m to 2.5 m at high tide. Current speeds varied considerably, deepening on the site and state of the tide. Maximum velocities of 145 cm/sec were recorded at the leeward edge of the reef on a rising spring tide, and minimum velocities of less than 5 cm/sec were recorded on the coral flat and in the lagoon. Wave heights were generally less than 10 cm, although in periods of rough weather wave heights in the lagoon were estimated at 0.5 to 0.7 m, with a short wavelength of 1.0 m. This paper describes the equipment and methods developed for determining sediment loads and water velocities on the reef. Similar equipment has since been used successfully on four other reefs in the Great Barrier Reef.

Collection of suspended-sediment samples

Sampling was achieved over both the rising and falling tides by mounting sample containers on a 3-m aluminium tower (Fig. 1) and collecting the samples using a technique comparable to that described by Collins (1976) and Evans & Collins (1975). Normally, the system was set up to collect three samples at different levels during both the flood and ebb of a tidal cycle. The sample inlet hoses were positioned so that water samples were collected at approximately half water depth for low-water, mid-water and high-water levels for a particular tidal range.

The sample containers were constructed of 100-mm ID heavy duty PVC stormwater pipe, with a capacity of either 2.0 litres or 4.0 litres. The bases of the containers were sealed, and the lids consisted of tightly fitting PVC stormwater pipe caps, which had soft rubber inserts placed inside to act as seals. The lids were held in position on the containers by clamping an aluminium bar across them. The inlet and air exhaust were 9-mm ID Nylex hose, fitted over PVC nozzles mounted in the lids.

Sampling during the flood tide was controlled by a siphon action, the time of sampling being controlled by the level of a 'goose-neck' bend in the inlet hose, and the depth at which the sample was taken, by the position of the inlet nozzle (Fig. 2). A PVC non-return valve in the air outlet hose minimised the exchange of water during the subsequent fall in water level.

Early in the development of the sampling towers it was decided that the ball-cock flat system used by Evans & Collins (1975) for collecting samples on a falling tide, might not be suitable in the more severe environments encountered on the windward and leeward margins of reefs in the southern Great Barrier Reef, particularly during periods of spring tides and southeast winds, which average 20-40 km/hr. A system was therefore developed, consisting of an operating level controlled by the movement of a polystyrene float, mounted inside a length of 100-mm ID PVC stormwater pipe to damp the effects of wave surge. The release mechanism which initiates the sampling on a falling tide is shown in Figure 3.

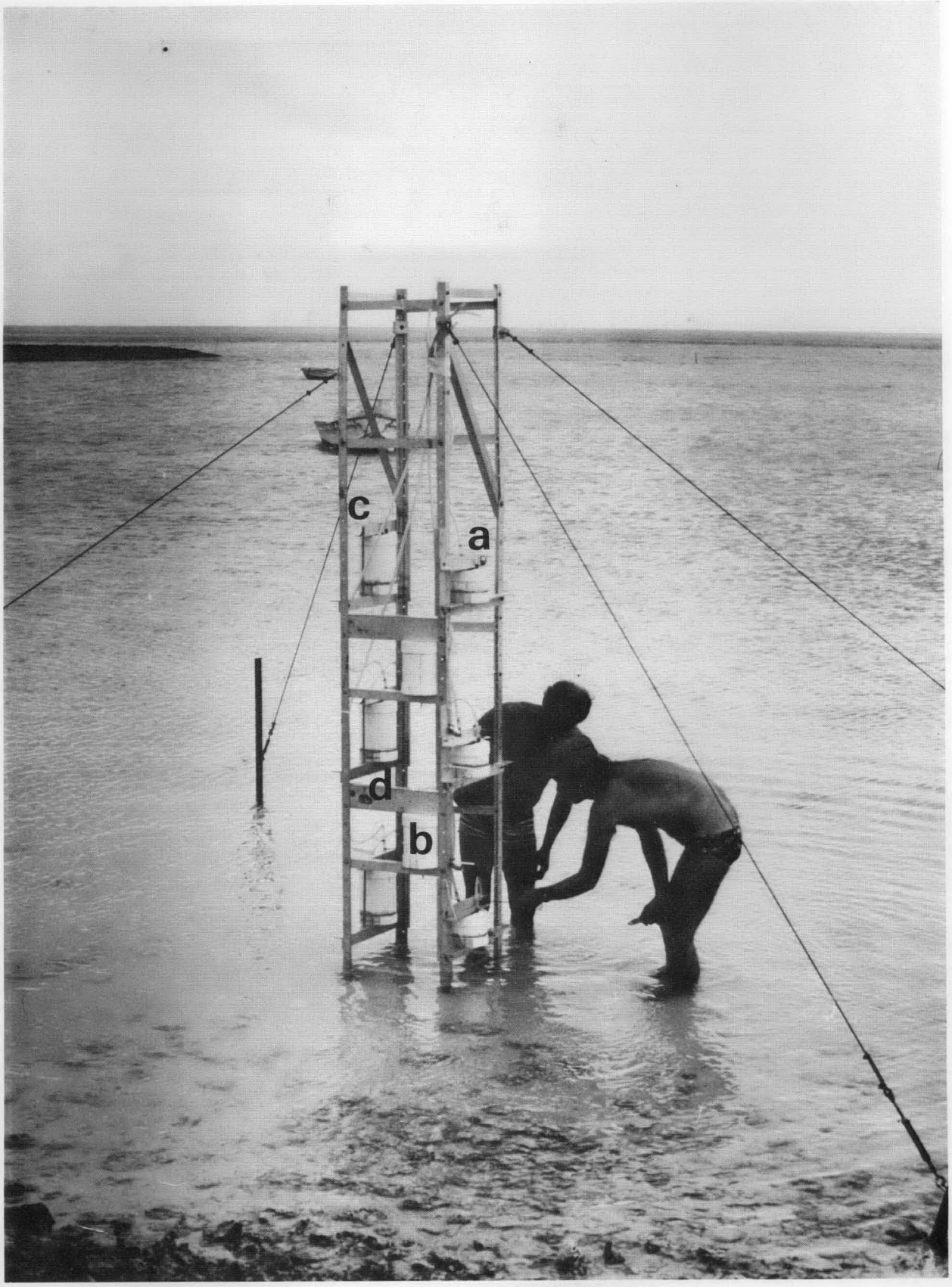

Figure 1. Tower system used to collect suspended sediment samples at One Tree Reef.
(a) rising tide sample containers; (b) PVC float containers for release mechanism; (c) falling tide sample containers; (d) housing for release mechanism.

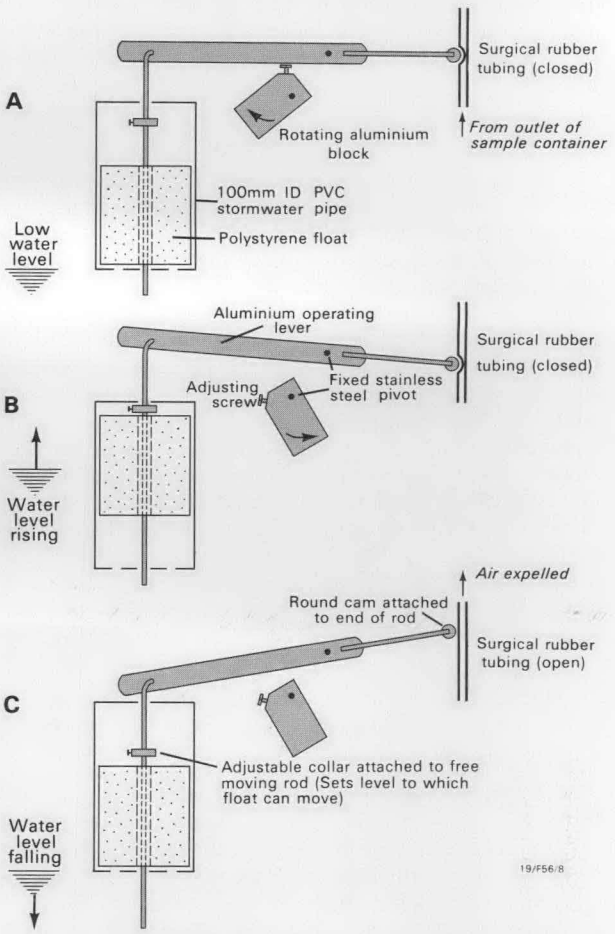

Figure 3. Operation of falling tide sampling mechanism. A. operating lever locked in position by rotating aluminium block; B. rotating block released—tubing remains closed; C. rubber tubing opened and air expelled.

The system is set prior to sampling (usually at low tide) by raising the float mechanism to seal the rubber tubing. The operating lever is locked in this position by a freely rotating block (Fig. 3a). As the water level rises, the pressure on the tubing is maintained by the buoyancy of the polystyrene float. At the same time, the rotating block is released (Fig. 3b). As the water level falls, the operating lever moves down, releasing the rubber tube and allowing a sample to be collected (Fig. 3c). The time of sampling is governed by the positioning of the float in relation to the state of the tide, and the level of sampling, by the positioning of the inlet nozzle, which was usually at half the water depth at which the float was positioned. A PVC non-return valve in the air outlet hose minimises water exchange during a following tidal cycle, but no attempt has been made to modify the mechanism to completely seal the sample container. Contamination is assumed to be minimal.

Because of the difficulty in traversing the reefs at night, samples were usually collected over one of two cycles in a 24-hour period, although there were short periods when samples were collected on successive

Figure 2. Arrangement of hoses for rising tide sampling. (a) sample container; (b) goose-neck bend in inlet hose; (c) inlet nozzle; (d) air exhaust hose.

tidal cycles. A total of 100 water samples was collected from One Tree Reef at four sites on the windward and leeward reef flats, and on the prograding sand sheets.

Measurement of current velocities

Current velocities were measured at the sampling sites of One Tree Reef on an irregular basis, for periods ranging from several hours to 4½ days. Two methods of data collection were used, (a) fluorescein dye casts, from which velocities were determined by timing the movement of dye cast over a measured distance; (b) bidirectional electromechanical current sensors mounted on the bottom. The output from the sensors is an analogue voltage, and is recorded on a modified Memodyne 16-channel data logger. This voltage is converted to a digital signal and recorded, along with a channel identifier, onto a cassette tape. Data on the cassette are processed on a Texas Instruments Silent 700 processor, which prints out time and current velocity (either forward or reverse direction). A total of 11 experiments was run at One Tree Reef using the continuous monitoring equipment in addition to 8 dye cast experiments.

Determination of particulate calcium carbonate

Sample preparation

The water sample is vacuum filtered at 25 psi through a 0.45-μm filter, using a Millipore aseptic filter system. As the sample is filtering, the sample container is flushed out with filtered seawater.

The filter paper containing the particulate material is placed in a 100-ml beaker with 50 ml of 0.3% HCl, and gently agitated until there is no visible sign of CO_2 effervescence, i.e. all the particulate $CaCO_3$ has been dissolved by the dilute HCl. The contents of the beaker are filtered through 0.45-μm filters, care being taken that the beaker is thoroughly rinsed out with distilled water. The filtrate of dilute acid solution and dissolved carbonate is made up to 100 ml in a volumetric flask with distilled water.

Sample analysis and experimental procedure

The concentration of Ca^{2+} in the prepared solution is determined by a complexometric titration of calcium, using a modification of the technique of Tsunogai & others (1968), and stoichiometrically recalculated as calcium carbonate. By using very low concentrations of ethyleneglycol-bis (2-aminoethylether)-tetra-acetic acid (EGTA) it is possible to determine calcium levels of less than 2×10^{-4} mmols.

Potential errors

A set of field experiments was carried out to determine the background level of calcium carbonate. Distilled water and filtered seawater were treated in the same way as that described for collected water samples. Prepared samples were then titrated against 0.1 mmol EGTA. Borax buffer was omitted from half the samples to see if any calcium impurity from sodium tetraborate was detectable.

Turtle grass *(Chlorodesma)* and a soft brown alga (*Laurencia*) are common organic constituents of the suspended material collected, and experiments were conducted to determine if they might be potential sources of Ca^{2+}. Both *Chlorodesma* and *Laurencia* were washed to remove particulate calcium carbonate. Small amounts (100 times more than occurred within collected suspended material) were soaked in 50 ml of dilute HCl for 30 minutes. The solutions were filtered, made up to volume and titrated as described earlier.

Table 1 shows the range of calcium levels as particulate calcium carbonate determined for the various sites at One Tree Reef, together with the background levels detected. Potential errors induced by all the background levels are insignificant compared with levels of particulate calcium carbonate, and have therefore been ignored.

	Range of calcium levels (mg/l)
Site 1 (Rising tide)	0.9-3.1
(Falling tide)	0.8-2.7
Site 2 (Rising tide)	0.6-7.2
(Falling tide)	0.6-2.0
Site 3 (Rising tide)	0.5-4.7
(Falling tide)	0.4-1.3
Site 4 (Rising tide)	0.8-1.3
(Falling tide)	0.5-1.1
Distilled water	Nil
Distilled water + borax buffer	0.017-0.02
Filtered seawater	Nil
Filtered seawater + borax buffer	0.017-0.02
Chlorodesma sp.	0.04
Laurencia sp.	0.004

Table 1. Range of calcium levels (as particulate calcium carbonate) from water samples, and background levels obtained from One Tree Reef. Sample sites are shown on Fig. 4.

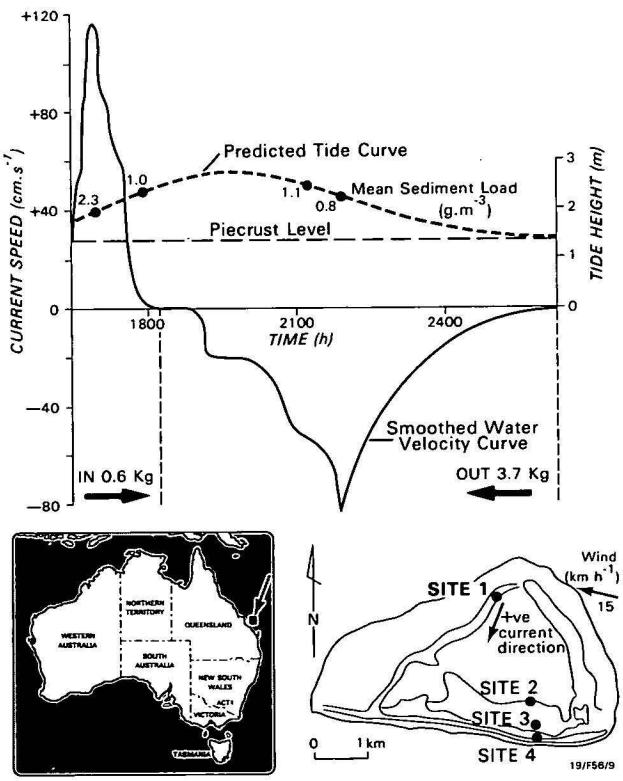

Figure 4. Graphical plot of water velocity data, tide curve, and suspended sediment loads, One Tree Reef, 26/27 March 1979.

Method of calculating total sediment flux over one tidal cycle

To derive a quantitative estimate over the total suspended sediment flux over one tidal cycle, a simple graphical technique is used to combine current velocity, tidal data, and suspended-sediment load.

The current-velocity data from the Memodyne data logger is read on a Texas Instruments Silent 700 in the field, and a time-velocity curve is sketched in the field, but is accurately plotted by computer manipulation of the data in the laboratory. A smoothed out velocity curve shown in Figure 4 has been subdivided into a number of segments denoting specific current-velocity ranges. On the same graph, the corresponding tide curve for One Tree Reef is plotted. This curve is extrapolated from predicted tide data for Heron Island (Queensland Department of Harbours and Marine, 1979), the low-tide values levelling off at about +1.4 m, owing to ponding of the waters in the lagoon (Davies & others, 1976, Ludington, 1979). This level of +1.4 m is taken to approximate the 'piecrust' level of One Tree Reef.

The current-velocity curve is divided into a number of segments, each approximating to a constant change in velocity. The volume of water moved a distance of 1 m by each segment is calculated as a ratio to 1 m^3. The sediment load moved by each segment volume over one tidal cycle is then calculated, and the loads summed.

Discussion

In attempting to measure sediment flux continuously, we initially measured suspension loads by various turbidometric or densitometric methods. While these have been applied successfully to fluviatile environments, they proved grossly inadequate in the reef environment, because calcium carbonate forms only a minor component of the total suspension load, particulate organic carbon being ten or a hundred times more abundant. Separation of these suspension load components can only be carried out by collecting samples. Collection of the samples is cumbersome, and analysis time-consuming, but no reliable alternative method has yet been devised.

References

COLLINS, M. B., 1976—Suspended-sediment sampling towers as used on the intertidal flats of the Wash, eastern England. *Estuarine and Coastal Marine Science*, 4, 45-57.

DAVIES, P. J., RADKE, B. M., & ROBISON, C. R., 1976—The evolution of One Tree Reef, Southern Great Barrier Reef, Queensland. *BMR Journal of Australian Geology & Geophysics*, 1, 231-40.

EVANS, G., & COLLINS, M. B., 1975—The transportation and deposition of suspended sediment over the intertidal flats of the Wash. *In* HAILS, J., & CARR, A. (editors), Nearshore sediment dynamics and sedimentation. *London, Wiley*, 273-306.

LUDINGTON, C. A., 1979—Tidal modifications and associated circulation in a platform reef lagoon. *Australian Journal of Marine and Freshwater Research*, 30, 425-30.

QUEENSLAND DEPARTMENT OF HARBOURS AND MARINE, 1979—Official tide tables for the coast of Queensland, 1979. *Queensland Department of Harbours and Marine, Brisbane.*

TSUNOGAI, S., NISHIMURA, M., & NAKAYA, S., 1968—Complexometric titration of calcium in the presence of larger amounts of magnesium. *Talanta*, 15, 385-90.

BMR Journal of Australian Geology & Geophysics, 6, 1981, 187-195

Suspended-sediment transport and water movement at One Tree Reef, southern Great Barrier Reef

Peter J. Davies & Barry G. West

One Tree Reef, in the southern Great Barrier Reef, is roughly triangular, with the southeast corner forming the windward margin, and the northwest side the leeward margin. In March/April 1979, water circulation and sediment flux were monitored over the reef margins. Generally, water moving from the ocean across the perimeters decreases in velocity when it reaches the lagoon. Over the windward margin coral and algal flats, water movement patterns are similar; i.e., in both environments flow reversal characterises the spring tide flood/ebb change, whereas on neaps, flow is continually towards the lagoon. On the southern prograding sand sheet, between the coral flat and the lagoon, flow is continually towards the lagoon. On the leeward margin, the flood/ebb flow reversal is again a dominant feature. Sediment flux for the different reef zones reflects the water flows. On the windward algal and coral flats, twice as much sediment leaves the reef towards the ocean on spring tides as is transported to the sand sheets, where there is a net loss; on neaps however, suspended sediment movement is continually towards the sand sheets. On the sand sheets, all sediment flux is towards the lagoon, with twice as much arriving in the springs compared with neaps. Spring tide sediment losses over the leeward margin are greater than neap tide gains made by the lagoon over the same margin. The distribution of mud in the lagoon, its concentration at the leeward margin, and its absence on the sand sheets can be explained by the observed energy pattern. Sediment is lost from the system mainly by spring tide flushing of the lagoon, most sediment leaving over the leeward margin.

Introduction

Sedimentological studies on coral reefs have traditionally concentrated on documenting sediment distribution patterns either as grain size or grain type populations. Valuable as these contributions are in indicating the general energy distribution across a reef, there is a need in many aspects of reef research for knowledge of the quantitative distribution and dissipation of energy impinging upon the ecosystem and of the changes in the energy pattern related to tidal and meteorological conditions. This paper is an attempt to understand the sediment flux at One Tree Reef, and to relate it to previously published qualitative sediment data.

One Tree Reef is located in the Capricorn Group in the southern Great Barrier Reef (Fig. 1). Its morphologic development has been shown to be related both to its Pleistocene substrate and to interaction with the modern hydrologic regime (Davies & others, 1976; Davies & Kinsey, 1977; Harvey & others, 1979). Sediment distribution, calcium carbonate production and overall Holocene growth have been studied over many years as part of a program aimed at understanding the processes affecting reef growth. Lagoon infill resulting largely from reef front destruction has been a major reef process ever since 500 yrs BP, when the windward margin reached stabilised sea level (Davies & Marshall, 1980). This lagoon infill implies transport of calcium carbonate from a source to a sink as a result of energy dissipation.

The present work reports on the energy and suspended sediment flux which occur across the perimeter margins at the present time, and attempts to integrate these data with what is known about the dynamics

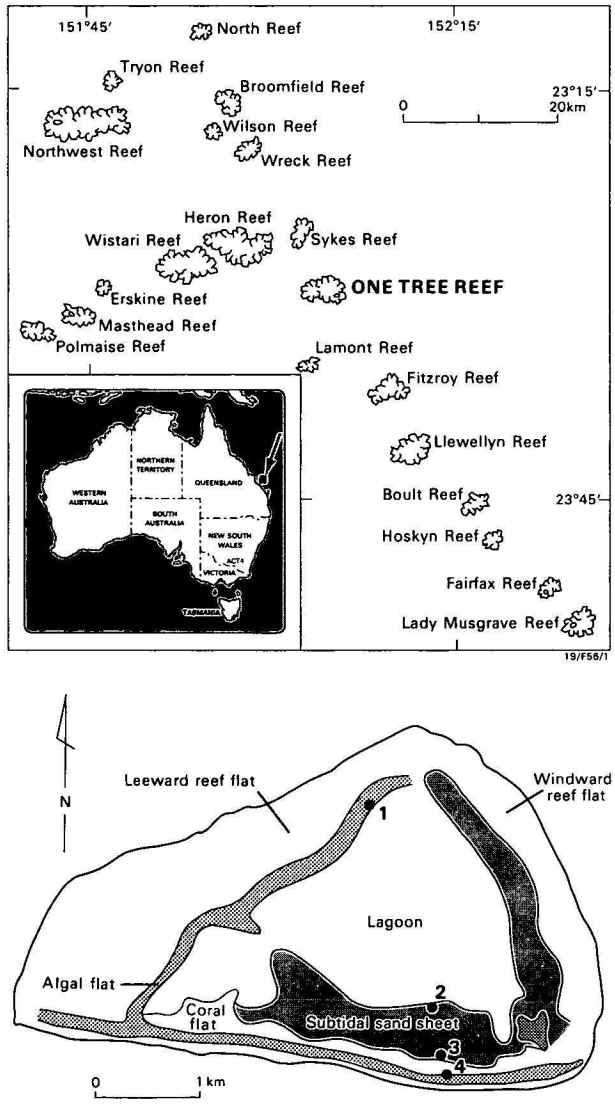

Figure 1. One Tree Reef, southern Great Barrier Reef. Numbers refer to locations of sample sites. 1—leeward margin; 2—prograding sand sheet; 3—sand sheet/coral flat junction; 4—coral flat/algal flat junction.

of the total system. The studies were conducted in March-April 1979 in the hope that monitoring would proceed through a wide spectrum of weather conditions. In the event, weather conditions remained relatively calm, and data reported in this paper may well represent under-estimates of gross suspended sediment transport. Extrapolation of our data outside the period of collection should be done with some caution.

Methods

The methods used for monitoring water and suspended sediment flux over the perimeter margins of One Tree Reef have been detailed elsewhere (West & Davies, this issue), and only a brief outline is given below.

Water movement was monitored by means of fluorescein dye casts and arrays of bidirectional ducted flow meters coupled to a 16-channel data logger. The current meters were installed only after an extensive series of dye casts had established the dominant pattern of water movement over the margins. No attempt was made to differentiate wave and current motion, although it is presumed that water movement over the perimeter margins is tidally and wind induced.

Suspension load was monitored by erecting modified Collins (1976) type towers on the perimeter margins, as described in West & Davies (this issue). Suspension loads were collected by siphon action at selected levels of the flooding tide and by a float-activated siphon system at selected levels of the falling tide. Usually three 4-litre or 2-litre samples were collected on both rising and falling tides. The samples therefore represent suspended material moving past fixed locations on the margins. Suspended calcium carbonate in the samples was determined by complexiometric titration using a modification of the technique detailed by Tsunogai & others (1968).

Current sensors and suspension load samplers were installed at the sites shown in Figure 1. Site 1, on the leeward margin is close to the junction of leeward coral flat and lagoon (Fig. 2A); Site 2 is the junction of prograding sand sheet and lagoon (Fig. 2B) and Site 4 is the junction of coral flat and algal flat (Fig. 2B). Because of the elevated nature of the reef margins, the lagoon is ponded during low tide (Davies & others, 1976; Ludington, 1979), so all sample locations were either dry or nearly dry at low spring tide. Most sites were monitored during springs and neaps, though not simultaneously. The maximum number of observations were made at sites 1 and 2 on the leeward margin and prograding sand flat respectively.

Results

Dye casts

Dye casts were made using fluorescein on the subtidal sand sheet and at the leeward edge of the lagoon. The results of several experiments at each site are shown in Table 1 and summarised in Figure 3.

Subtidal sand sheet. On the rising tide, water leaving the coral flat moves slowly at 10 cm/sec, but this increases to 17 cm/sec as the water mass reaches the centre of the sand sheet. By the time this water mass has reached the edge of the sand sheet it is moving at 13 cm/sec, but this reduces drastically to 6 cm/sec at the lagoon edge. Lagoonal water moves at around 4 cm/sec. During this particular experiment, wind velocities average 16 km/h from the south. Water movements were therefore wind-assisted. On the falling tide similar results were obtained, but with slightly higher velocities in the middle and on the edge of the sand sheet.

Leeward edge of lagoon. On the rising tide, water velocity decreases rapidly from 100 cm/sec on the leeward flat to zero only 400 m into the lagoon. On the falling tide this area of zero movement disappears, water velocities increasing as the leeward edge is approached.

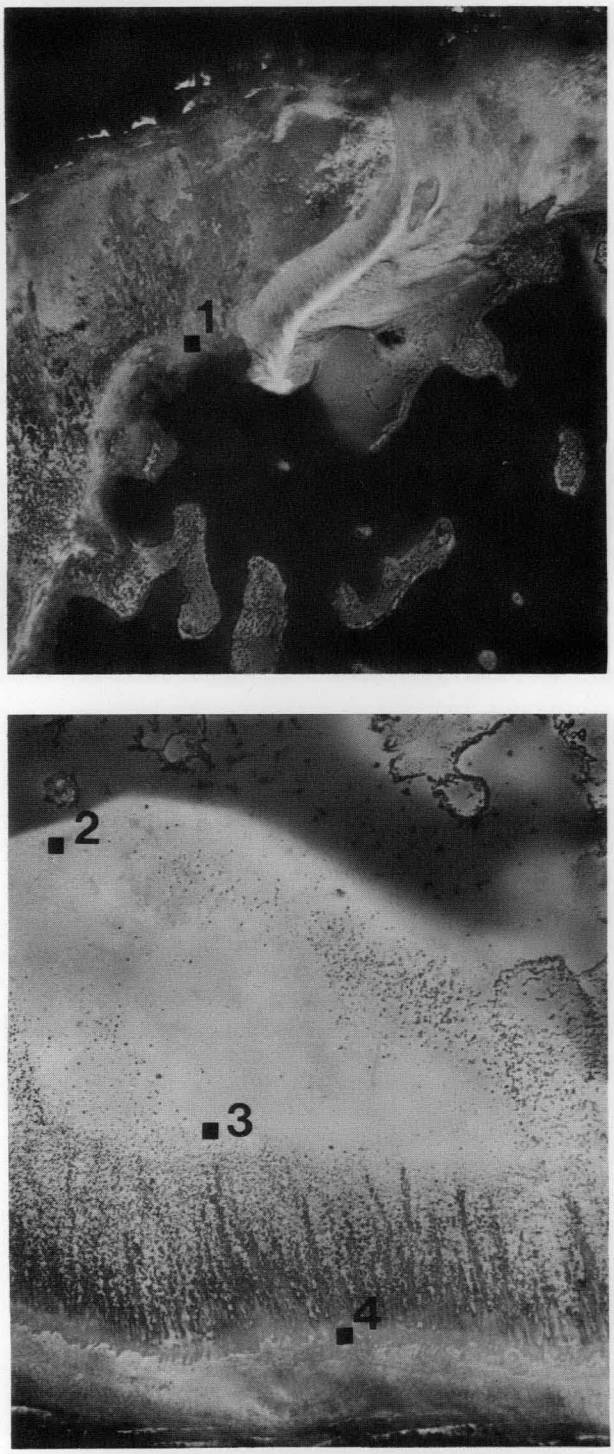

Figure 2. Aerial photographs of sites at which experiments conducted.
A—leeward margin; B—windward side—sites 2, 3, and 4.

Site	Date, time	Tide, condition	Wind speed (km/h) direction (°T)	Water movement Velocity (cm/s)	Direction (°T)
			LEEWARD MARGIN		
1–1	15 March 0700 hrs	Spring rising	15-20 135°	100 (2)	160°
1–2	,,	,,	,,	17 (1)	160°
1–3	,,	,,	,,	13 (1)	160°
1–4	,,	,,	,,	8 (1)	160°
1–5	,,	,,	,,	0 (4)	—
1–4	14 March 1030 hrs	Spring falling	20-25 100°	25	315°
1–3	,,	,,	,,	22 (1)	285°
1–2	,,	,,	,,	33 (1)	315°
1–1	17 March 0640 hrs	Off spring rising	12 130°	36 (8)	160°
1–2	27 March 0715 hrs	Spring high tide	20-25 135°	0 (2)	—
1–2	27 March 0757 hrs	Spring falling	,,	18 (1)	315°
1–2	27 March 0939 hrs	,,	,,	27 (1)	315°
1–1	27 March 0952-1051 hrs	Spring falling	,,	80-132 (13)	315°
			SUBTIDAL SAND SHEET		
2–1	12 March 0900 hrs	Spring falling	25-35 120°	20 (1)	340°
2–2	,,	,,	,,	26 (1)	340°
2–4	,,	,,	,,	6 (2)	340°
2–1	16 March 0630 hrs	Spring rising	16 160°	13 (1)	355°
2–2	,,	,,	,,	10 (3)	345°
2–3	,,	,,	,,	17 (3)	340°
2–4	,,	,,	,,	0-6 (3)	330°
2–5	,,	,,	,,	6	350°
2–6	,,	,,	,,	4	350°
2–1	18 March 1400 hrs	Off spring falling	Calm	12	045°

Table 1. Water velocity data obtained from dye cast studies.
The dye used was fluorescein. Numbers in parentheses in water velocity column refer to number of dye casts.

Results of current meter studies

A resumé of the results is shown in Table 2, and examples of results from each location are shown in Figures 4 and 5. These are discussed below.

Site 1—leeward margin. Maximum water velocities of 145 cm/sec were recorded over the leeward margin, the water moving towards the lagoon. Two examples of the continuous records are shown in Figures 4A-B, both obtained during situations approximating closely to springs. The following conclusions are drawn from the data.

(a) In both instances reversal of water-flow characterises the flood/ebb cycle.

(b) On the 2.8-m tide (Fig. 4A), maximum rising-tide velocities occur some three hours before the top of the tide, and maximum falling-tide velocities some three hours after the top of the tide. Further, on the rising tide, maximum flow is not coincident with the first tidal inrush. On the 2.5-m tide (Fig. 4B) identical conclusions can be drawn.

(c) Higher water velocities characterise the rising tide compared with falling tide on both the 2.8 and 2.5-m tides. A greater velocity difference between rising and falling tides is seen on the 2.5-m tide.

(d) Reversal is nearly instantaneous at the top of the 2.5-tide (Fig. 4B), whereas a slack-water period characterises the 2.8-m tide (Fig. 4A). On the 2.8-m tide, reversal occurs before the top of the tide, i.e. water is flowing back out over the leeward margin while the tide is still rising. The wind data in Table 2 offer some explanation of this phenomenon: on the 2.8-m tide, a southeast wind at 20–25 km/h drove lagoonal water down over the leeward margin. This did not occur in the monitored 2.5-m tide, when winds of only 4 km/h prevailed.

Site 2—sand sheet/lagoon junction. Measurements were made close to spring tide (2.9 m) and neap tide (2.3 m). The data in Figures 4C-D contrast these two situations, from which the following conclusions are drawn.

(a) Maximum water velocities of 25 cm/sec and 15 cm/sec characterise the spring and neap tides, respectively.

(b) On the spring tide, peak velocities occur immediately before the top of the tide, whereas on neaps maximum velocities occur some two hours before the top of the tide. Such differences cannot be attributed to wind speed variations.

(c) On both tides, water velocities are pulsing, and towards the lagoon only. No flow reversal occurs.

Site 3—sand sheet/coral flat junction. Measurements were made when the tide was going off springs and on

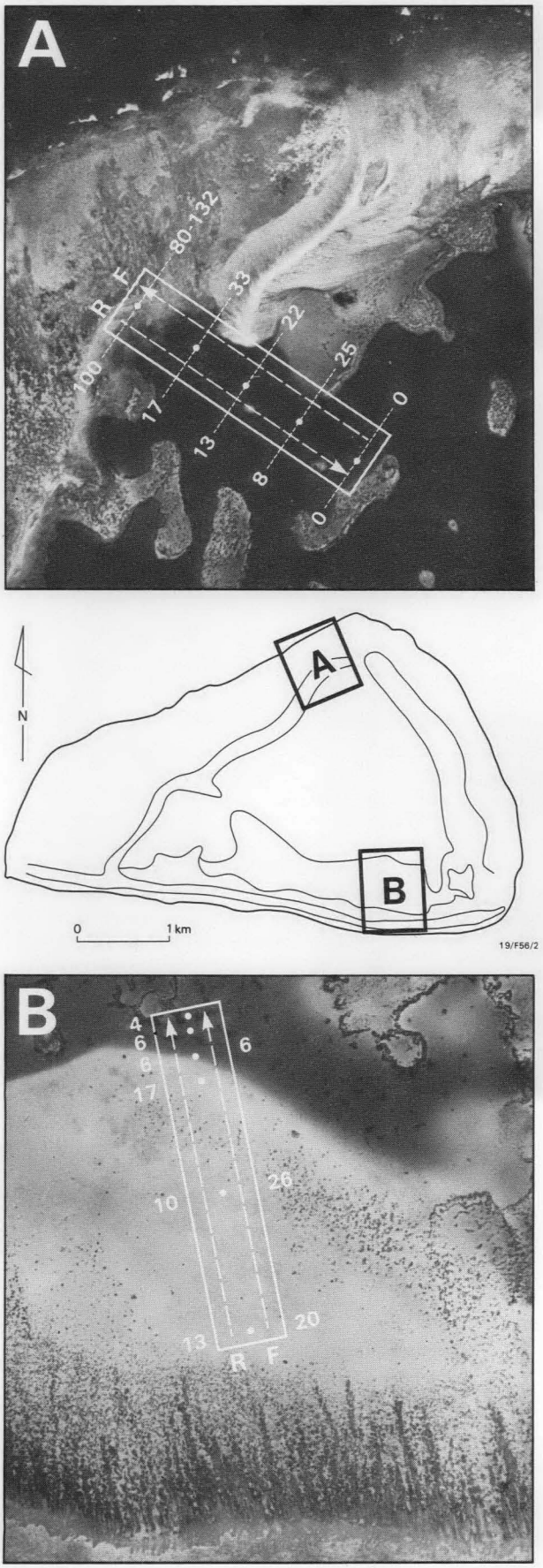

neaps, and both situations are shown in Figures 5A-B, from which the following conclusions are drawn.

(a) Maximum water velocities of 15 cm/sec on springs and 10 cm/sec on neaps were measured; winds were similar in both instances (around 14 km/h).

(b) Flow reversal characterises the rising-tide phase of the 2.6-m tide, with oscillatory backward and forward motion characterising the falling tide. No reversal is seen on the 1.9-m tide, water movement being towards the lagoon, as a series of pulses. Small oscillations in water velocity characterise the falling tide.

(c) The reversed water flow on the 2.6-m tide occurred some one and a half hours before the top of the tide, so that water was running out towards the reef edge while the tide was still rising.

Site 4—coral flat/algal flat junction. Monitoring at this location occurred at tidal states very similar to those at site 3. Examples of results are shown in Figures 5C-D, from which the following conclusions are drawn.

(a) Maximum velocities of 45 cm/sec and 25 cm/sec characterise the 2.5-m and 1.9-m tides, respectively; little wind occurred during either period.

(b) Flow reversal characterises the rising-tide phase of the 2.6-m tide, occurring some hours before the top of the tide and slightly before a similar reversal at station 3. Outward flowing velocities reach 25 cm/sec, but these are reduced during the falling tide.

(c) No flow reversal is seen on the 1.9-m tide, water movement being entirely inwards in a series of pulses at velocities up to 25 cm/sec.

Suspension-load monitoring

Suspended calcium carbonate was monitored at each site on rising and falling tides (Table 2). Together with a knowledge of water volume and velocity, gross estimates of suspended calcium carbonate can be made according to published methods (West & Davies, this issue), and these data are shown in Table 3. Sediment movement is designated as either towards lagoon or towards ocean. The results are summarised below.

Site 1—leeward margin. Large differences are seen in gross suspension loads on the 2.8 and 2.5-tides. On the 2.8-m spring tide and with prevailing winds of 20–25 km/h, more calcium carbonate is transported off the reef than is brought onto the reef. However, as the tide goes off springs (2.5 m), a greater amount of calcium carbonate is brought into the lagoon than leaves. In terms of carbonate measured in collected samples, however, there is little difference between the two tidal states. The gross variation in carbonate load must, therefore, relate to velocity differences in the two tidal conditions.

Figure 3. Water movement at the leeward end of the lagoon (A) and on the windward sand sheet (B), measured by means of fluorescein dye casts. The zone in Fig. 3A where water velocity drops from 100 cm/sec to zero is approximately 400 m long. R—rising tide; F—falling tide.

Date	Tide height (m)	Wind		Water speed		Suspended calcium carbonate (mg/litre)				
						Rising tide			Falling tide	
		Speed (km/h)	Direction	Max. (cm/s)	Min. (cm/s)	R1	R2	R3	F1	F2
SITE 1—Leeward margin										
9/10 March	2.3	20-25	090°-110°	—	—	1.0	1.6	1.4	0.8	1.4
11/12 March	2.5	25-35	100°-120°	—	—	1.6	1.2	1.5	1.7	2.7
15 March	2.8	15	135°	100	0	3.1	2.3	1.4	0.8	1.0
17 March	2.6	12	130°	36	0	2.1	1.5	2.1	1.3	1.1
22/23 March	2.5	calm	010°	103	0	—	—	—	—	—
23/24 March	2.7	0-20	270°-290°	114	0	—	—	—	—	—
25/26 March	2.7	20-25	155°	125	0	1.9	1.5	2.2	1.0	1.4
26/27 March	2.8	20-25	110°-120°	115	0	2.3	1.2	0.9	1.1	0.8
27/28 March	3.0	20-25	135°	—	—	—	—	—	—	—
SITE 2—Sand sheet/lagoon junction										
9/10 March	2.3	20-25	090°-110°	—	—	2.5	2.9	1.0	—	1.3
11/12 March	2.5	25-35	100°-120°	26	2	2.1	7.2	1.8	1.0	0.6
15 March	2.8	15	135°	—	—	1.2	1.1	1.4	1.4	2.0
17 March	2.6	12	130°	—	—	1.9	1.2	—	—	0.8
29/30 March	3.0	25-35	120°-140°	25	0	1.7	—	2.0	1.3	1.4
30 March	2.8	25-35	140°	—	—	1.3	0.9	—	—	1.1
30/31 March	2.9	25-35	100°-140°	36	0	1.1	1.2	1.2	1.1	1.5
1/2 April	2.6	13-20	115°125°	—	—	1.9	0.6	1.3	0.8	0.8
2/3 April	2.5	10-13	090°	—	—	0.8	0.8	—	—	0.4
SITE 3—Sand sheet/coral flat junction										
1/2 April	2.6	13-20	115°-125°	20	0	1.7	4.7	0	1.3	1.0
2 April	2.2	13	115°	13	0	0.5	0.6	—	0.7	0.4
3 April	2.0	10-13	090°	11	0	0.9	0.8	—	0.5	0.7
4 April	1.9	10-13	090°	18	0	0.7	0.7	—	0.6	0.7
SITE 4—Coral flat/algal flat junction										
5 April	2.3	10-13	090°	—	—	1.3	0.8	—	0.9	1.1
5 April	1.9	10-13	090°	33	0	1.7	2.1	—	0.9	0.9
6 April	2.3	13	110°	33	0	0.6	0.7	—	0.6	0.5
8 April	2.5	10	290°-100°	45	0					

Table 2. Résumé of water and suspended-sediment data collected on One Tree Reef in March/April 1979.

Site 2—sand sheet/lagoon junction. Spring and near neap conditions were monitored, and the results indicate a large influx of suspended sediment into the lagoon under both conditions. Twice as much suspended sediment is carried on springs (2.8 m) compared with neaps (?-2.3 m), owing to the greater velocities on the springs.

Site 3—sand sheet/coral flat junction. Under conditions closer to springs than neaps (2.5 m), twice as much suspended sediment moves towards the ocean as moves onto the sand flat. Under conditions closer to neaps however (2.2 m), small but consistent sediment loads are carried onto the sand flat.

Site 4—coral flat/algal flat junction. Under conditions closer to springs (2.5 m) than neaps (2.5 m), twice as much suspended sediment moves off the reef into the ocean as moves onto the coral flat. This inbalance is, however, reversed under neap tide conditions, all suspended load sediment moving onto the coral flat.

Microscopic inspection of particulate calcium carbonate collected on 0.45-μm filter papers showed only mud grade particles forming the suspension loads. No sand grade material was detected.

Discussion

This discussion attempts first to define causes for the circulation pattern, and then appraises important lagoonal sedimentation processes in the light of the sediment flux and circulation patterns.

Wind speed and direction clearly play important forcing or retarding roles in water movement, as predicted by simulation experiments for this reef (Davies & others, 1976) and confirmed by the data in this paper. Tidal currents outside the reef have little direct bearing on water movements over the reef; for example, the flooding tide sets to the west (British Admiralty, 1962), whereas maximum concomitant water velocity occurs on the leeward margin and is to the east. The lagoon at One Tree Reef is ponded because of the elevated reef rims (Kinsey, 1972), and Ludington (1978) used the effect of reef geometry on tidal patterns to deduce the likely water circulation patterns over the reef (Fig. 6). However, our data suggest that Ludington's circulation patterns are partly incorrect, because she has not considered likely circulation differences induced by spring and neap conditions. On spring tides and with southeasterly winds, circulation on the windward margin at high tide is outwards, and this continues throughout the falling tide (cf. Fig. 6A). However, on the neaps, circulation on the windward margin is similar to that proposed by Ludington, except that, during the ebb, movement is continuously to leeward (cf. Fig. 6B). On rising spring tides, the leeward margin shows flow reversal well before the top of the tide, whereas the same situation on neaps produces a slack-water period of little movement (cf. Fig. 6F).

The suspended sediment data presented in our paper relate to silt and clay grade calcium carbonate. The importance of these data in explaining sedimentation on this reef may be gauged from the distribution of

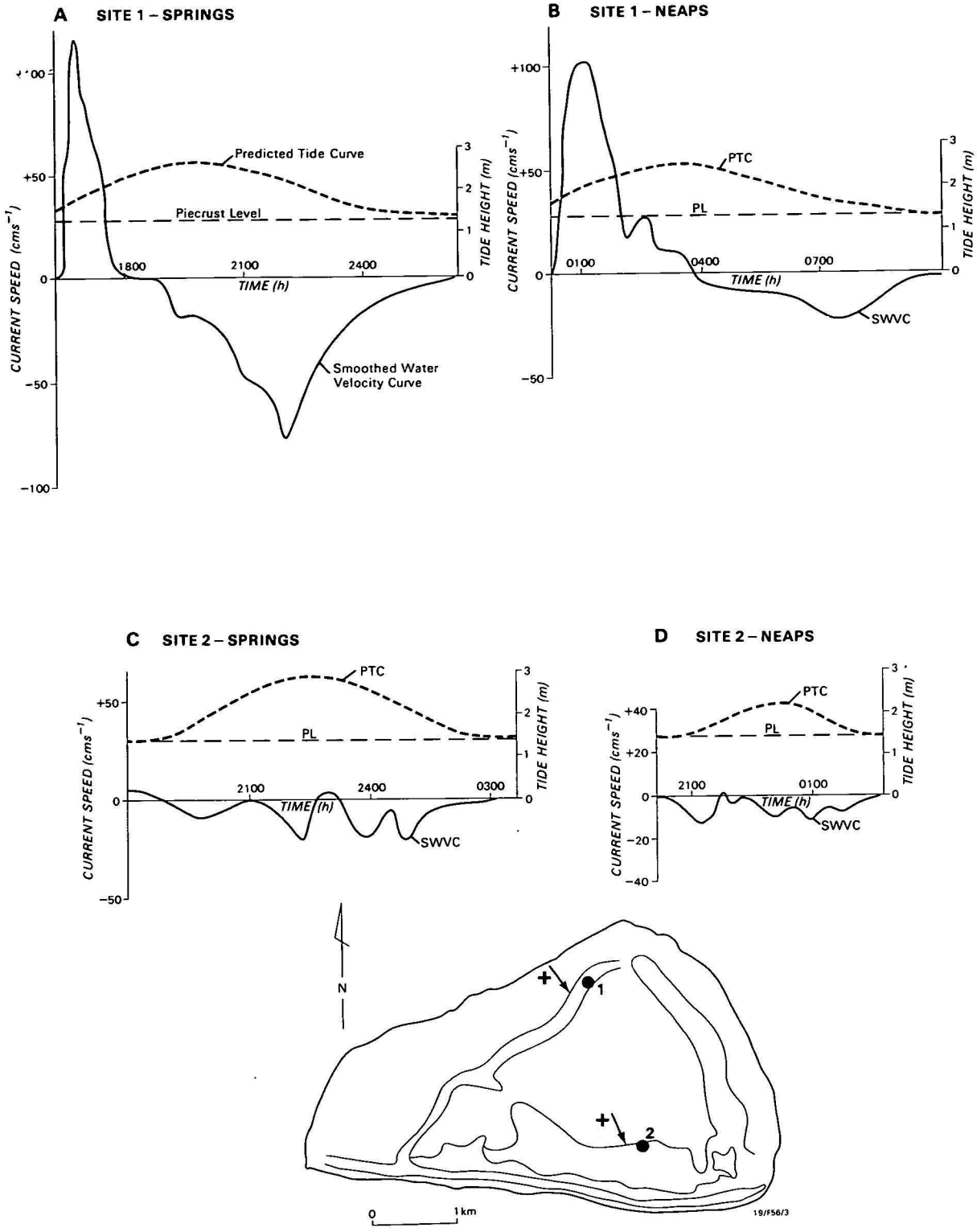

Figure 4. Time-velocity curves for sites 1 and 2.
Arrows refer to positive directions of movement on the time-velocity curves. The predicted tidal curve (PTC) is computed and verified in the field. The piecrust is the ponded water level on the reef.

such material in the sediments (Fig. 7). Three features stand out in this diagram: (1) the high mud content (20-30%) at the leeward end of the lagoon, (2) the sharp entry of mud into the sediment at the junction of sand sheet and lagoon, and (3) the absence of mud in the sand sheet sediments. These three features may be considered in the light of our monitoring studies.

An important feature of the water circulation pattern of the leeward end of the lagoon is the 400-m zone (Fig. 3A), where water velocity drops from 100 cm/sec to zero during the flood tide. We believe this arises from the difference in height between leeward and windward margin, i.e. water penetrates the lagoon first from the leeward end, further penetration being in-

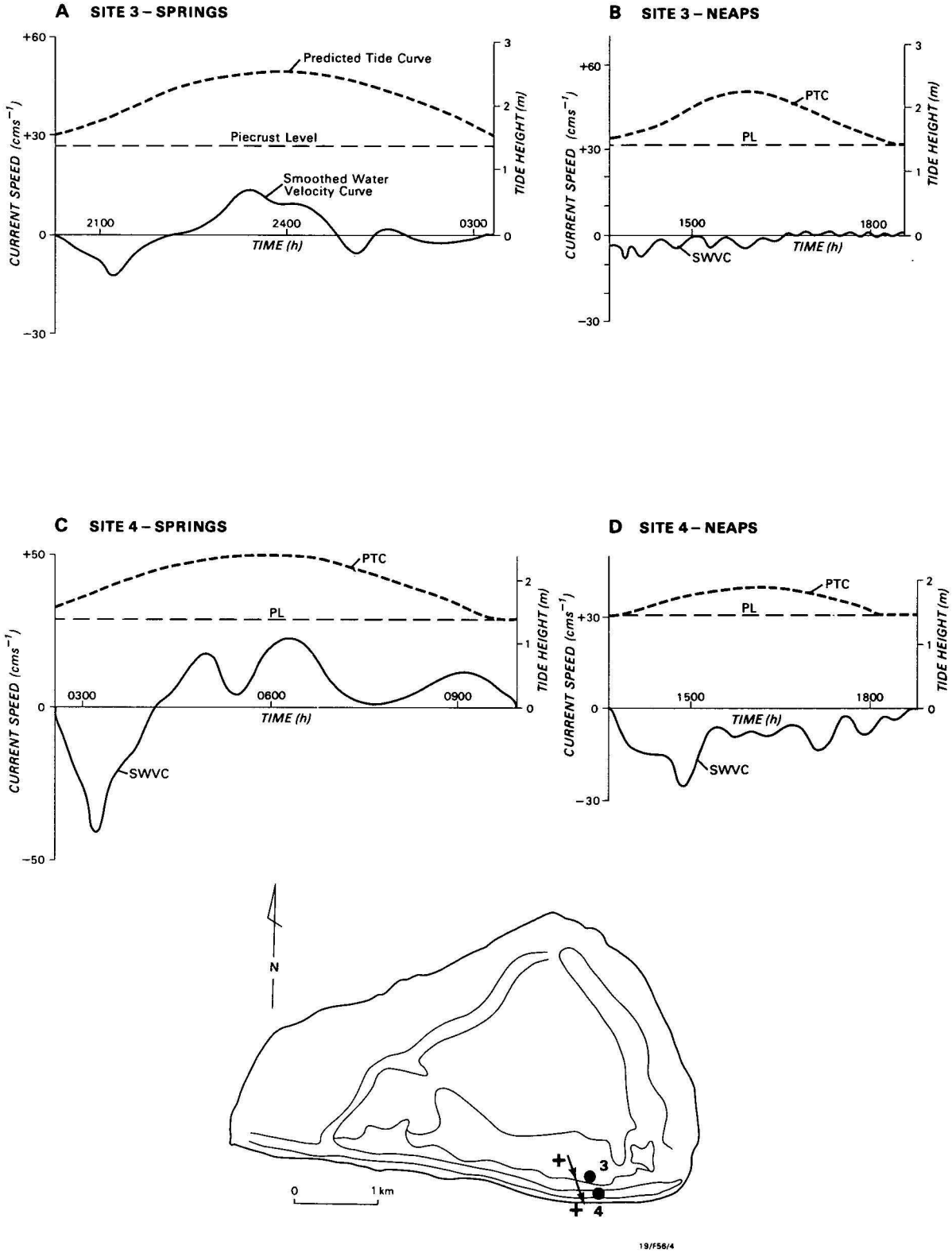

Figure 5. Time-velocity curves for sites 3 and 4.
Arrows refer to positive direction of movement on the time-velocity curves. The predicted tidal curve (PTC) is computed and verified in the field. The piecrust is the ponded water level on the reef.

hibited when water flows over the higher windward edge. The width of this zone is, therefore, likely to vary both with the state of the tide (neaps/springs) and the intensity of the winds. It will be widest on springs with no wind, and narrowest on the neaps with strong southeasterlies. This oscillating zone of marked velocity gradient provides a plausible explanation for the distribution of mud at the leeward end of the lagoon, shown in Figure 7. High mud values (20-30%) would accrue both because of the large amounts enter-

ing the lagoon from the leeward margin, especially on neaps, and because of the rapid velocity decrease which occurs within this zone.

Previous work at One Tree Reef (Davies & others, 1976; Davies, 1977; Kinsey & Davies, 1979) has indicated that the lagoon is acting as a trap for sediment generated, especially on the windward margins. For suspension-load transport our data (Table 3) confirm this general hypothesis, but with certain modifications. Lagoonal trapping of silts occurs mainly under neap or near neap conditions. This is verified by the usually poor visibility in the lagoons during neap tides. However, on the rising tide, under springs or near spring-tide conditions, sediment generated near the windward margins is split into inward moving and outward moving components, i.e. a large proportion of the sediment generated is not in fact incorporated into the reef system. On the falling tide, a large amount of suspended calcium carbonate again leaves the reef, particularly on the leeward margin. Clearly therefore, while the lagoon certainly acts as a trap in neap-tide conditions, both it and the margins are flushed of suspended carbonate during the springs. An estimate of the daily movement of calcium carbonate (Fig. 8A-B) gives some indication of the budgetry losses and gains. We have not extrapolated these reasonably accurate daily figures to annual estimates, although we should be surprised if further studies did not support our contention of a loss of calcium carbonate from the system, especially over the leeward margin under spring-tide conditions.

A comparison of the data at sites 2 and 3 in Table 3 points towards two important sedimentological processes affecting the sand sheet and the lagoon. First,

Predicted tide height at One Tree Reef (m)	*Tide height at Gladstone (m)*	*Condition*	*Calculated sediment loads (kg/m width of reef/day)* Onto reef*	*Out into ocean*
SITE 1—Leeward margin				
2.8	4.2	Springs	1.2	7.4
2.5	3.7	Off springs	4.2	3.6
SITE 2—Sand sheet/lagoon junction				
2.9	4.3	Springs	1.4	—
2.3	3.4	Approaching neaps	0.6	—
SITE 3—Sand sheet/coral flat junction				
2.6	3.8	Off springs	0.15	0.2
2.2	3.2	Approaching neaps	0.06	—
SITE 4—Coral flat/algal flat junction				
2.5	3.7	Off springs	0.4	0.8
1.9	2.8	Neaps	0.6	—

* Calculated for a transect 1 m wide.

Table 3. Relations between suspended-sediment transport and tidal state at One Tree Reef.

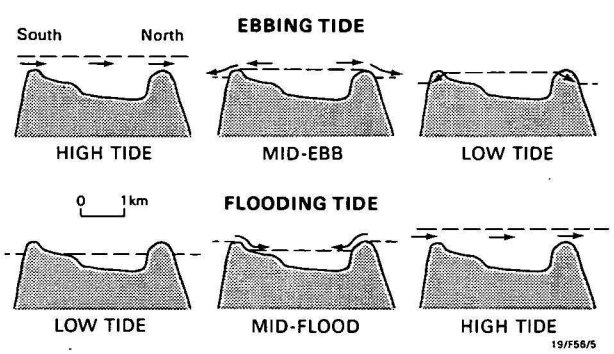

Figure 6. Water circulation patterns at One Tree Reef (after Ludington, 1979).

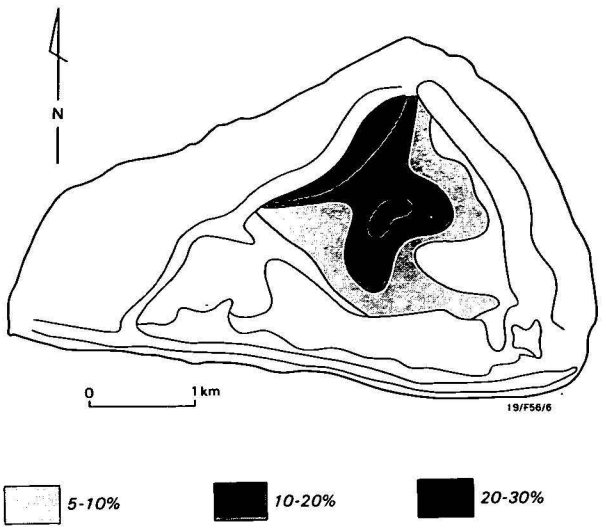

Figure 7. Distribution of mud in the lagoon at One Tree Reef.
Note the close proximity of mud to the sand sheet on the southern side and the high mud values (20-30%) at the leeward end of the lagoon.

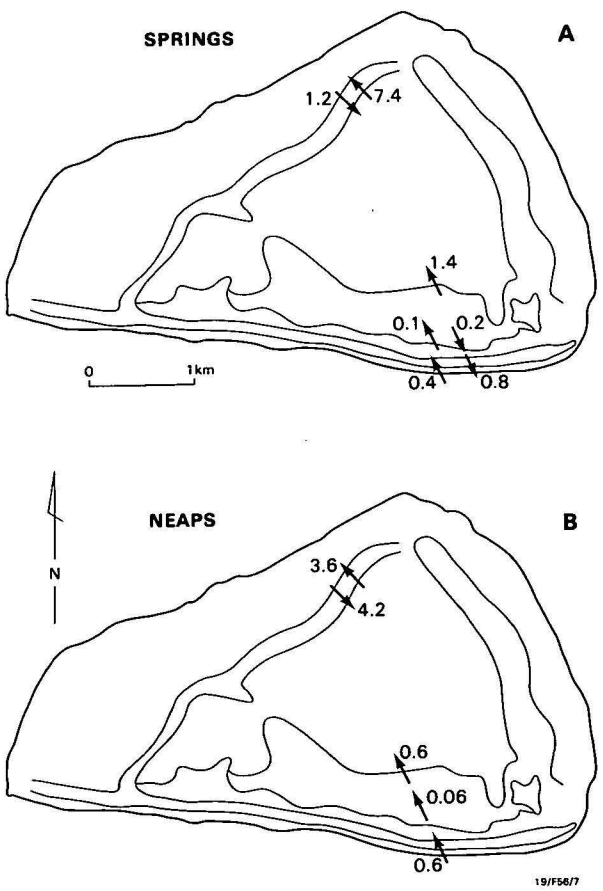

Figure 8. Daily movements of sediment on spring and neap tides during the period of investigation, over a 1-m wide transect.
Figures are kg $CaCO_3$/m width of reef/day.

more suspended calcium carbonate is leaving the sand sheet at station 2 than is entering the sand sheet at station 3. Clearly therefore, erosion of silt-grade components of the sand sheet is occurring between the two zones; and this is borne out by bathymetric profiles across the sand sheet, which show a saucer-shaped surface. Secondly, a relatively large amount of suspended calcium carbonate is being added to the lagoon on both spring and neap tides. Dye casts showed a marked drop in water velocity only 10 m lagoonward of site 2, and it is not unreasonable, therefore, to propose that this suspension load is deposited in the deeper-water marginal lagoonal environment. The mud distribution map (Fig. 7) confirms this to be the case, as high mud values were found in this deeper-water environment.

Analysis of the data indicates significant suspension-load transport into the lagoon and over the leeward margins, the fluxes depending on the state of the tide. Suspended sediment loads calculated for a transect 1 m wide range from a minimum of 0.06 kg/m width of reef/day over the coral flat during neap tides, where water movement is continually towards the lagoon at peak velocities of 10 cm/sec, to a maximum of 7.4 kg/m width of reef/day leaving the system over the leeward margin during spring tides, where water movement is characterised by flood/ebb reversals, with velocities up to 145 cm/sec (Fig. 8).

References

BRITISH ADMIRALTY, 1962—Australia Pilot, IV, Fifth Edition. *Hydrographer of the Navy, London.*

COLLINS, M. B., 1976—Suspended sediment sampling towers as used on the intertidal flats of the Wash, Eastern England. *Estuarine and Coastal Marine Science,* 4, 45-57.

DAVIES, P. J., 1977—Modern Reef Growth—Great Barrier Reef. *Proceedings Third International Coral Reef Symposium,* 2, 325-30.

DAVIES, P. J., & KINSEY, D. W., 1977—Holocene reef growth—One Tree Island, Great Barrier Reef. *Marine Geology* 24, M1-M11.

DAVIES, P. J., & MARSHALL, J. F., 1980—A model of epicontinental reef growth. *Nature* 287, 37-8.

DAVIES, P. J., RADKE, B. M., & ROBISON, C. R., 1976—The evolution of One Tree Reef, Southern Great Barrier Reef, Queensland. *BMR Journal of Australian Geology & Geophysics,* 1, 231-40.

HARVEY, N., DAVIES, P. J., & MARSHALL, J. F., 1979—Seismic refraction, a tool for studying coral reef growth. *BMR Journal of Australian Geology & Geophysics,* 4, 141-7.

KINSEY, D. W., 1972—Preliminary observations on community metabolism and primary productivity of the pseudo-atoll reef at One Tree Island, Great Barrier Reef. *Proceedings, Symposium on Corals and Coral Reefs, Marine Biological Association of India,* 13-32.

KINSEY, D. W., & DAVIES, P. J., 1979—Carbon turnover, calcification and growth in coral reefs. *In* TRUDINGER, P.A., & SWAINE, D. J. (editors), Biogeochemical cycling of mineral forming elements. *Elsevier Amsterdam,* 131-62.

LUDINGTON, C. A., 1979—Tidal modifications and associated circulation in a platform reef lagoon. *Australian Journal of Marine and Freshwater Research,* 30, 425-30.

TSUNOGAI, S., NISHIMURA, M., & NAKAYA, S., 1968—Complexiometric titration of calcium in the presence of larger amounts of magnesium. *Talanta,* 15, 385-90.

WEST, B. G., & DAVIES, P. J., 1981—Determination of suspended sediment loads—southern Great Barrier Reef. *BMR Journal of Australian Geology & Geophysics,* 6(2), (this volume).

Report 222
Microform MF119

Geological Branch Summary of Activities 1979.

ISSN 0084-7100

ISBN 0 642 04890 8

318 pp., 46 figs., 1980. 4 fiche, **$2.50**

Report 223
Microform MF120

Geophysical Branch Summary of Activities 1979.

ISSN 0084-7100

ISBN 0 642 04889 4

239 pp., 1980. 3 fiche, **$2.00**

Report 225
Microform MF150

Definitions of new stratigraphic units in the Seigal and Hedleys Creek 1:100 000 Sheet areas, Northern Territory and Queensland.

ISSN 0084-7100

by *I. P. Sweet*

ISBN 0 642 06025 8

17 pp., 1981. 1 fiche, **$1.00**

This Report contains definitions of eleven new stratigraphic units which were recognised during semi-detailed mapping of the Seigal and Hedleys Creek 1:100 000 Sheet areas in 1972–74. All the new units are of Proterozoic age. The geology of the two Sheet areas is described by Sweet, Mock, & Mitchell (1981).

In the following summary the names of the newly defined units are *italicised*. The *Nicholson Granite Complex* consists of several granite bodies formerly called the Nicholson and Norris Granites. The complex intrudes the Cliffdale Volcanics, the youngest member of which is the *Billicumidji Rhyolite Member*. The Nicholson Granite Complex and Cliffdale Volcanics form an east-northeast trending belt and are overlain unconformably to both the north and south by sedimentary and volcanic rocks. To the north is the Tawallah Group, containing the *Seigal Volcanics*. To the south is the *Wire Creek Sandstone*, which is overlain by the Peters Creek Volcanics containing the *Buddawadda Basalt Member*. Unconformable on these units is the *Fickling Group*, comprising the *Fish River Formation*, the *Walford Dolomite*, the *Mount Les Siltstone*, and the *Doomadgee Formation*. The youngest Proterozoic group south of the basement belt is the South Nicholson Group. The basal formation in the group is the Constance Sandstone, which contains three siltstone members; the youngest one is the *Bowthorn Siltstone Member*.

Report 226
Microform MF151

Chemical analyses of igneous rocks from the Seigal and Hedleys Creek 1:100 000 Sheet areas, Northern Territory and Queensland.

ISSN 0084-7100

by *I. P. Sweet & others*

ISBN 0 642 06026 6

14 pp., 1981. 1 fiche, **$1.00**

Tables of chemical analyses are presented for the Cliffdale Volcanics (36 samples), dyke rocks (10, of which most cut the Cliffdale Volcanics), xenoliths in the Nicholson Granite Complex (4), the Nicholson Granite Complex (25), and the Peters Creek Volcanics (14).

Report 227
Microform MF 147

Petrological data catalogue for Boisa Island, an andesitic volcano in Papua New Guinea: whole rock, mineral, and modal analyses, and modelling data.

ISSN 0084-7100

by *D. A. Gust & others*

ISBN 0 642 05816

3 pp., 14 tables, 1980. 1 fiche, **$1.00**

Seven rock samples from the andesitic volcano Boisa have been chemically analysed and the compositions of their constituent minerals determined by the electron microprobe. These data are presented together with the results of petrogenetic calculations in 14 Tables; all the results are discussed in a paper by Gust & Johnson (1981).

GUST, D. A., & JOHNSON, R. W., 1981—Amphibole-bearing inclusions from Boisa Island, Papua New Guinea: evaluation of the role of fractional crystallisation in an andesitic volcano. *Journal of Geology*, 89, 219-32.

Report 229
Microform MF158

1937 Rabaul eruptions, Papua New Guinea: translations of contemporary accounts by German missionaries.

ISSN 0084-7100

by *A. Arculus (translator) & R. W. Johnson (compiler)*

ISBN 0 642 066175

78 pp., 2 figs., 1981. 1 fiche, **$1.00**

German staff of the Mission of the Sacred Heart in the Rabaul area of northeastern New Britain, Papua New Guinea, observed the explosive eruptions of Vulcan and Kaia (Tavurvur) volcanoes in late May and early June 1937. The missionaries also played a major role in setting up an evacuation camp at their mission headquarters at Vunapope for several thousand refugees from Rabaul and surrounding areas. Letters, accounts based on the letters, and additional articles by the missionaries were published in 1937 in the German mission journals Hiltruper Monatshefte and Liebfrauen Monatshefte. Translations of these reports provide a substantial addition to the English-language record of the 1937 Rabaul eruptions.

BMR Journal of Australian Geology & Geophysics, 6, 1981, 197-198

New microform publications

The reports whose titles and abstracts appear below have recently been issued as microfiche. (The price quoted includes surface postage.)

Report 214
Microform MF92

Adelaidean and Early Cambrian stratigraphy of the southwestern Georgina Basin: correlation chart and explanatory notes.

ISSN 0084-7100

by *M. R. Walter*

ISBN 0 642 05835 6

21 pp., 1 chart, 1980. 1 fiche, **$1.00**

A study has been made of the Adelaidean and Early Cambrian stratigraphy of the southwestern Georgina Basin, and the basic results are presented as lithologic and chronostratigraphic correlation charts and a palinspastic section. Within the Adelaide sequence four tectosomes are recognised; two of these are correlated with the two Adelaidean tillites of other Australian basins. Tectonic movements preceding the deposition of each tectosome have been recognised and named. The palinspastic section shows that Adelaidean deposition took place in fault-bounded troughs. An unconformity separating the Adelaidean and Early Cambrian sequences has been recognised.

The following stratigraphic units are defined or redefined: Black Stump Arkose, Donkey Creek beds, Elkera Formation, Elyuah Formation, Gnallan-a-gea Arkose, Grant Bluff Formation, Mount Baldwin Formation, Mount Cornish Formation, Oorabra Arkose, Wonnadinna Dolomite, Yackah beds, Yardida Tillite, Keepera Group and Mopunga Group. Trace fossils are reported from several Early Cambrian sandstones.

Report 218
Microform MF106

Bibliography of gravimetry in Australia.

ISSN 0084-7100

by *W. Anfiloff & O. Terron*

ISBN 0 642 05061 9

69 pp., 1980. 1 fiche, **$1.00**

This bibliography contains references covering the full range of activities associated with gravity work in Australia. It includes references to field surveys, data reduction methods, map production, geological interpretation, and geodetic work.

BMR will welcome any contributions to the bibliography for inclusion in a later edition.

Report 219
Microform MF114

Permian and Late Carboniferous palynostratigraphy of the Galilee Basin, Queensland.

ISSN 0084-7100

by *M. Norvick*

ISBN 0 642 05980 2

149 pp., 16 figs., 1981. 2 fiche, **$1.50**

Palynological information from the Upper Carboniferous and Permian of 42 petroleum exploration well sections and two outcrop sections in the Galilee Basin, central Queensland, is compiled and re-evaluated. These data are used firstly to test and refine the eastern Australian Late Palaeozoic spore-pollen stage zonation of Evans (1967a, 1969), and secondly to show the broad geological evolution of the basin. The stratigraphic ranges of selected spore-pollen species and species groups are used to define a sequence of nine Late Carboniferous and Permian palynologic intervals, with wide application in eastern Australia. The relationship between these stages and existing zonations is discussed. In the Galilee Basin, Late Carboniferous stage 1 is represented by a thick, glaciogenic, coarse clastic sequence. Early Permian stage 2 comprises coarse clastics, passing up into a possibly glaciogenic fine clastic unit. Coal measure sedimentation began in Early Permian stage 3, possibly indicating warmer climatic conditions. A basin-wide hiatus removed all of stage 4 and the lower part of stage 5. Upper stage 5, of late Early to Late Permian age, saw the widespread development of coal measures. Uppermost Permian rocks have not yet been recorded. The Galilee Basin was outside the influence of the sea, except during upper stage 5, when short-lived marine incursions extended into its southeastern margin.

Report 220
Microform MF110

Seismicity of the New Guinea/ Solomon Islands region, 1972.

ISSN 0084-7100

by *I. B. Everingham & S. N. Sheard*

ISBN 0 642 05880 6

12 pp., 7 tables, 11 figs., 1980. 1 fiche, **$1.00**

Earthquakes which occurred in the New Guinea/Solomon Islands region (0°–12°S, 130–163°E) and intensity data for earthquakes felt in Papua New Guinea are listed for 1972. The level of activity was less than during 1971, when several major earthquakes occurred, but greater than during the 1966–1970 period. One major earthquake with M 6.9 occurred, and twenty-three had magnitudes in the range M 6.0–6.9. No serious damage was caused in the region. The highest level of seismic activity was along the northern area of the Solomon Sea between 151° and 155°E. Intense activity also occurred in smaller isolated areas near the north coast of New Guinea (145°E) and off San Cristobal Island (162°E). Four deep earthquakes occurred in the subduction zone beneath southern New Ireland and Bougainville. Isoseismal maps have been drawn for seven of the most strongly felt earthquakes in Papua New Guinea. The maximum intensities of these earthquakes were MM VII (18 January), MM VI-VII (28 April, 5 May, 17 August, 28 October) MM VI (30 October) and MM VII (5 November). The magnitude frequency relation for 1972 was: $\log N = 6.90 - 0.94M$.

CORRECTION

Volume 6, Number 1: In the paper by P. R. Gidley—
'Discrimination of surficial and bedrock magnetic sources in the Cobar area, NSW', the artwork of Figures 3 and 5 is transposed; the captions are correct.

LANDSAT 81

CONFERENCE AND EXHIBITION

1981 marks the first complete year of operations for the Australian Landsat Station at Alice Springs and its associated processing facility in Canberra. For the first time Australian users of Landsat satellite data have access to timely repetitive coverage. The upsurge of interest that this had triggered in remote sensing is extending beyond the confines of Landsat itself into the fields of complimentary study that augurs well for the future use and development of remotely sensed data and systems throughout this decade.

Given these advances the Australian Academy of Science, the Department of Science & the Environment, CSIRO, the INDUSAT group, and the Canberra College of Advanced Education in association with the Remote Sensing Association of Australia and the Australian National University have announced details of LANDSAT 81, the 2nd Australasian Remote Sensing Conference and Exhibition which will be held at the Australian National University in Canberra from 31st August to 4th September, 1981. The Exhibition will display a wide range of equipment, goods and services related to remote sensing from all over the world. Equipment will include: digital image processing equipment, remote sensing imagery, graphics, image analysis systems, photo geological and geophysical interpretation maps, aerial photographs, sar imagery, computer software and hardware, interpretation and interactive data.

The Exhibition will be held in the same building as the Conference, enabling delegates to attend the Exhibition on a regular basis. People wishing to visit the Exhibition are asked to contact the organisers for complimentary trade passes and special rates on accommodation and airfares that have been negotiated especially for the event. There is limited space still available in the Exhibition for companies wishing to participate and they are asked to contact the organisers direct.

The Conference theme will focus on the application of Landsat data to problems within the Australasian region, with an emphasis on current achievements. Other facets of remote sensing and remotely sensed data will be addressed that complement Landsat or lead to a better understanding of tthe observed data and their effective applications.

Invited speakers from Australia and overseas will present review papers in the areas of:

- Geology and mineral exploration
- Agriculture/land use
- Water resources
- Technical development

CONFERENCE ORGANISERS' ADDRESS

LANDSAT 81,
Australian Academy of Science,
P.O. Box 783,
Canberra City, A.C.T. 2601
Phone: (02) 47 5385

EXHIBITION ORGANISERS' ADDRESS

Exhibition & Trade Fairs Pty Ltd,
49 Cardigan Place,
Albert Park, Vic. 3206
Phone: (03) 699 9100

CONTENTS

Note

R80/207(2) Cat. No. 80 2203 0